Summary

I. Introduction 3
I.1. Epidemiology 3
I.2. Etiology 5
I.2.1 Inherited forms 7
I.3. Pathogenesis 8
I.3.1 Pathogenesis of Colorectal Carcinoma and Molecular Pathways 8
I.4 Histopathological Framework 11
I.5 Prognostic factors 12
I.6. Clinical picture 13
I.6.1 Diagnosis 13
I.6.2 Stadiation 14
I.8 Metastatic setting and predictive factors for therapy response 15
I.8.1 Molecular profiling 15
I.8.2 Immune system and immunosenescence 20
I.8.3 Extracellular vesicles, metabolomics and lipidomics 23
I.9 Rationale of the study 24
II. Methods and materials 25
II.1 Design of the study 25
II.1.1 Inclusion and exclusion criteria 25
II.2 Study objectives 26
II.3. Data collection 26
II.4. Biological Sample Preparation 27
II.4.1 Peripheral Blood Analysis 27
II.4.2 Faecal Analysis 29
II.5 Statistical analysis 29
III. Results 30
III.1. Demographic and clinicopathological data 30
III.2. Tumor-related clinical data 31
III.2.1 Molecular and mutational profiling data 32
III.2.2 Response and Survival Data 34
III.3 Analysis of T cell subpopulations 34

III.4 Metabolomic panel data 48
III.4.1 Stool metabolic panel data 48
III.4.2 Plasma metabolic panel data - responders vs non responders analysis 52
III.4.3 Plasma metabolic panel data - pre vs post analysis 54
***III.4.4* Relationship between T Cells and baseline plasma metabolites** 60
III.4.5 Metabolomic Signatures Associated with T-cell Subsets Linked to Progression-Free Survival 61
III.4.6 Relationship between T Cells and baseline faecal metabolites 61
IV Discussion and conclusions 63
V Future perspectives 69
VI Bibliography 69
VII List of publications of the candidate 83

I. Introduction

I.1. Epidemiology

The colorectal tumor is the third most frequent neoplasm and the second leading cause of cancer-related death worldwide, with a total of 1,931,590 new cases and 935,173 estimated deaths for the year 2020 [1]. In the 1990s, this neoplasm accounted for approximately 783,000 new cases per year, with 437,000 deaths, ranking as the fourth most frequent cancer[2].

In females at the European level, colorectal cancer is the second most common tumor after breast cancer, while in males, it ranks third, following prostate and lung cancer.

The incidence of colorectal cancer is approximately 25% higher in men than in women and varies significantly across different countries. The highest incidence is found in Europe, North America, and Oceania, whereas the lowest is observed in less developed regions such as South-Central Asia and Africa[3], [4].

In the general population, it has been estimated that a male individual has a 4.5% lifetime risk of developing colorectal cancer, while a female individual has a 3.2% risk. The risk of developing the disease begins at 40 years of age and increases exponentially in subsequent decades; in fact, approximately 70% of cases occur in individuals aged 65 years or older.

The disease is predominantly localized in the left colon and rectum, where approximately 60% of large intestine tumors develop. However, the incidence of right colon tumors is increasing in Europe, the United States, and Asia[5].

In Italy, it is estimated that in 2024, the incidence of this neoplasm was 24,473 new cases in men and 21,233 in women, with a total combined incidence of 48,706 new cases per year. In 2020, the incidence of colorectal cancer was estimated to have decreased by 11% compared to 2019, by 17.5% compared to 2017, by 20% compared to the peak in 2013, and by more than 23% compared to the estimated projection in 2011. This significant data confirms the role of primary prevention through colorectal screening, which also provides an additional benefit in secondary prevention, allowing for earlier-stage diagnosis and, consequently, a higher 5-year survival rate[6].

Over the decades, the 5-year overall survival rate has increased from 28.5% to 57% in men and from 30.9% to 60% in women, likely due not only to the greater use of screening investigations but also to the improvement of therapeutic strategies in more advanced stages. The mortality rate in Europe is 15-20 per 100,000 among males and 9-14 per 100,000 among females[4], [5].

Conversely, the incidence has increased among patients under 65 years of age, with a 1% annual increase among those aged 50 to 64 years and a 2% annual increase in individuals under 50 years. Mortality rates have also shown age-dependent trends, with a 3% annual decline in patients over 65 years, a 0.6% annual increase among those aged 50 to 64 years, and a 1.3% annual increase in those under 50 years[8].

A retrospective study conducted using SEER registry data has confirmed this increasing incidence trend of colorectal tumors in patients under 50 years, though the causes remain unclear[9].

Approximately 40% of colorectal tumors are diagnosed at a localized stage (I and II); tumors with regional lymph node involvement (stage III) account for about 36% of new diagnoses, while around 20% of patients present with metastatic disease at diagnosis[7].

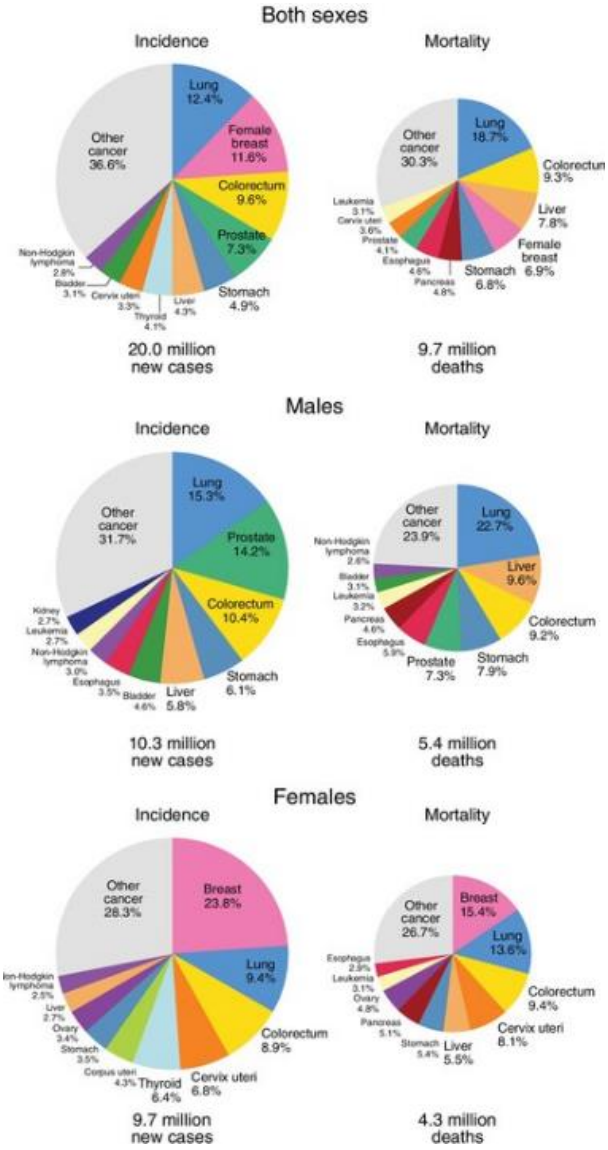

Figure 1. Incidence and mortality estimates in 185 countries or territories for the year 2022. GLOBOCAN 2022

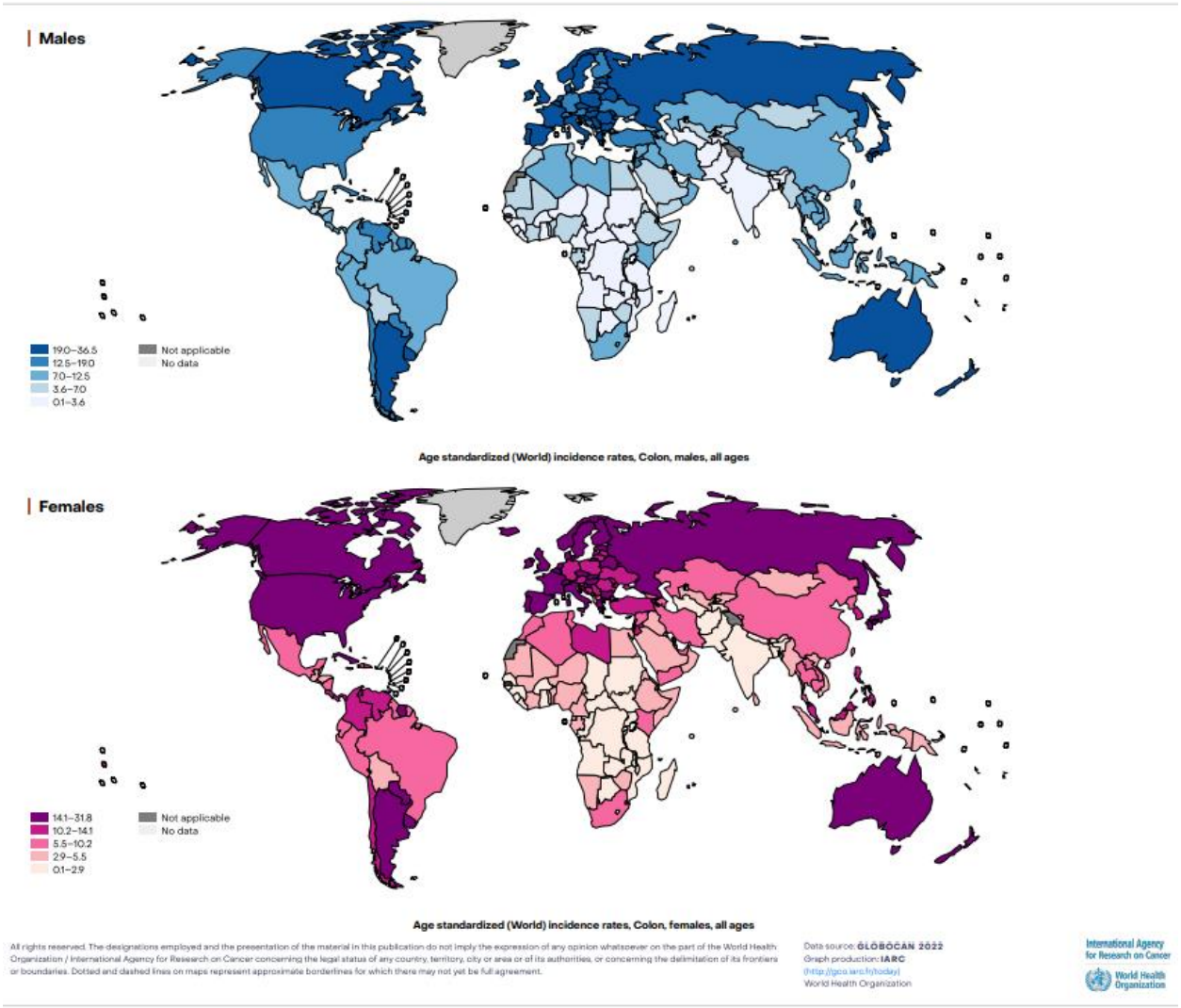

Figure 2. Age standardized (world) incidence rate: men and women. GLOBOCAN 2022

I.2. Etiology

The etiology of colorectal carcinoma is complex and multifactorial. It is hypothesized that, on a background of genetic susceptibility specific to each individual, other factors, generally defined as environmental, come into play, capable of promoting or triggering the carcinogenesis process.

Regarding lifestyle, there is a relationship between colorectal cancer and high caloric intake, obesity, and a sedentary lifestyle; cigarette smoking and excessive alcohol consumption also seem to have a promoting role 10,11. Further studies have shown that foods such as fiber and fats influence the risk of tumor onset, likely due to increased bile acid secretion.

According to the criteria outlined by WHO/FAD, reducing risk by increasing the amount of fruits and vegetables in the diet is possible and likely: raw vegetables and fruits appear to have an anticancer effect. Similarly, a decreased risk is likely associated with the intake of whole grains, whereas eggs and meat have shown the opposite effect. High red meat consumption has been associated with a

relative risk of approximately 2 (1.5 and 2.5); well-cooked or fried meat further increases this risk by another twofold.

This phenomenon is primarily explained by the presence of nitrosamines, which form due to prolonged exposure to high cooking temperatures, and these compounds appear to act as carcinogens or cancer-promoting agents. A high-calorie diet, predominantly rich in fats and carbohydrates, increases the risk of obesity, which is directly correlated with an increased cancer risk. Obesity, particularly visceral obesity, is considered a promoting factor for carcinogenesis.

Alcohol consumption (especially strong liquors and beer) seems to have a direct impact on risk, particularly when combined with tobacco use; this has a significant influence even on moderate smokers.

Regarding medications, many studies have suggested a preventive role for the chronic use of NSAIDs and aspirin [12,13], due to their inhibition of cyclooxygenase, a key enzyme in arachidonic acid metabolism. Some data suggest a reduced risk in women undergoing hormone replacement therapy. Prospective cohort studies indicate that folic acid supplementation from multivitamins is associated with a lower probability of developing cancer.

However, different vitamins, such as vitamin E, as well as calcium and selenium, have not shown clear evidence of efficacy in preventing colorectal neoplasms. Retrospective studies on vitamin D have indicated that its deficiency is linked to a higher incidence of colorectal cancer and that supplementation may reduce the risk of developing this type of tumor [14,15,16,17]. Additionally, retrospective studies have demonstrated that vitamin D deficiency is associated with increased mortality in patients with colorectal cancer [18,19,20].

Nevertheless, no study has analyzed whether vitamin D supplementation improves outcomes in patients already diagnosed with colorectal cancer. In a recent report, the Institute of Medicine concluded that data supporting the role of vitamin D are conclusive only in preserving bone health, but not in cancer prevention or other diseases [21]. Due to a lack of significant data, routine screening for vitamin D deficiency and supplementation in colorectal cancer patients is not currently recommended [21].

The study "Colorectal Cancer: Lifestyle and Dietary Factors," conducted from 1994 to 2004, also demonstrated an important correlation between exposure to plastic-origin dust and fumes or fuel oil and the likelihood of developing colorectal neoplasms [22]. Chronic inflammatory bowel diseases, particularly ulcerative colitis, are another risk factor.

Patients with a previous history of colon cancer have a higher risk of developing a second tumor; for those with a positive family history, the risk is about twice that of the general population. A portion of colorectal carcinomas arises from the malignant transformation of benign adenomas; the transformation potential of adenomas depends on their size, degree of dysplasia, presence of a villous component, and the patient’s age. The risk of transformation for an adenoma larger than one centimeter is estimated to be 3% at five years, 8% at ten years, and 25% at twenty years.

As primary prevention, a diet rich in fruits, fiber, vegetables, whole grains, and legumes should be recommended. This should be combined with a low daily intake of fats, poultry, sweets, refined white

flour, and red meat, along with moderate alcohol consumption and abstinence from tobacco use [22]. Physical activity has proven to be an important ally in prevention, as a sedentary lifestyle predisposes individuals to weight gain and, eventually, obesity [23].

I.2.1 Inherited forms

About 5% of patients with colonic neoplasia have a hereditary predisposition syndrome for colorectal cancer. The most common are: Familial Adenomatous Polyposis (FAP), with its variants, Gardner syndrome and Turcot syndrome, and Lynch syndrome or Hereditary Non-Polyposis Colorectal Cancer (HNPCC).

- **FAP** is the archetype of adenomatous polyposis syndromes. It is an autosomal dominant disorder caused by mutations in the Adenomatous Polyposis Coli (APC) gene, located on chromosome 5q21, and is responsible for about 1% of all colon cancers. The same genetic mutation causes a wide spectrum of clinical manifestations. Based on the clinical presentation, FAP can be divided into classic FAP and attenuated FAP. In classic FAP, patients typically develop between 500 and 2500 colonic adenomas, which carpet the mucosal surface. Numerous adenomas can also be found elsewhere in the gastrointestinal tract, such as in the ampulla of Vater, stomach, and small intestine. Histologically, they are adenomatous polyps with either a tubular or sessile appearance, which, if not removed, undergo malignant transformation in 100% of cases. This explains why one of the preventive measures for carcinoma includes prophylactic total proctocolectomy. Furthermore, FAP is associated with a higher risk of developing other conditions and neoplasms, such as congenital hypertrophy of the retinal epithelium and hepatoblastoma. In attenuated FAP (AFAP), patients tend to have fewer polyps (on average 30), mostly located in the proximal colon, with a lifetime risk of developing carcinoma of about 50%.
- **Gardner Syndrome**: Patients exhibit intestinal polyposis identical to that of classic FAP, combined with numerous osteomas (of the mandible, skull, and long bones), epidermoid cysts, and fibromas. Less frequent are dental abnormalities such as supernumerary or unerupted teeth, as well as thyroid and duodenal carcinomas.
- **Turcot Syndrome**: This is a rare syndrome characterized by the association of colonic adenomatous polyposis and central nervous system tumors. Two-thirds of patients with Turcot syndrome have an APC gene mutation and develop medulloblastomas, while the other third have mutations in one of the genes associated with HNPCC and develop glioblastomas.
- **HNPCC**: This is an autosomal dominant syndrome responsible for about 3-5% of colorectal cancers. It is characterized by an increased risk of developing colorectal and extraintestinal carcinomas, particularly in the endometrium, often at an early age. Colonic carcinomas are frequently multiple and generally do not arise from pre-existing adenomas. A hallmark of HNPCC is a mutation in MMR (mismatch repair) genes, leading to microsatellite instability (MSI). Given the benefits of Lynch syndrome diagnosis, all patients with a colorectal neoplasia diagnosis are screened for this condition through dMMR testing. dMMR can be

identified via PCR, diagnosing microsatellite instability (MSI, MSI-H, or MSI high), or via immunohistochemistry (IHC) to detect the loss of protein expression from one of the four main MMR genes involved in Lynch syndrome diagnosis (MLH1, MSH2, MSH6, PMS2). If a tumor shows loss of MLH1 expression on IHC, it is recommended to analyze the BRAFV600E mutation and/or MLH1 promoter methylation status in the tumor sample. The presence of MLH1 promoter hypermethylation and/or a BRAF mutation indicates that MLH1 expression is downregulated due to a somatic, rather than germline, mutation, thereby ruling out Lynch syndrome [24, 25, 26, 27, 28].

I.3. Pathogenesis

The carcinogenesis of colorectal cancer is a multiphasic process that involves the progressive accumulation of genetic and epigenetic alterations over a generally long period (15-20 years), leading to modifications of the colonic mucosa, first transforming it into an adenoma and then into a carcinoma. The adenoma → carcinoma sequence (Figure 3) is characterized by successive mutations of specific genes, both tumor suppressor genes (p53, APC, DCC, MCC) and proto-oncogenes (c-SYS, c-ERB, c-Myc, c-Fos, c-Jun, c-Ras). Additionally, mutations in DNA repair genes (hMSH2, hMSH1, hPMS1, and hPMS2) play a crucial role in the development of carcinoma in HNPCC syndromes, which are characterized by a high frequency of microsatellite instability.

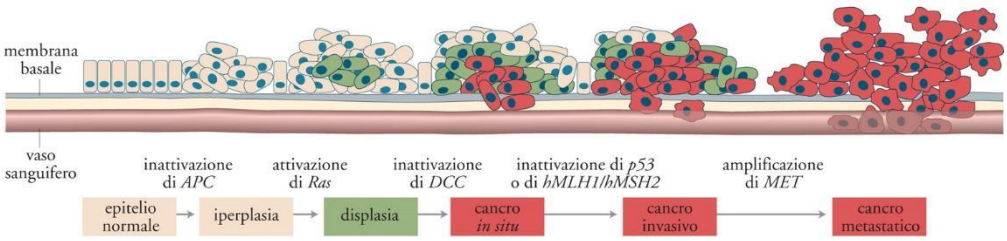

Figure 3

I.3.1 Pathogenesis of Colorectal Carcinoma and Molecular Pathways

There are three main molecular pathways considered responsible for the onset of most colorectal tumors:

1. Chromosomal instability (CIN);
2. Mutation in mismatch repair genes (MIN);
3. CpG island methylator phenotype (CIMP).

1. Chromosomal Instability:

This is a very common pathway and results from "gain of function" mutations. This can lead to hyperactivation of growth pathways and oncogenes or a decrease/inactivation of tumor suppressor genes or apoptotic pathways; among the most common mutations are those in the APC/beta-catenin system. Tumors originating from this pathway can be both sporadic and hereditary and are characterized by large chromosomal abnormalities, including deletions, insertions, and loss of heterozygosity.

2. Mismatch Repair Pathway:

This is less common than the CIN phenotype. The key element is the dysfunction of DNA-mismatch repair enzymes, caused by mutations in one or more genes of the MMR family, particularly MLH1 and MSH. The inactivation of MMR genes can be congenital (Lynch syndrome/HNPCC, where there is a germline mutation of MLH1 and MSH2 [less frequently MSH6 and PMS2] followed by LOH of the second allele due to epigenetic inactivation) or somatic (19% of cases, biallelic silencing of MMR gene promoters by promoter methylation).

The loss of MMR activity leads to an accumulation of errors, resulting in genetic instability, which can contribute to tumor onset 29. The biological "footprint" is the accumulation of abnormalities in small nucleotide base sequences (1-5 base pairs) that are normally repeated dozens to hundreds of times in the genome. These non-coding monodinucleotide repeated DNA sequences have no pathological significance and are called microsatellites. Tumors with high-frequency abnormalities in these areas are phenotypically described as having microsatellite instability. MSI-H (high-frequency microsatellite instability) occurs when mutations are present in more than one microsatellite locus, whereas MSI-L (low-frequency microsatellite instability) is defined by mutations in a single locus.

In HNPCC, MSI is attributed to mutations in loci encoding MSH2 and MLH1, both crucial for regulating the DNA MMR system. Somatic mutations have also been described in sporadic microsatellite instability colorectal carcinoma, but they are present in a minority of tumors. Thibodeau et al. described a lack of hMLH1 expression in more than 90% of MSI-H tumors. A defect in the mismatch repair system results in the failure to correct errors in microsatellite loci. Some microsatellite sequences are located in regions that encode or promote the expression of genes involved in cell growth regulation and apoptosis, leading to mutations in genes such as TGFβRII (Transforming Growth Factor beta Receptor II), IGFIIR (Insulin Growth Factor 2 Receptor), and BAX (Bcl-2 associated X protein) [30]. Other possible gene targets of mutations in colorectal cancer with MMR system alterations include APAF1 (Apoptotic Protease Activating Factor 1), BCL 10 (B-cell Lymphoma 10), Caspase-5, PTEN (Phosphatase and Tensin homolog), TCF-4 (Transcription Factor-4), and ACTRII (Activin Receptor Type II) [31].

Mutations in TGFβRII occur in more than 90% of MSI-H colorectal carcinomas and play a fundamental role in the carcinogenesis process. MMR-deficient cells are 100 times more resistant to apoptosis induced by methylating agents and, respectively, 10 and 2 times more resistant to apoptosis mediated by thioguanine and cisplatin, compared to cells with intact MMR 32, 33. MSI-H tumors

predominantly arise in the right and transverse colon (86-100%), in contrast to MSI-L and MSS tumors, which occur in these locations only in 25% of cases [34].

From an epidemiological perspective, MSI-H colorectal tumors appear to have equal incidence in males and females between 60 and 70 years of age, whereas, beyond 70 years, unstable tumors are 3-4 times more frequent in females [31]. Microscopically, MSI-H colorectal tumors tend to be poorly differentiated, mucinous, and show significant peritumoral lymphocytic infiltration. Despite this apparently aggressive aspect, high-frequency microsatellite instability seems to be associated with a better prognosis compared to MSS.

In a multivariate analysis, Gryfe et al. demonstrated that MSI-H status is an independent positive prognostic factor; patients under 60 years old with MSI-H tumors have increased survival compared to MSS patients [35].

3. CpG Island Methylator Phenotype:

Nucleotide sequences of 20-50 bp rich in CG dinucleotides (CpG islands) are recognized as gene transcription initiation sequences (promoters). Aberrant methylation of C (5-methylcytosine) with hypomethylation, hypermethylation, and loss of imprinting leads to gene silencing of various genes, such as MLH1, resulting in microsatellite instability [34]. Subgroups are defined based on the number of genes inactivated via the CIMP mechanism (H and L).

The term "loss of imprinting" refers to the loss of expression of a specific gene lineage due to selective methylation of one allele. Imprinting is a programmed pattern set in the zygote and maintained during development to suppress the expression of maternal or paternal copies of the same allele.

In the genome, there are small areas, usually located upstream of promoters, characterized by CG dinucleotide repeats called CpG islands. These sequences exist in two main states: methylated and unmethylated. It has been observed that methylation status can influence gene expression, with methylated sequences being associated with transcription inhibition. In normal cells, many CpG-rich promoter regions crucial for transcription remain unmethylated. However, in some neoplasms, these CpG sequences change their state for reasons not yet fully understood, shifting from "unmethylated" to "methylated," thereby preventing the normal function of the corresponding promoter and suppressing gene expression [32].

Neoplasms with a particularly high frequency of CpG island methylation are considered CIMP+ (CpG Island Hypermethylation Phenotype) tumors. The defect may affect promoter regions of genes encoding MMR enzymes like MLH1, leading to gene silencing. Activating mutations in the BRAF gene (V-raf murine sarcoma viral oncogene homolog B1) are almost exclusively found in MSI-H, CIMP+ tumors that do not carry KRAS (V-Ki-ras2 Kirsten rat sarcoma viral oncogene homolog) mutations. BRAF mutations are particularly prevalent in smokers with colorectal cancer. Sporadic tumors with high-frequency microsatellite instability and high BRAF mutation incidence form a distinct subgroup widely regarded as evolving from serrated polyps [35].

Furthermore, this type of epigenetic pathway-driven neoplasia appears to have a preference for the female sex, particularly at advanced ages [31].

Another pathogenetic characteristic of microsatellite instability concerns metastases: studies [34, 36] have shown that highly unstable tumors have a lower frequency of lymph node and hematogenous metastases. This observation was also noted in the study by Kochhar R. et al. (1997), where only 2.5% of liver metastases from colorectal cancer were unstable [30].

The significance of this low incidence may reflect the role of microsatellite instability in carcinogenesis. No secondary tumors exhibited MSI-H without the primary tumor also showing it. This supports the theory that microsatellite instability plays a role in tumorigenesis rather than in distant dissemination. This suggests that CIN and MSI tumors are actually two distinct types of tumors with different prognoses and clinical outcomes [37].

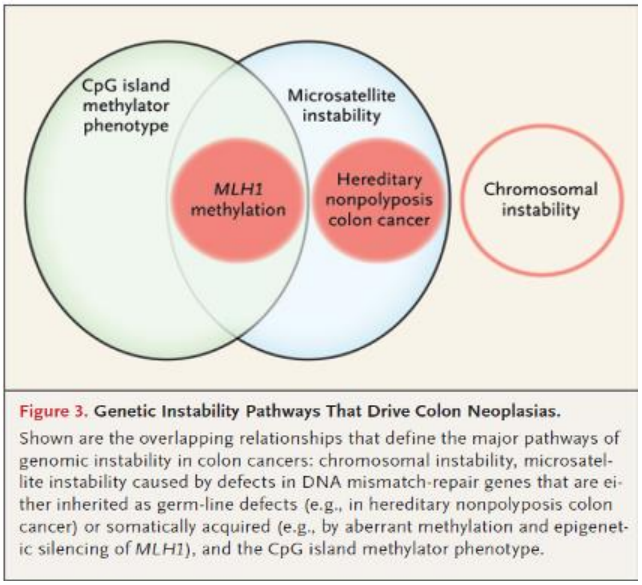

Figure 3. Genetic Instability Pathways That Drive Colon Neoplasias.
Shown are the overlapping relationships that define the major pathways of genomic instability in colon cancers: chromosomal instability, microsatellite instability caused by defects in DNA mismatch-repair genes that are either inherited as germ-line defects (e.g., in hereditary nonpolyposis colon cancer) or somatically acquired (e.g., by aberrant methylation and epigenetic silencing of *MLH1*), and the CpG island methylator phenotype.

Figure 4

I.4 Histopathological Framework

Macroscopically, colorectal carcinoma can present as polypoid, nodular, or ulcerated lesions. The primary histological type of colorectal carcinoma is adenocarcinoma, which accounts for 90-95% of colon carcinomas. Other histological types include:

- Mucinous adenocarcinomas
- Signet ring cell carcinoma
- Squamous cell carcinomas
- Adenosquamous carcinomas
- Carcinoma with endocrine component/small cell carcinoma [38]

Signet ring cell carcinomas and mucinous adenocarcinomas are predominantly located in the right colon. Squamous cell carcinomas are almost exclusively found in the distal colon-rectum, primarily

at the rectoanal level. Signet ring cell carcinomas, squamous carcinomas, and adenosquamous carcinomas are associated with an unfavorable prognosis [5]. From a pathological-anatomical perspective, the minimum diagnostic criteria that must necessarily be included in the pathology report are as follows:

- Histological type
- Degree of differentiation
- Level of wall infiltration and infiltration of the serosa and perivisceral fat
- Distance from the proximal and distal resection margins
- Number of lymph nodes examined (at least 12)
- Number of metastatic lymph nodes
- Presence/absence of vascular invasion
- Presence/absence of perineural invasion
- Tumor budding
- For rectal tumors, the report must also indicate the integrity of the mesorectal fascia and the distance from the radial margin.

I.5 Prognostic factors

The prognosis of patients with colorectal carcinoma is primarily related to TNM staging (where T represents the depth of tumor invasion, N the presence of lymph node involvement, and M the presence or absence of distant metastases).

The 5-year survival probability for patients with colorectal carcinoma is fundamentally correlated with the tumor stage. This probability has improved over the years thanks to intraoperative and pathological staging. In particular, greater attention to pathological details has revealed that prognosis after tumor resection is not solely related to the presence or absence of regional lymph node involvement but can be more precisely assessed through the number of lymph nodes removed. In fact, for an accurate definition of tumor staging, the removal of at least 12 lymph nodes is necessary.

Factors predicting an unfavorable prognosis after total surgical resection include tumor penetration through the intestinal wall into the pericolonic fat, poorly differentiated histotype, tumor perforation and/or adhesion to adjacent organs, and vascular and/or perineural invasion by the tumor. The presence of aneuploidy and specific chromosomal deletions, such as allelic loss on chromosome 18q (involving the DCC gene) in tumor cells, appears to predict a high risk of metastatic spread [5, 24].

Conversely, microsatellite instability appears to be an important prognostic factor. Some studies 39 have shown that high-frequency microsatellite instability (MSI-H) is associated with a better prognosis in stages II and III compared to patients with low-frequency microsatellite instability (MSI-L) or microsatellite stability (MSS). The BRAF gene (V-raf-murine sarcoma viral oncogene homolog

B1) plays a crucial role in this context, as its mutation (mutV600E) is often associated with hypermethylation of hMLH1 promoters. The mutational status of BRAF thus appears to influence the prognosis of MSI-H patients (generally favorable), dividing this group into two subgroups: one with a good prognosis with BRAF Wild Type (WT) and one with an intermediate prognosis with mutated BRAF.

I.6. Clinical picture

About 70% of tumors are located at the level of the sigmoid-rectum. In descending order, the next most common locations are the right colon (cecum and ascending, 15%), the transverse colon (10%), and the descending colon (5%). Many early colorectal carcinomas are asymptomatic, and when symptoms do appear, they are nonspecific. This depends on the tumor's location, its local or distant extent, and the possible presence of complications such as bleeding, obstruction, and intestinal perforation. The presence of blood in the stool, tenesmus, or difficulty in evacuation are more frequent in left-sided locations; nonspecific symptoms include fatigue, anorexia, anemia, or lower abdominal pain and are more common in right-sided colon locations. The clinical presentation at onset may also be influenced by the spread of the disease locally and thus by the involvement of other organs or abdominal structures. The neoplastic mass originating from the intestinal lumen can invade the entire wall and then nearby structures such as the loops of the small intestine, the ureter, the bladder, the stomach, or the prostate. Neoplastic cells can spread into the peritoneal cavity, colonizing the entire surface of the peritoneum (peritoneal carcinomatosis) or the ovaries (Krukenberg syndrome). Additionally, massive lymph node involvement or a large mass originating from the rectum may affect the nervous structures of the small pelvis, causing painful syndromes or functional disturbances. About 20% of tumors are diagnosed already with distant metastases. The most frequent site is the liver, associated with symptoms such as a feeling of gastric fullness, nausea, dull pain in the right hypochondrium, and loss. A colorectal cancer may present with a clinical picture related to complications such as obstruction, bleeding, or perforation [40].

I.6.1 Diagnosis

The symptoms of colon cancer are often subtle and characterized by the absence of macroscopically evident clinical signs when the neoplasm is in its early stage. For this reason, the main diagnostic tools are associated with careful population screening, primarily selected based on age and risk factors (such as family history). The primary diagnostic examination is pancolonoscopy with the possibility of biopsy, which should be conducted until the cecum is visualized; the sensitivity is 96-97% and the specificity is 98%. Alternative investigations include rectosigmoidoscopy combined with a double-contrast enema, which has lower sensitivity. In centers with high expertise, virtual colonoscopy can be used, but it must be followed by an endoscopic examination for histological diagnosis. For rectal tumors, it is essential to define the distance of the neoplasm from the anal margin, its longitudinal and circumferential extension, and the degree of fixation. For these parameters, transrectal endoscopic ultrasound and pelvic MRI are used. The search for hepatic and pulmonary metastases should be performed preoperatively by abdominal ultrasound and chest X-ray, followed by CT in positive or doubtful cases; for tumors of the middle or lower rectum, chest CT is essential. PET and SOF are not

routine tests but should be used in selected doubtful cases. The determination of CEA should be performed at the time of diagnosis, given its prognostic role and its possible use in follow-up. CA 19.9 is also widely used, although its use is not supported by scientific evidence [24].

I.6.2 Stadiation

The most commonly used classification is the TNM system, recommended by the AJCC (American Joint Committee on Cancer), which includes a clinical classification (prefix c) and a pathological classification (prefix p); for rectal cancer, there is also a "y" classification for staging after neoadjuvant treatment. The classification of surgical margins is defined as R0 (clear margins), R1 (microscopic invasion), or R2 (macroscopic invasion).

American Joint Committee on Cancer (AJCC) TNM Staging Classification for Colon Cancer 8th ed., 2017

Table 1. **Definitions for T, N, M**

T	**Primary Tumor**
TX	Primary tumor cannot be assessed
T0	No evidence of primary tumor
Tis	Carcinoma *in situ*, intramucosal carcinoma (involvement of lamina propria with no extension through muscularis mucosae)
T1	Tumor invades the submucosa (through the muscularis mucosa but not into the muscularis propria)
T2	Tumor invades the muscularis propria
T3	Tumor invades through the muscularis propria into pericolorectal tissues
T4	Tumor invades* the visceral peritoneum or invades or adheres** to adjacent organ or structure
T4a	Tumor invades* through the visceral peritoneum (including gross perforation of the bowel through tumor and continuous invasion of tumor through areas of inflammation to the surface of the visceral peritoneum)
T4b	Tumor directly invades* or adheres** to adjacent organs or structures

N	**Regional Lymph Nodes**
NX	Regional lymph nodes cannot be assessed
N0	No regional lymph node metastasis
N1	One to three regional lymph nodes are positive (tumor in lymph nodes measuring ≥0.2 mm), or any number of tumor deposits are present and all identifiable lymph nodes are negative
N1a	One regional lymph node is positive
N1b	Two or three regional lymph nodes are positive
N1c	No regional lymph nodes are positive, but there are tumor deposits in the subserosa, mesentery, or nonperitonealized pericolic, or perirectal/mesorectal tissues
N2	Four or more regional lymph nodes are positive
N2a	Four to six regional lymph nodes are positive
N2b	Seven or more regional lymph nodes are positive

M	**Distant Metastasis**
M0	No distant metastasis by imaging, etc.; no evidence of tumor in distant sites or organs. (This category is not assigned by pathologists)
M1	Metastasis to one or more distant sites or organs or peritoneal metastasis is identified
M1a	Metastasis to one site or organ is identified without peritoneal metastasis
M1b	Metastasis to two or more sites or organs is identified without peritoneal metastasis
M1c	Metastasis to the peritoneal surface is identified alone or with other site or organ metastases

Table 1. TNM-AJCC 2017, 8th ed.

American Joint Committee on Cancer (AJCC)
TNM Staging System for Colon Cancer 8th ed., 2017

Table 2. **Prognostic Groups**

	T	N	M
Stage 0	Tis	N0	M0
Stage I	T1, T2	N0	M0
Stage IIA	T3	N0	M0
Stage IIB	T4a	N0	M0
Stage IIC	T4b	N0	M0
Stage IIIA	T1-T2	N1/N1c	M0
	T1	N2a	M0
Stage IIIB	T3-T4a	N1/N1c	M0
	T2-T3	N2a	M0
	T1-T2	N2b	M0
Stage IIIC	T4a	N2a	M0
	T3-T4a	N2b	M0
	T4b	N1-N2	M0
Stage IVA	Any T	Any N	M1a
Stage IVB	Any T	Any N	M1b
Stage IVC	Any T	Any N	M1c

Table 2. TNM-AJCC 2017, 8th ed., prognostic groups

I.8 Metastatic setting and predictive factors for therapy response

I.8.1 Molecular profiling

The therapeutic option for patients with metastatic colorectal cancer who are eligible for systemic treatment is guided by molecular profiling of the disease, in particular it's crucial to determine the:

- Microsatellite status;
- Mutational status of RAS (KRAS, NRAS);
- Mutational status of BRAF.

either at the primary tumor site or in metastatic tissue.

Patients with a wild-type RAS and wild-type BRAF genotype (35-40% of cases) can currently be treated with chemotherapy combined with the monoclonal antibody cetuximab or panitumumab in clinical practice. Cetuximab (CTX) is a chimeric monoclonal antibody (derived from a combination of mouse/human) that targets the epidermal growth factor receptor (EGFR).

The EGFR (Epidermal Growth Factor Receptor) is a transmembrane glycoprotein weighing 170 kD and is the prototype of the erb-B receptor family [41]. It consists of 3 domains: an extracellular binding domain, a transmembrane domain, and an intracellular catalytic domain. Upon receptor-ligand interaction, the monomers conjugate to form homodimers or heterodimers, leading to activation of

tyrosine kinase function, autophosphorylation of the receptor, and downstream phosphorylation of several intracellular target proteins, initiating the signal transduction cascade. There are several endogenous ligands for EGFR: EGF (Epidermal Growth Factor), TGF-α (Transforming Growth Factor Alpha), amphiregulin, and betacellulin. The main transduction pathways include the RAS/RAF/MAPK (mitogen-activated protein kinase) pathway, the phosphoinositide 3-kinase (PI3K)/AKT/mTOR (mammalian target of rapamycin) pathway, and the JAK-STAT pathway. Activation of these pathways promotes cellular proliferation, neoangiogenesis, metastasis, and resistance to apoptosis, playing a fundamental role in neoplastic growth and progression.

EGFR is overexpressed in 60-80% of colorectal carcinomas. Initial data suggested that increased EGFR expression could correlate with a worse prognosis and reduced survival [42]. Subsequent studies have demonstrated that there is no correlation between receptor overexpression and treatment response [43].

Mutations in the KRAS gene (V-Ki ras2 Kirsten rat sarcoma viral oncogene homolog) are generally found in approximately 40% of colorectal carcinomas. Contradictory data exist regarding the correlation between KRAS mutations and prognosis in this neoplasm. Some studies have suggested a weak negative prognostic role for the G12V mutation alone, but no conclusive data support this hypothesis. The protein encoded by this gene is one of the main effectors in the signaling pathway originating from the EGFR membrane receptor. The KRAS mutation prevents treatment with anti-EGFR monoclonal antibodies (Cetuximab and Panitumumab); indeed, numerous clinical studies have consistently shown that mutations in KRAS codons 12 and 13 (exon 2, 40% of total KRAS mutations) lead to resistance to anti-EGFR monoclonal antibodies in patients with metastatic colorectal cancer [44, 45]. A retrospective analysis of samples from the PRIME study demonstrated not only that other KRAS mutations (exons 3 and 4) and mutations in NRAS (exons 2, 3, and 4) can cause resistance to anti-EGFR antibody treatment, but also that the use of such EGFR inhibitors may worsen patient outcomes when combined with FOLFOX [46]. Similarly, a retrospective analysis of results from the PEAK study (FOLFOX+Panitumumab vs FOLFOX+Bevacizumab as first-line treatment in metastatic colorectal cancer patients) highlighted the superiority of anti-EGFR antibodies in the RAS wild-type population [47]. Similar conclusions were reached in the FIRE-3 study, in which patients with metastatic colorectal cancer were randomized to receive first-line therapy with FOLFIRI+Cetuximab or FOLFIRI+Bevacizumab [48]. Mutations in KRAS or NRAS often lead to the activation of signaling pathways involved in tumor proliferation, independent of EGFR, thus leading to intrinsic resistance to this type of treatment.

Based on these results, AIFA (Italian Medicines Agency) has restricted the use of Cetuximab and Panitumumab to RAS wild-type patients (i.e., patients without mutations in exons 2, 3, and 4 of KRAS and NRAS). Cetuximab and Panitumumab are used in combination with irinotecan-based chemotherapy, as first-line therapy with FOLFOX, or as monotherapy in patients whose oxaliplatin and irinotecan-based therapy has failed and who are intolerant to irinotecan. The role of the G13D KRAS codon mutation (5% of cases) remains uncertain [49, 50].

In 30-40% of patients with metastatic colorectal cancer with KRAS Wild-Type (WT) who do not respond to anti-EGFR antibody treatment, the role of the BRAF protein (V-raf-murine sarcoma viral oncogene homolog B1), a major downstream effector of KRAS, is hypothesized [51].

BRAF mutation, found in about 10% of patients, seems to explain the lack of efficacy of anti-EGFR monoclonal antibody treatment in KRAS WT cancers [52, 53, 54, 55]. Numerous studies have shown that patients with the V600E BRAF mutation have a worse prognosis. Activation of the protein encoded by the unmutated BRAF gene occurs downstream of the activation of the RAS protein in the EGFR pathway [56, 57, 58]; thus, the protein encoded by mutated BRAF is constitutively activated and is not affected by EGFR inhibition carried out by Cetuximab and Panitumumab. Retrospective data from patients with metastatic colorectal cancer undergoing first-line chemotherapy treatment show that despite the V600E mutation being associated with a worse prognosis regardless of therapy, patients with disease characterized by this mutation may benefit from the presence of Cetuximab in the treatment regimen [59, 60]. In general, BRAF-mutated patients are considered to be less responsive to anti-EGFR treatments unless combined with BRAF inhibitors [69, 70].

The phase III BEACON CRC trial demonstrated that encorafenib plus cetuximab, with or without binimetinib, significantly improved overall survival (OS) compared to cetuximab combined with chemotherapy in previously treated patients with BRAF V600E-mutant metastatic colorectal cancer, leading to regulatory approval of the encorafenib–cetuximab combination for this indication [107]. Historically, first-line chemotherapy has achieved limited success in BRAF V600E-mutant mCRC. The phase III BREAKWATER trial evaluated encorafenib plus cetuximab with mFOLFOX6 versus standard chemotherapy in previously untreated patients. Results showed a notably higher, rapid, and durable response rate with manageable toxicity profile and no new safety signals. Although OS data remain immature, early findings suggest a prolonged survival advantage with the experimental regimen [106].

Unfortunately, the efficacy remains limited to only 25% of wild-type KRAS, NRAS, and BRAF tumors [71]; thus, there is a population of cells that survives treatment and is resistant to Cetuximab and PAnitumumab. Therefore, numerous studies have been conducted to explore the mechanisms of secondary resistance to EGFR blockade, and several biomarkers and pathways involved in the development of resistance to anti-EGFR therapy have been reported.

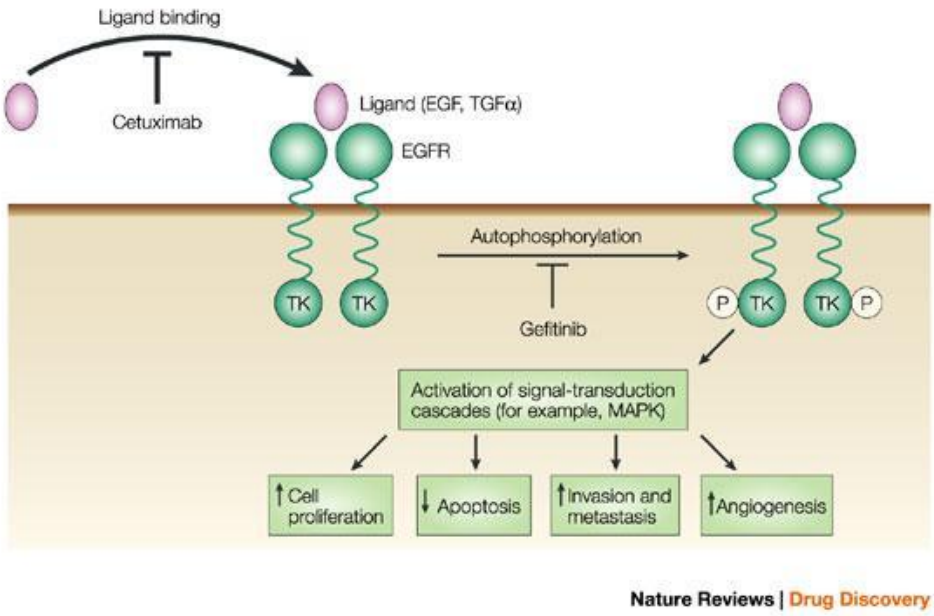

Figure 5. Mechanism of Action of Cetuximab

Another biological drug used in the treatment of metastatic colon cancer is bevacizumab (monoclonal antibody against vascular endothelial growth factor, VEGFA), which blocks the ligand binding to its receptor. VEGF (Vascular Endothelial Growth Factor) is a growth factor involved in the angiogenesis process.

Activation of the VEGF receptor pathway triggers a network of signaling processes that promote carcinogenesis, independent of the EGF/EGFR axis.

The meta-analysis by Chen 76 showed a significant efficacy advantage of adding bevacizumab to chemotherapy. Two randomized phase III clinical trials (FIRE 3 and CALGB) 77, 78 compared the efficacy of chemotherapy + cetuximab vs chemotherapy + bevacizumab, showing a substantial equivalence between the two combinations in KRAS wt patients.

There are no effective markers that can predict the therapeutic action of the monoclonal anti-VEGF antibody (Bevacizumab), as its efficacy does not depend on KRAS or BRAF, nor on VEGFR or plasma levels of VEGF. The levels of VEGF-D in tumor tissue and variations in angiogenetic factors during Bevacizumab treatment seem to have considerable potential. The roles of topoisomerase-1 overexpression (an enzyme that regulates DNA supercoiling) in treatment with Irinotecan, a chemotherapy drug that selectively inhibits its action, and the importance of ERCC1 (excision repair cross-complementing rodent repair deficiency, complementation group 1), thymidine phosphorylase, and thymidylate synthase in treatment with 5-FU and Oxaliplatin remain uncertain.

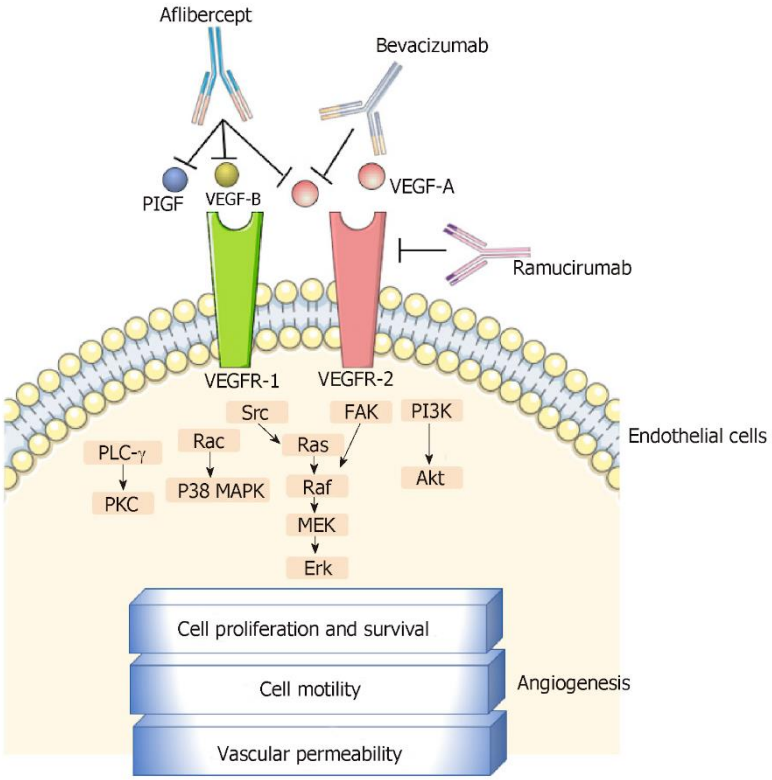

Figure 6. Mechanism of Action of antiVEGF

Approximately 3 – 4% of mCRC cases exhibit HER2 amplification (HER2 3+ or 2+ in IHC with FISH confirmation) and treatment with trastuzumab and lapatinib in advanced lines has proven to be effective in this patients subgroup. Recent studies have also shown encouraging results with the

combination of pertuzumab and trastuzumab along with the antibody conjugate deruxtecan trastuzumab. Despite that none of these anti-HER2 treatments are reimbursed by AIFA.

Moreover, surgery is indicated for patients with a resectable liver or lung metastasis or those that become resectable after chemotherapy.[80,82]

Immunotherapy has recently emerged as a viable treatment option for mCRC. In patients with high microsatellite instability (MSI-H) or mismatch repair deficiency (dMMR, approximately 4% of cases) checkpoint inhibitors targeting PD-1, such as pembrolizumab (KEYNOTE 177), have demonstrated greater efficacy compared to chemotherapy (approved by AIFA in first line and subsequent lines in patients previously treated with fluoropyrimidine-based chemotherapy).

Promising results have also been achieved with anti-PD1 nivolumab as monotherapy and in combination with anti-CTL4 ipilimumab (approved by AIFA in the second line after prior chemotherapy).

The use of immunotherapy in the neoplasm treatment, including mCRC, allows:

- the optimization of tumor cell recognition by the immune system;

- the enhancement of the immune response;
- the eradication of cancer cells' immune system evasion programs.

I.8.2 Immune system and immunosenescence

The immune system is classically divided into innate and adaptive branches. Innate immunity provides a nonspecific, immediate defense against pathogens in individuals without prior immunization. This response is mediated by a range of effector cells, including natural killer (NK) cells, mast cells, eosinophils, basophils, macrophages, neutrophils, and dendritic cells, all capable of pathogen recognition and elimination.
Adaptive immunity, in contrast, involves highly specific responses against microbial pathogens and is subdivided into humoral and cell-mediated immunity. Humoral immunity is driven by B lymphocytes (B cells), which produce antigen-specific antibodies to neutralize infectious agents. Cell-mediated immunity is orchestrated by T lymphocytes (T cells), distinguished by the presence of a T cell receptor (TCR) complexed with CD3 molecules.
Upon recognition of the MHC-antigen complex, alongside appropriate co-stimulatory signals, TCR engagement initiates intracellular signaling cascades leading to T cell activation.
The primary T cell types include:

- **CD4+ T lymphocytes (Helper T cells)**: these cells coordinate immune responses by activating B lymphocytes, cytotoxic T lymphocytes, and phagocytes, crucial for defending against infections and pathogens.
- **CD8+ T lymphocytes (Cytotoxic T cells)**: specialized in the direct elimination of virus-infected and tumor cells, CD8+ T cells recognize antigens presented by MHC class I molecules on target cells.
- **Regulatory T lymphocytes (Tregs)**: Tregs maintain immune homeostasis by suppressing autoreactive T cells, preventing autoimmune responses, and promoting immune tolerance.
- **Memory T lymphocytes**: these cells "remember" previous pathogen encounters, enabling a more rapid and robust response upon re-exposure. They are classified into central memory (residing in lymphoid tissues) and effector memory (circulating in peripheral tissues).
- **Naive T lymphocytes**: naive T cells have not encountered their specific antigen and remain dormant until activation, at which point they differentiate into effector or memory T cells.
- **Gamma-delta (γδ) T lymphocytes**: these cells, lacking CD4 and CD8 markers, are primarily found in mucosal tissues and provide an early immune response to infections and tumors without requiring MHC-mediated antigen presentation.

One of the major immunological escape techniques employed by neoplastic cells is represented by immunosuppression of regulatory T cells through mechanism of exhaustion, anergy and senescence.

Immunesenescence is a process characterized by the progressive decline of immune system functions which is typically associated with physiological aging. However, high levels of senescent T cells can also be found in young patients with chronic viral infections, autoimmune diseases, or cancer.

The process of Immunesenescence is intrinsically linked to changes in the cell cycle and immune cell responses, including:

- Reduced proliferation capacity;
- Slowdown in cell cycle progression;
- Accumulation of senescent cells;
- Alterations in responses to proliferation and cell death signals;
- Reduction of receptor diversity.

Growth arrest is mainly achieved through the activation of the DNA damage Response (DDR) pathways, resulting in the activation of p16INK4a/Rb and p53/p21 pathways and in the entry of cells into a state of senescence. Senescent cells are characterized by increased expression of cell cycle inhibitors (e.g. p16 and p21), a specific phenotype (CD28- CD27+ CD57+ KLRG1+), and a unique secretory profile known as senescence-associated secretory phenotype (SASP). SASP exhibits dual roles: it promotes immune clearance of potentially oncogenic cells, facilitates tissue regeneration, and limits fibrosis, while simultaneously contributing to chronic inflammation and enhancing tumor cell proliferation. This duality is particularly significant in T cells, which, due to continuous activation by antigens and modulation by pro-inflammatory cytokines, can acquire the SASP, thereby disrupting the immune microenvironment.[83, 84]

Every cell undergoes senescence, including those of the immune system and it is known that senescent T cells can be involved in the mechanisms of tumour escape. The study and characterization of circulating T cells are becoming increasingly valuable tools for understanding their potential use of both predictive and prognostic biomarkers. In the case of neoplasm, it has been observed that in patients with higher levels of senescent T cells in the blood, overall survival is significantly shorter.[85, 86.] On the other hand, other studies have demonstrated that pre-treatment levels of senescent circulating T cells are associated with treatment response. Furthermore, changes in senescent T cell levels after chemotherapy can be used as prognostic biomarkers for refractory or recurrent disease.[87, 88]

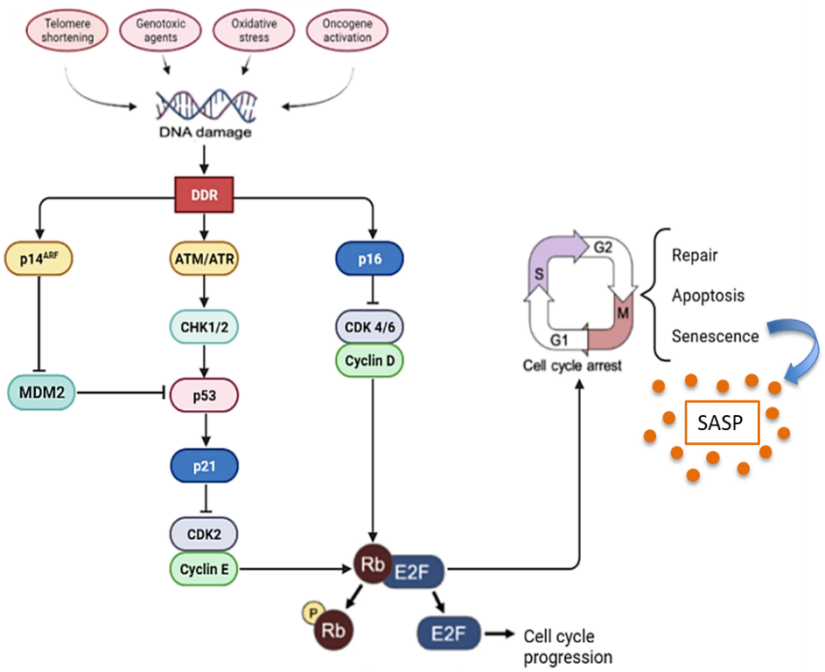

Figure 7. Immunosenescence

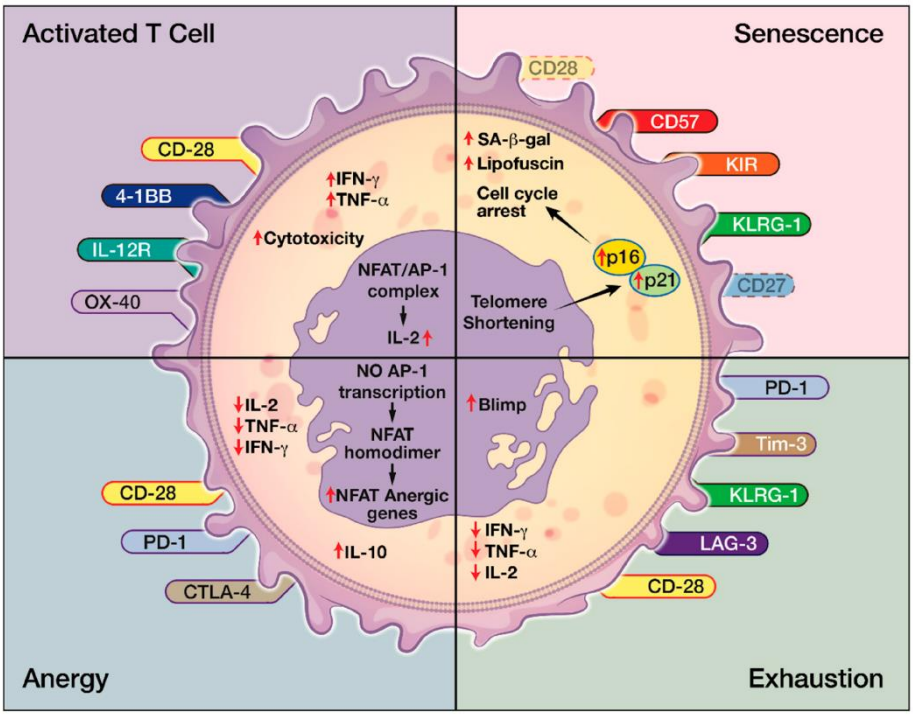

Figure 8. Expression patterns of markers across different T cell phenotypes.

Another important aspect to take into account is that the tumor microenvironment (TME) and many factors, including cytokines, transcription factors, and cell–cell interactions can impact on cells of the immune system, and it specifically can induce the exhaustion of T cells. Exhausted CD3+ T cells are lymphocytes that express several inhibitory receptors such as PD1, LAG3, CTLA4, and TIM3. Therefore, they are characterized by the progressive loss of effector functions, becoming unable to proliferate and produce cytokines [89, 91].

Most T cells in advanced CRC patients are exhausted, and this phenotype is considered to be an important factor affecting the efficacy of immunotherapy in patients with CRC. Studies have shown that low levels of immunostimulatory tumor neoantigens and exhaustion of TILs can contribute to lack of benefit from ICIs in MSS CRC in part due to a hypoxic TME [89, 92].

Investigating the potential prognostic or predictive role of exhausted T lymphocytes may be an intriguing avenue to pursue in light of these results.

In conclusion, recent studies have shown that elevated levels of circulating senescent cells are associated with a reduced response to PD-1 inhibitors. Only exhausted CD8+ CD28+ PD-1+ T cells can be reactivated by the activation of the PD-L1/PD-1 axis, while senescent T cells which are CD8+ CD28- PD-1- naturally remain in a senescent state. Consequently, the prevalence of senescent T cells could be used as a potential predictive marker for response to immunotherapy [93, 95].

The number of CRC-related biomarkers utilized in clinical practice remain limited, therefore the identification of molecules detectable through non-invasive methods represents an interesting tool for dynamically monitoring the course of the disease [96, 97].

I.8.3 Extracellular vesicles, metabolomics and lipidomics

Extracellular vesicles (EVs) derived from blood play a crucial role in intracellular communication by facilitating biomolecules transfer and influencing the extracellular microenvironment in various pathological conditions, including cancer. In addition, EVs represent potential circulating tool useful for profiling the status of disease, improving early diagnosis and prognosis of CRC, as well as predicting treatment response because it can also provide insights into the dynamics immunomodulation and identify potential predictive markers [96, 98, 99].

Metabolomics is defined as the direct analysis, identification and quantification of metabolites which provides a functional insight into the alteration of metabolic processes caused by the biochemical interaction between cancer and the host [100, 101].

Specific alterations characteristic of tumor cells, such as uncontrolled proliferation, results from disruptions in metabolic pathways, especially those related to glucose metabolism (e.g. PI3K-AKT, mTORC1, and RAS). Furthermore, dysregulation of certain pathways leads to the abnormal accumulation and release of products known as “oncometabolites” [100, 102, 103].

Several studies have demonstrated that there was a variation in the levels of various metabolites (aminoacids, fatty acids, and lysophosphatidylcholine) in patients at different stages of CRC

compared to healthy controls or adenomatous polyps. It's important to highlight that at least some of these differences are influenced by the distinct composition of the intestinal microbiota. [104]

In addition, lipid metabolism is described as an essential component in various aspects of CRC carcinogenesis. Different research findings have shown that tumor cells are also characterized by the dysregulation of these metabolic pathways which can contribute to tumour development, aggressiveness, and to the decline of prognosis. Specifically, an increase in omega-6 polyunsaturated fatty acids and a decrease in omega-3 fatty acids have been observed, both of which are associated with tumor progression [105, 108.]

However, the exact contribution of lipids to tumorigenesis and tumor progression remains currently unknown, underscoring the need for further research in this field.

The comprehensive integration of extracellular vesicle characterization with lipidomic and metabolomic profiling delineates a detailed molecular landscape of colorectal cancer, offering transformative potential for the advancement of early diagnostic frameworks, real-time surveillance of disease dynamics, and the precision assessment of therapeutic outcomes.

I.9 Rationale of the study

Despite advances in precision medicine through mutational profiling, clinically implemented biomarkers for CRC remain limited. There is a growing interest in identifying non-invasive, dynamic biomarkers capable of reflecting disease progression and treatment response. In this context, the immune system—particularly circulating T lymphocytes—has emerged as a potential source of clinically relevant information, yet most studies have focused on tissue-resident cells, leaving the systemic immune landscape underexplored. Concurrently, metabolic reprogramming and lipid dysregulation, influenced in part by gut microbiota, have been implicated in CRC progression, with alterations in amino acids, fatty acids, and lysophospholipids observed across disease stages. However, the precise role of lipid metabolism in tumorigenesis remains unclear. This study aims to address these knowledge gaps by characterizing peripheral T cell phenotypes and integrating extracellular vesicle, lipidomic, and metabolomic profiling in patients with metastatic CRC undergoing systemic treatment. The goal is to identify immunometabolic signatures associated with clinical and molecular features, offering novel insights for prognostic refinement and personalized therapeutic strategies.

II. Methods and materials

II.1 Design of the study

"CRC – Tsen: Assessment of the Predictive and Prognostic Role of Circulating T Cells in Patients with Colorectal Cancer Undergoing First-Line Treatment" is a single-centre, observational study with a prospective and translational design. The aim is to identify novel predictive and prognostic biomarkers of treatment response in patients with mCRC who are eligible for first-line therapy, in accordance with standard clinical practice. All patients are treated at the Department of Oncology of the Azienda Ospedaliera Universitaria – Ospedale Maggiore della Carità, Novara, Italy. The biological specimens collected for the translational research component are processed at the University Centre for Translational Research in Autoimmune and Allergic Diseases (UPO-CAAD), also located in Novara. The study protocol received ethical approval from the Ethics Committee of the Azienda Ospedaliera Universitaria – Ospedale Maggiore della Carità di Novara in March 2024

II.1.1 Inclusion and exclusion criteria

Patients enrolled in the study are required to meet the following inclusion criteria:

- Subject has provided informed consent prior to initiation of any study specific activities/procedures
- Age ≥ 18 years
- Pathologically documented mCRC
- Subjects will have received the first-line treatment of therapy for metastatic disease
- Life expectancy of > 3 months, in the opinion of the investigator

Exclusion criteria are:

- Patients with psychological, familiar, social and geographic conditions that could contraindicate compliance and adherence to the proposed therapies
- Significant uncontrolled concomitant diseases that could affect compliance with protocol procedures or interpretation of results or that pose a risk to subject safety, in the opinion of the investigator

II.2 Study objectives

The primary objective of this study is to investigate the impact of circulating T cells functional state on treatment response and survival in patients with metastatic colorectal cancer (mCRC) undergoing first line therapy.

Secondary objectives include:

- The assessment of the predictive and/or prognostic value of circulating leukocytic and tumour-derived extracellular vesicle (EV) levels, along with the evaluation of PD-L1 expression, at baseline and at subsequent time points during therapy or at the time of disease progression.
- The identification of a metabolomic signature that may serve as a predictive and/or prognostic biomarker for treatment response, with longitudinal analysis throughout first-line therapy.
- The identification of a lipidomic signature at baseline with potential predictive and/or prognostic significance in the context of mCRC treatment and progression.

II.3. Data collection

Patient data were obtained through the review of electronic medical records and included the following information:

- Demographic information, including full name, sex, and date of birth;
- Medical history, comprising body mass index (BMI), smoking habits, predisposing genetic conditions, alcohol consumption, and comorbidities affecting lipid, glycaemic, or immune profiles;
- Medication history, with particular attention to drugs influencing lipid, glycaemic, or immune parameters (e.g., metformin and other antidiabetic agents, statins, vitamin D, and related medications);
- Date of initial diagnosis, anatomical location of the primary tumour, pathological staging according to the TNM classification, and disease status (resected vs. unresected);
- Date of metastatic diagnosis, along with the site and extent of metastases (visceral and/or involving soft tissues and bone);
- Histopathological findings, including the date of biopsy or surgical specimen collection, tumour grading, microsatellite instability status, and the mutational status of *KRAS*, *NRAS*, *BRAF*, and other relevant genes;
- Date of initiation of first-line therapy, along with the corresponding treatment regimens;

- Serum levels of tumour markers (CEA and CA19-9) at baseline and during subsequent evaluations;
- Date of enrolment in the study;
- Date of baseline and follow-up blood sampling, including corresponding laboratory values for total cholesterol, HDL, LDL, triglycerides, and blood glucose;
- Date of completion of first-line therapy;
- Date of study-related blood and faecal sample collection.
- Date of progressive disease
- Type of radiological response during study follow up

II.4. Biological Sample Preparation

Biological samples were collected, processed, and stored in accordance with standardized protocols to ensure the integrity and reproducibility of downstream analyses. All specimens were appropriately labeled, anonymized, and maintained under controlled temperature conditions, in full compliance with ethical guidelines and biobanking standards.

II.4.1 Peripheral Blood Analysis

Peripheral venous blood (10ml) was obtained in EDTA tubes. The patients donated two blood samples (first before starting chemotherapy and the second after the chemotherapy). Peripheral blood mononuclear cells (PBMCs) were isolated using a density gradient (Lympholyte-H, Cedarlane, Netherlands)

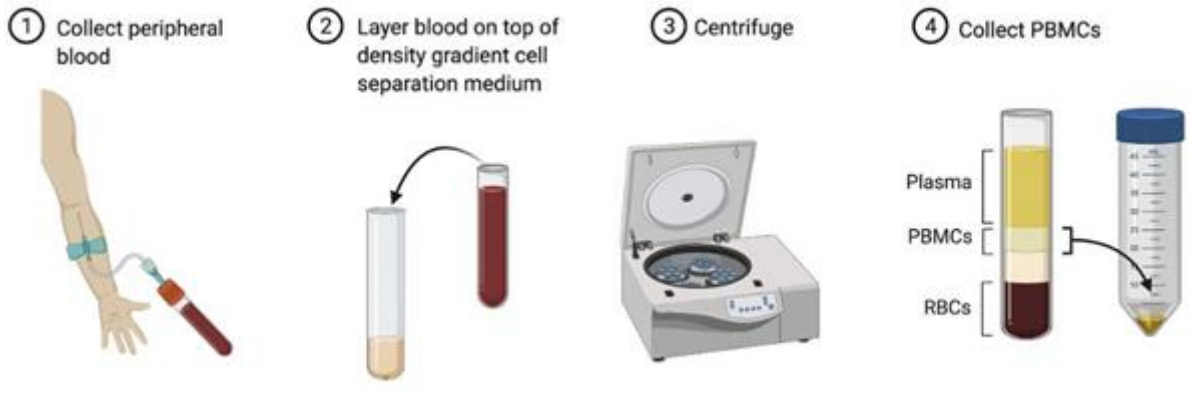

PBMCs isolation begins with peripheral blood collection from patients in an EDTA tube. Blood is then layered over the Ficoll-Paque, and through centrifugation (with brake OFF) its components are separated into plasma and platelets, PBMCs (lymphocytes and monocytes) and other red blood cells indicated as RBCs (granulocytes and erythrocytes). The PBMCs layer can be extracted along with

residual platelets and washed to purify only the lymphocytic and monocytic populations. Adapted from (Turocy J, Williams Z. Fertility and Sterility 2021)

T-cell senescence and exhaustion staining

200 ul of whole blood or $1*10^6$ cryopreserved PBMCs were stained and incubated for 20 min at room temperature with a viability dye (FV780) and with monoclonal antibodies against senescent and exhausted markers (all provided by BD Bioscience, Milan, IT Tab.)

Table: Anti-human antibodies used for staining procedures.

ANTIBODY	FLUOROPHORE	VOLUME (ul)
KLRG1	PE	1
PD-1	BV650	1
TIGIT	BB700	1
LAG-3	BV480	1
CD45	BUV395	0,5
CD8	BUV496	1
CD4	FITC	1
CD57	BV421	0,5
CD3	BV786	1
CD28	APC-R700	2

Following incubation, the remaining reticulocytes were lysed with a 1x lysis buffer (BD biosciences, Milan, IT). Finally, stained cells were analysed for T-cell phenotyping by FACS, using the latest updated version of FlowJo software. Circulating T-lymphocytes subpopulations were classified and quantified according to Weili Xu et al. as follows:

- · Exhausted T lymphocytes: CD4+/CD8+ CD28+PD1+TIGIT+LAG3+
- · Senescent T lymphocytes: CD4+/CD8+ CD28-CD57+KLRG1+

Metabolomics GCxGC/TOFMS analysis on plasma

A total of 1.5 ml of the original peripheral whole blood was centrifuged to extract 4 vials of 200 µl plasma, which were stored at -80°C.

For each patient, a vial was thawed and prepared for metabolomics analysis as follows: 30 µl of plasma was treated with 1 ml of acetonitrile (VWR, Milan, IT) and isopropanol (Scharlab, Barcelona, ES) water solution (3:3:2), with tridecanoic acid (Merck, Darmstadt, DE) at 1 ppm, added as internal standard. The solution was then vortexed and centrifuged at room temperature for 15 minutes at 14.500 g, the resulting supernatant was collected and dried in a speed-vacuum. Then, the sample was derivatized by adding 20 µl of Methox at 80°C for 20 minutes, followed by 90 µl of N,O-Bis(trimethylsilyl) trifluoroacetamide (both reagents were purchased from Merck, Darmstadt, DE) at 80°C for 20 minutes, respectively for methoximation and sialylation.

For GCxGC/TOF-MS metabolomic analysis, 1 ml of derivatized solution was injected in splitless mode at 250°C into a LECO Pegasus BT 4D GCXGC/TOFMS instrument (Leco Corp., St. Josef, MI, USA) equipped with a LECO dual stage quad jet thermal modulator. High-purity helium (99.9999%) was used as a carrier gas.

Chromatograms were acquired in total ion current (TIC) mode, and we rejected those peaks with a signal-to-noise value lower than 500. Finally, the ChromaTOF software (ver. 5.51) was utilized for raw data processing, spectral assignments were achieved by matching the results with the NIST MS Search 2.3 library and implemented by FiehnLib. The alignment of chromatographic signals was performed by LECO ChromaTOF Statistical Compare® optimized for Pegasus® 4D.

II.4.2 Faecal Analysis

The faecal metabolomic profile was evaluated using comprehensive two-dimensional gas chromatography coupled with mass spectrometry (GC×GC-MS). Samples were treated with ethanol, dried, and derivatized with methoxyamine prior to analysis. An untargeted metabolomic approach was applied to identify key metabolites involved in host–microbiota interactions.

Required Materials

Faecal samples were self-collected by patients using a dedicated sterile container provided during clinical visits. Collection was carried out after informed consent was obtained, prior to the initiation of therapy (T0), and at follow-up intervals every 6 months or at the time of disease progression (T1), whichever occurred earlier.

II.5 Statistical analysis

Statistical analyses were performed using a range of methods tailored to the specific endpoints and data structures. Progression-free survival (PFS) was assessed through univariate and multivariate Cox proportional hazards models, as well as Kaplan–Meier survival curves. The Mann–Whitney U test was used to compare the distribution of lymphocyte subsets across groups defined by distinct clinical characteristics. For matched data (comparisons between baseline and T1 values) the Wilcoxon signed-rank test was applied. Logistic regression was employed to investigate associations with progressive disease (PD) as a binary outcome. Correlations between plasma and fecal metabolites and T cell subpopulations were evaluated using the Spearman rank correlation test. All analyses were conducted using RStudio (R version 4.4.3)

III. Results

III.1. Demographic and clinicopathological data

From March 11, 2024, to May 9, 2025, a total of 33 patients were enrolled in the study, including 21 males (64%) and 12 females (36%). The mean age at CRC diagnosis was 67 years (range: 37–84 years; median: 69 years), while the mean age at mCRC diagnosis was 69 years (range: 37–86 years; median: 69 years).
Regarding medical history, 4 patients (12%) were current smokers and 11 (33%) were former smokers. Body mass index (BMI) was calculated by dividing body weight (in kilograms) by the square of height (in meters). Based on the resulting values, each patient was classified into one of the World Health Organization (WHO) BMI categories: underweight (<18.5), normal weight (18.5–24.9), overweight (25–29.9), and obese (≥30). One patient (3.03%) was underweight, 13 patients (39%) had normal weight, 14 (42%) were overweight, and 5 (15%) were classified as obese. With regard to comorbidities, 8 patients (24%) had diabetes, and 12 patients (36%) had dyslipidemia and were undergoing statin therapy.

Characteristic	Value
Study period	March 11, 2024 – May 9, 2025
Total patients enrolled	33
Sex	21 males (64%)
	12 females (36%)
Mean age at CRC diagnosis	67 years (range: 37–84), median: 69
Mean age at mCRC diagnosis	69 years (range: 37–86), median: 69
Smoking status	4 current smokers (12%)
	11 former smokers (33%)
BMI classification (WHO)	
– Underweight (<18.5)	1 patient (3.03%)
– Normal weight (18.5–24.9)	13 patients (39%)
– Overweight (25–29.9)	14 patients (42%)
– Obese (≥30)	5 patients (15%)
Comorbidities	
– Diabetes	8 patients (24%)
– Dyslipidemia (on statins)	12 patients (36%)

Table 3 Demographic and clinicopathological data

At baseline, both fecal and plasma samples were collected from all 33 enrolled patients. Subsequent plasma samples were obtained either after 6 months in cases of sustained stable disease (SD), or at the time of PD or objective response. During the study period, 8 patients experienced PD; among them, 6 underwent a follow-up sampling, whereas 2 presented with rapid clinical progression and were not sampled. In total, 16 patients underwent restaging blood collection, with the following clinical outcomes: 3 partial responses (PR), 6 PD, and 7 SD.

III.2. Tumor-related clinical data

Regarding tumor-related clinical data, the primary tumor site was located in the right colon in 15 patients (45%), the left colon in 12 patients (37%), and the rectum in 6 patients (18%).

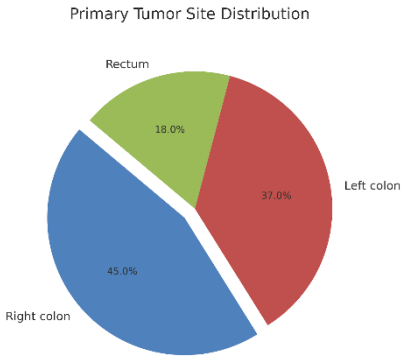

Figure 9. primary tumor site distribution

Based on the anatomical distribution of metastatic lesions, disease stage can be classified as stage IV A when a single metastatic site is involved, and stage IV B when multiple metastatic sites are affected. In cases of peritoneal involvement, the disease is categorized as stage IV C.

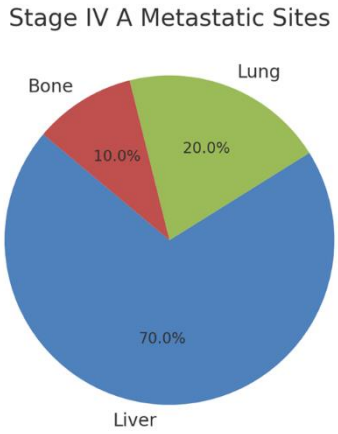

Figure 10. stage IVA metastatic site

All enrolled patients underwent first-line treatment for CRC: 11 patients (33%) received anti-EGFR therapy with or without chemotherapy, 15 (45%) received anti-VEGF combined with chemotherapy, 4 patients (12%) received immunotherapy, and 3 patients (9%) were treated with chemotherapy alone.

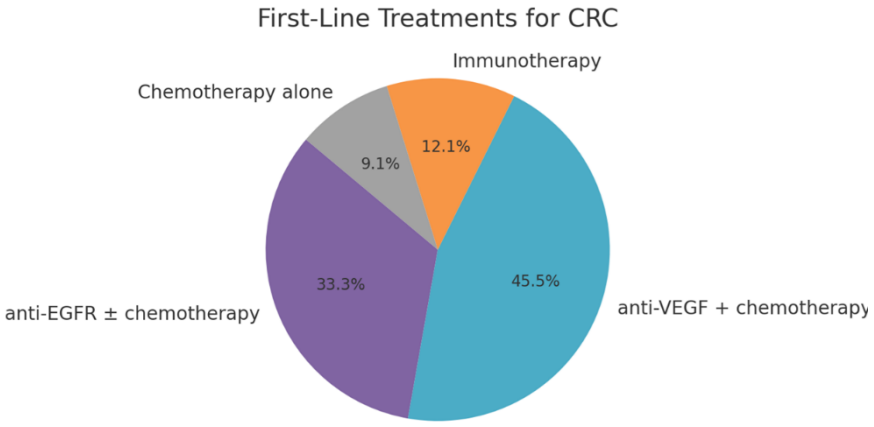

Figure 11. first line treatments

III.2.1 Molecular and mutational profiling data

As per clinical practice, all enrolled patients underwent mutational profiling by next-generation sequencing (NGS) performed on either primary tumor tissue or metastatic lesions. Among them, 17 patients (52%) were found to carry a KRAS mutation, including: 2 patients with the G12A variant (12%), 1 with G12C (6%), 8 with G12D (47%), 2 with mutations in exon 4 (12%), 1 with G12S (6%), 1 with G12V (6%), 1 with G13D (6%), and 1 with a Q61x mutation (6%).

In addition, 4 patients (12%) harbored the BRAF V600E mutation, while no NRAS mutations were detected.

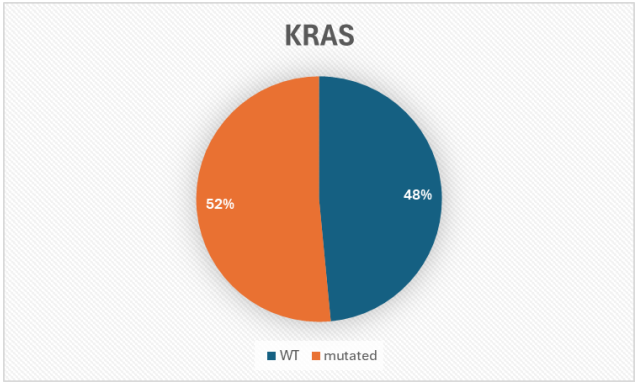

Figure 12. KRAS status

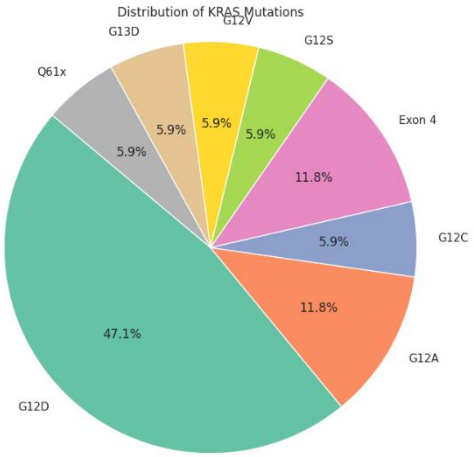

Figure 13. KRAS mutations

Beyond the canonical RAS/RAF genes, the molecular panel also identified additional alterations in other genes: 7 patients (21%) showed PIK3CA mutations, and 5 patients (15%) had mutations in TP53. Notably, 2 of these patients carried concomitant mutations in both PIK3CA and TP53.

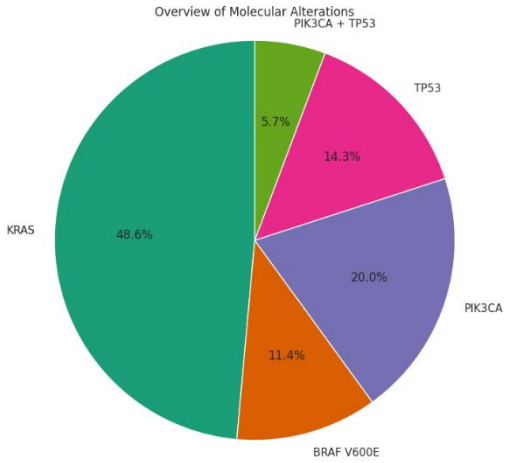

Figure 14. Molecular alterations

These findings underscore the molecular heterogeneity of colorectal cancer and reflect the mutational landscape typically observed in metastatic settings. The predominance of KRAS mutations, particularly the G12D variant, is consistent with previously reported data and is clinically significant, as such mutations confer resistance to anti-EGFR monoclonal antibodies and are associated with distinct biological behavior and outcomes. The detection of less common KRAS variants (e.g., G12A, G12C, Q61x) further highlights the need for precise molecular characterization, as emerging targeted therapies—such as KRAS G12C inhibitors—may offer novel treatment opportunities in selected patient subgroups.

The presence of BRAF V600E mutations in 12% of patients, a well-established negative prognostic marker, is also in line with literature data and may indicate an aggressive tumor phenotype with a poor response to conventional chemotherapy. The absence of NRAS mutations in this cohort may reflect either the relatively lower frequency of such alterations or possible selection bias.

Mutations in PIK3CA and TP53, both of which were observed in a significant proportion of patients, represent additional layers of complexity. PIK3CA mutations are implicated in the activation of the PI3K-AKT pathway and may be associated with resistance mechanisms and potential sensitivity to pathway-specific inhibitors. Conversely, TP53 mutations are frequently associated with genomic instability and tumor progression. The coexistence of PIK3CA and TP53 mutations in a subset of patients may reflect a particularly aggressive molecular phenotype, warranting further investigation.

As part of standard clinical practice, microsatellite status was assessed in all patients, revealing MSI-H in 4 cases (12%), all of whom received immunotherapy. Notably, the prevalence of MSI-H in our cohort is higher than typically reported in the literature (~4%), suggesting a potential selection bias or cohort-specific characteristics. Among the MSI-H patients, two also harbored concomitant BRAF mutations. None of the MSI-H cases were associated with a diagnosis of Lynch syndrome.

Overall, these data reinforce the clinical utility of comprehensive genomic profiling, not only for guiding targeted therapy decisions but also for stratifying patients based on molecular risk and potential therapeutic vulnerabilities.

III.2.2 Response and Survival Data

PFS was calculated as the time interval between the date of enrollment/baseline (start of treatment) and the date of PD, death, or last available follow-up. The mean PFS observed in the analyzed cohort (n = 32) was 6.9 months, with a range spanning from 0.1 to 14 months.

Regarding treatment response:

- 8 patients (25%) experienced PD,
- 3 patients (9.4%) achieved PR,
- 13 patients (40.6%) showed SD,
- 8 patients (25%) had not yet undergone restaging at the time of analysis.

III.3 Analysis of T cell subpopulations

In this study, peripheral blood samples were analyzed from mCRC patients at three different time points: baseline (T0, *n*=32), re-evaluation (T1, *n*=14; including 12 non-progressors [NON-PD] and 2 progressors [PD]), and PD after first revaluation (T2, *n*=3). T cell subpopulations were characterized based on the expression of surface markers, with particular focus on the CD28 molecule and co-inhibitory receptors associated with T cell exhaustion and senescence. Functional T cells were identified as ($CD3^+/CD4^+/CD8^+$)$CD28^+$, while dysfunctional T cells lacked CD28 expression ($CD3^+/CD4^+/CD8^+$)$CD28^-$. Exhausted T cells were defined by the co-expression of CD28, LAG-3, PD-1, and TIGIT ($CD28^+LAG\text{-}3^+PD\text{-}1^+TIGIT^+$), whereas a less differentiated exhausted-like phenotype was marked by the expression of CD28, PD-1, and TIGIT without LAG-3 ($CD28^+PD\text{-}1^+TIGIT^+$). Transitional phenotypes were also observed, including cells expressing either LAG-3 or

TIGIT alongside CD28 ($CD28^+LAG\text{-}3^+/TIGIT^+$), which may represent an intermediate state towards exhaustion. In addition, senescent T cells were identified as $CD28^-CD57^+KLRG1^+$, with a potential pre-senescent subset characterized by the expression of CD57 alone in the absence of CD28 ($CD28^-CD57^+$). This phenotypic stratification provides insight into the dynamic alterations of T cell functionality during disease progression and treatment response in CRC patients.

Relationship with PFS

Univariate Cox Model

Immune_population	n	n_event	HR	Lower_HR	Upper_HR	p-value
CD3+CD28- (on CD3+)	32	9	1.05	1.01	1.10	0.013
CD3+CD28-CD57+ (on CD3+)	32	9	1.08	1.01	1.15	0.018
CD8+CD28+LAG3+ (on CD3+)	32	9	663097.76	8.76	50198277810.63	0.019
CD4+CD28+ (on CD3+)	32	9	0.96	0.92	1.00	0.067
CD3+CD28+LAG3+ (on CD3+)	32	9	26.30	0.72	957.86	0.075

Figure 15. Results of univariate Cox model analysis

A univariate Cox model was applied to assess the relationship between PFS and the frequency of specific T cell subpopulations in CRC patients (Figure 15). The analysis demonstrated that an increased proportion of $CD3^+CD28^-$ T cells, representing a dysfunctional phenotype, was significantly associated with a higher risk of disease progression. Similarly, elevated levels of $CD3^+CD28^-CD57^+$ cells, indicative of a pre-senescent state, and $CD8^+CD28^+LAG3^+$ cells, suggestive of a transitional phenotype toward exhaustion, were also significantly correlated with shorter PFS. These findings align with existing literature, where co-expression of LAG-3 and other inhibitory receptors on T cells has been linked to T cell dysfunction and poor clinical outcomes in chronic infections and cancer [133, 134]. Such cells are characterized by impaired proliferative capacity and reduced cytokine production, leading to an ineffective antitumor response. In contrast, the non-significant but consistent trend toward improved PFS in patients with higher frequencies of $CD4^+CD28^+$ cells may reflect the preservation of a more functional helper T cell compartment, capable of supporting effective immune responses and sustaining cytotoxic activity. These findings suggest that the phenotypic diversity of T cells may hold prognostic value in CRC, providing insights into immune competence and exhaustion states at the initiation of treatment, and underlining the importance of T cell functionality in predicting disease progression.

Multivariate Cox Model

Variabile	HR	Lower_HR	Upper_HR	P_value
CD3+CD28- (on CD3+)	1.06	1.01	1.12	0.033
ETA' DIAGNOSI(≤65 vs >65)	0.92	0.07	12.03	0.949
STADIO Iva	0.00	0.00	Inf	0.999
TERAPIA	0.65	0.19	2.25	0.494
STATINE	1.26	0.18	9.00	0.821
BRAF(WT vs MUT)	7.24	0.34	153.11	0.203

Variabile	HR	Lower_HR	Upper_HR	P_value
CD3+CD28-CD57+	1.09	1.01	1.19	0.042
ETA' DIAGNOSI(≤65 vs >65)	1.00	0.10	10.58	0.997
STADIO Iva	0.00	0.00	Inf	0.999
TERAPIA	0.81	0.21	3.09	0.761
STATINE	1.05	0.18	6.21	0.957
BRAF(WT vs MUT)	7.14	0.29	173.64	0.227

Variabile	HR	Lower_HR	Upper_HR	P_value
CD8+CD28+LAG3+	84806300792.67	410.22	2E+19	0.01
ETA' DIAGNOSI(≤65 vs >65)	39.89	1.23	1297.58	0.04
STADIO Iva	0.00	0.00	Inf	1.00
TERAPIA	0.35	0.09	1.39	0.13
STATINE	0.04	0.00	0.97	0.05
BRAF(WT vs MUT)	1.76	0.15	21.05	0.66

Figure 16. Results of multivariate Cox model analysis

The previously observed results remained statistically significant after adjustment for potential confounders, including age at diagnosis, tumor stage, first-line therapy, statin use, and BRAF mutational status in a multivariate Cox proportional hazards regression analysis (Figure 16). Notably, age >65 years was independently associated with a markedly increased risk of the event (Hazard Ratio [HR] = 39.89, p = 0.04). A significantly association was also observed for the frequency of $CD8^{+}CD28^{+}LAG3^{+}$ T cells—a subpopulation expressing the inhibitory receptor LAG-3, suggestive of a shift toward an exhausted phenotype — (HR = 8.5×10^{10}, p = 0.01). Interestingly, statin treatment was associated with a potentially protective effect (HR = 0.04, p = 0.05). This observation aligns with growing evidence supporting the immunomodulatory and antitumor properties of statins. Two recent meta-analyses encompassing over a million patients and multiple cancer types, including CRC, have demonstrated a consistent association between statin use and reduced all-cause mortality, cancer-specific mortality, and improved progression-free survival, relapse-free survival, and disease-free survival. Proposed mechanisms include the inhibition of the mevalonate pathway, suppression of tumor cell proliferation, induction of apoptosis, and enhancement of antitumor immune responses [135]. Specifically in CRC, statins have been shown to inhibit key oncogenic drivers such as MACC1, downregulate pro-survival pathways (e.g., IGF-1/ERK), and reduce post-colonoscopy CRC incidence. These findings support a potential role for statins in modulating immune senescence and tumor progression, underscoring the need for prospective studies to evaluate statin effects in defined molecular and immunological CRC subtypes [136].

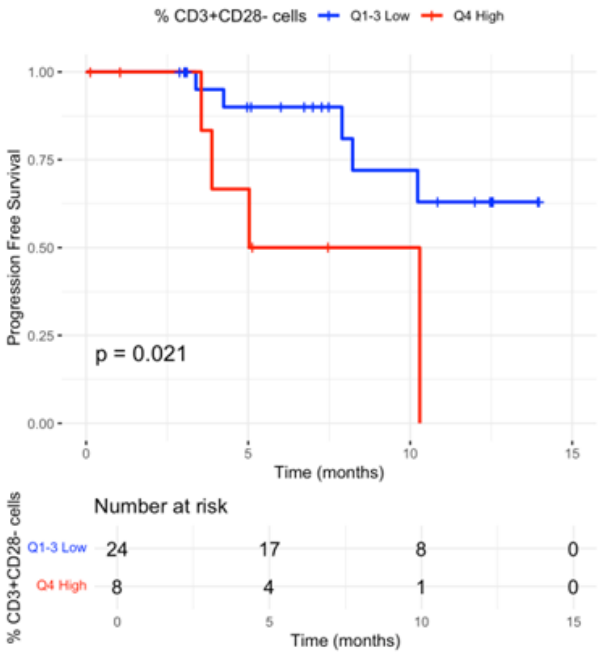

Figure 17 Kaplan Meier Curves;: PFS and dysfunctional T cells

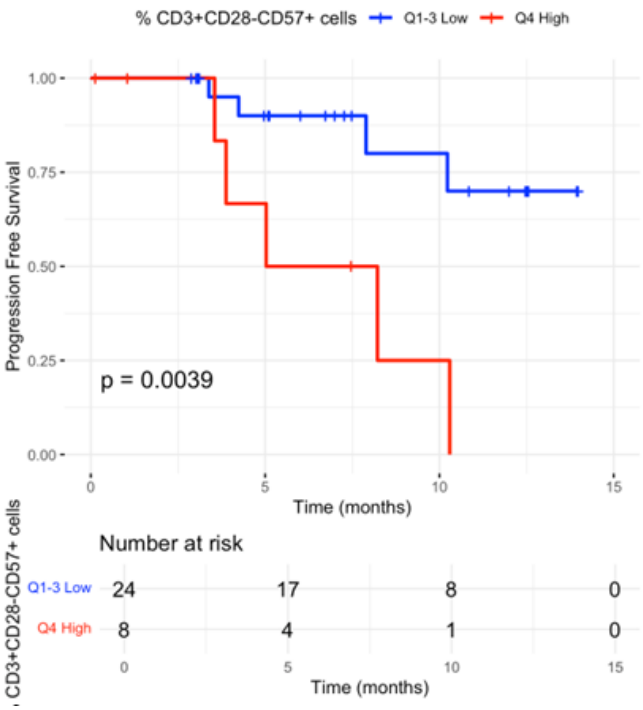

Figure 18 Kaplan Meier Curves: PFS and T cells with a potential pre-senescent subset

Kaplan–Meier survival analyses further substantiated the prognostic relevance of immunosenescent T cell subpopulations in CRC patients. As shown in Figure 17, patients were stratified according to the frequency of $CD3^{+}CD28^{-}$ T cells, a subset indicative of T cell dysfunction and senescence. Patients in the highest quartile (Q4) exhibited significantly shorter PFS compared to those in the lower three quartiles (Q1–Q3) ($p = 0.021$). This suggests that an elevated proportion of $CD3^{+}CD28^{-}$ cells may impair effective immune surveillance, thereby accelerating disease progression. In Figure 18, Kaplan–Meier curve presents survival data based on $CD3^{+}CD28^{-}CD57^{+}$ T cell frequency, a subset representing a more advanced stage of senescence. The separation between the curves was even more pronounced ($p = 0.0039$) and statistically significant, with patients in the Q4 group showing markedly poorer PFS. This finding supports the hypothesis that progressive T cell senescence — characterized by both loss of costimulatory signaling ($CD28^{-}$) and acquisition of terminal differentiation markers ($CD57^{+}$) — correlates with worse clinical outcomes in CRC. In both cases, the number-at-risk tables confirm an early and sharp drop in survival probability for patients in the high-frequency groups, reinforcing the clinical significance of these phenotypic markers. Taken together, these data demonstrate that the accumulation of senescent T cells at baseline serves as a negative prognostic factor and may reflect an underlying state of immune exhaustion that compromises the efficacy of the host antitumor response.

Relationship with tumor characteristics and stadiation

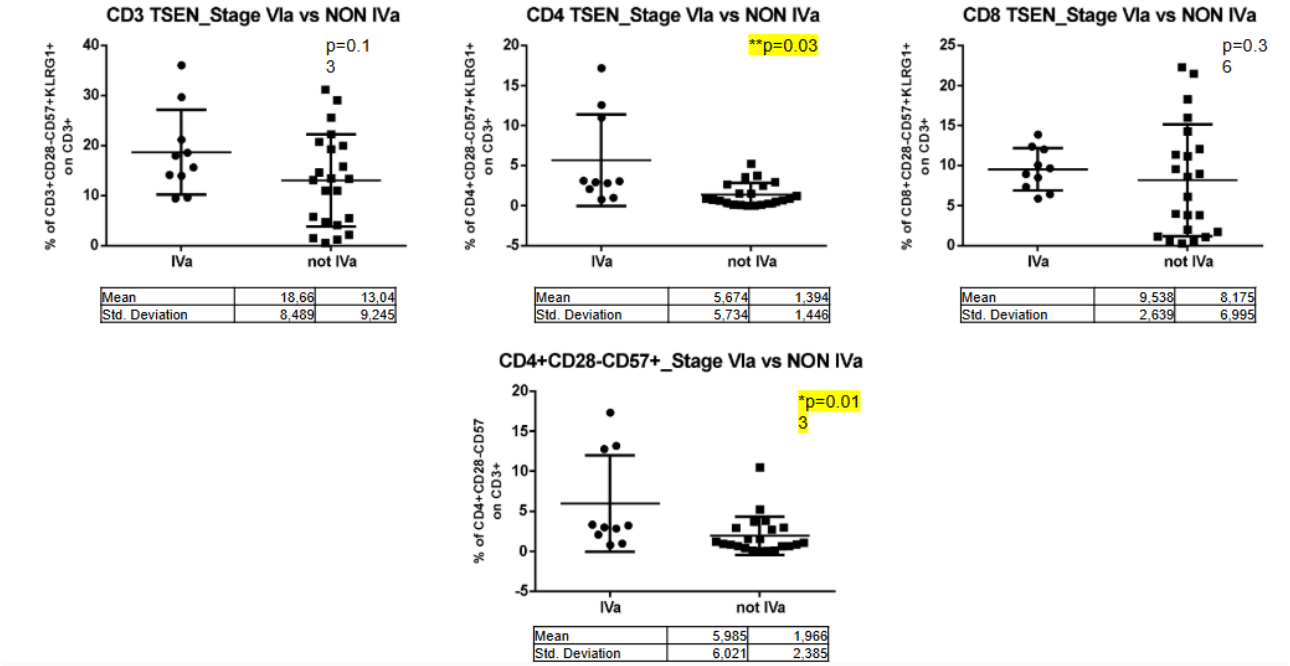

Figure 19 Dot Plots – Baseline T Senescent Cells: Stage IVa vs Non-IVa

Among the 32 analyzed patients, 10 (31%) presented with stage IV A disease: 7 with hepatic metastases, 2 with pulmonary metastases, and 1 with a solitary bone lesion. To investigate whether the distribution of T cell senescence and activation phenotypes differs by metastatic burden at baseline (T0), we compared immune cell subpopulations between patients with stage IVa CRC, defined by a single metastatic site, and those with more advanced disease (non-IVa: multiple metastatic sites or peritoneal involvement). As shown in Figure 19 at baseline, a trend towards higher frequencies of total $CD3^+$ TSEN cells ($CD3^+CD28^-CD57^+KLRG1^+$) was observed in IVa patients compared to non-IVa, though the difference did not reach statistical significance (mean 18.66% vs 13.04%, p=0.103). Notably, a significant increase in $CD4^+$ TSEN cells ($CD4^+CD28^-CD57^+KLRG1^+$) was detected in IVa patients (mean 5.67%) compared to non-IVa (mean 1.39%, p=0.030), suggesting a selective enrichment of senescent $CD4^+$ T cells in patients with limited metastatic dissemination. Similarly, a higher proportion of $CD4^+CD28^-CD57^+$ T cells was observed in the IVa group (mean 5.98%) relative to non-IVa patients (mean 1.97%, p=0.013), indicating potential differences in the early stages of T cell senescence. In contrast, no significant differences were identified in the $CD8^+$ TSEN compartment (mean 9.54% vs 8.18%, p=0.306), suggesting that $CD4^+$ rather than $CD8^+$ T cell senescence may be more closely associated with a lower metastatic burden at therapy initiation.

Although T cell senescence is frequently associated with immune dysfunction, the enrichment of $CD4^+$ TSEN cells in patients with stage IVa disease may reflect a more regulated or functionally effective immune landscape in individuals with limited metastatic spread. This could indicate the presence of a senescent subset retaining immunomodulatory or residual effector capacity, potentially

contributing to immune surveillance. These findings align with recent evidence suggesting that T cell senescence, particularly in the CD4⁺ compartment, may not uniformly signify dysfunction, but rather reflect prior immune engagement and tumor control in certain oncological contexts [137, 138, 139, 140].

These findings highlight distinct immunosenescence profiles according to metastatic extent at baseline and warrant further investigation into their potential prognostic or predictive value.

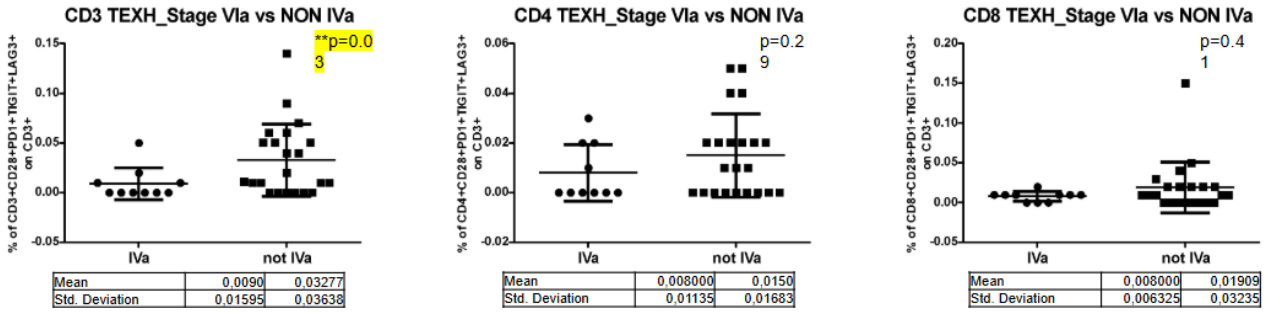

Figure 20 Dot Plots – Baseline T Exhausted Cells: Stage IVa vs Non-IVa

In contrast to the distribution of senescent T cells, we observed a significantly higher proportion of exhausted T cells (CD3⁺PD-1⁺TIM-3⁺) in patients with more advanced metastatic disease (non-IVa stage). This increase in global T cell exhaustion was accompanied by similar, albeit non-statistically significant, trends within both the CD4⁺ and CD8⁺ compartments (Figure 20). These findings are consistent with the well-established association between T cell exhaustion and chronic antigen exposure, often observed in patients with higher tumor burden and prolonged immunological engagement. Exhausted T cells are characterized by impaired effector functions and sustained expression of inhibitory receptors such as PD-1 and TIM-3, which reflect a dysfunctional immune state unable to mount effective anti-tumor responses [141].

The enrichment of exhausted T cells in non-IVa patients may therefore represent a consequence of immune overstimulation in the setting of systemic tumor dissemination, where persistent antigenic stimulation promotes progressive functional decline. This is in line with previous findings in metastatic CRC and other solid tumors, in which high levels of exhausted T cells have been associated with poor prognosis and reduced responsiveness to immunotherapy [134]. Importantly, the parallel enrichment of senescent T cells in patients with limited metastatic spread (IVa) and exhausted T cells in patients with more extensive disease suggests that distinct dysfunctional T cell phenotypes dominate different stages of tumor progression. This dichotomy may reflect differing immune regulatory dynamics at baseline, with potential implications for treatment response and immunotherapeutic targeting.

Immune_population	mediana_W	sd_W	mediana_M	sd_M	P_value
CD4+CD28- (on CD3+)	3.82	6.76	0.82	1.53	0.029
CD3+CD28+ (on CD3+)	75.82	14.76	90.30	10.46	0.034
CD3+CD28- (on CD3+)	23.90	16.95	9.63	10.52	0.040
CD8+CD28-CD57+KLRG1+ (on CD3+)	9.28	5.97	2.95	3.44	0.054
CD8+CD28- (on CD3+)	14.02	7.14	5.27	5.90	0.056

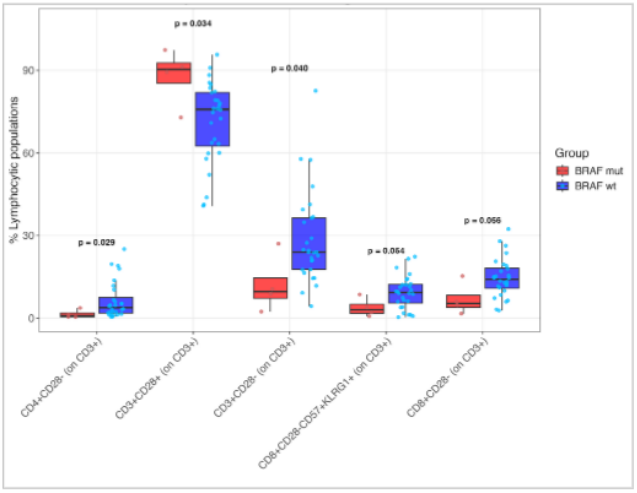

Figure 21 Mann-Withney test– Baseline T Cell subpopulation: BRAF wild type vs mutated

BRAF V600E mutations were identified in 4 patients (12% of the cohort), in line with reported frequencies in mCRC and known to be associated with poor prognosis and resistance to conventional chemotherapy [142]. Figure 21 presents the distribution of various lymphocytic populations at baseline in BRAF-mutated versus BRAF wild-type mCRC patients, as assessed by the Mann–Whitney U test. Notably, the proportion of senescent $CD8^+$ T cells ($CD28^-CD57^+KLRG1^+$) within the $CD3^+$ compartment was higher in the BRAF wild-type group (mean ± SD: 9.29 ± 5.97%) compared to the BRAF-mutated group (3.77 ± 3.44%), with a p-value of 0.054, indicating a trend towards significance. In addition to senescent T cells, several other T cell subpopulations showed statistically significant differences between the two molecular subgroups. Specifically, BRAF-mutated patients exhibited significantly higher frequencies of $CD4^+CD28^+$ and $CD3^+CD28^+$ cells ($p = 0.029$ and $p = 0.034$, respectively), while BRAF wild-type patients displayed an increased percentage of $CD3^+CD28^-$ cells ($p = 0.040$), further suggesting differential T cell activation and exhaustion states associated with BRAF mutational status. Trends were also observed in $CD8^+CD28^+$ and $CD8^+CD28^-$ subsets ($p = 0.054$ and $p = 0.056$, respectively), though these did not reach conventional levels of significance. Collectively, these findings highlight immunophenotypic distinctions between BRAF wild-type and BRAF-mutated tumors at baseline, potentially reflecting divergent immune regulatory mechanisms driven by oncogenic BRAF signaling. The observed differences in T cell subset composition may contribute to the immune evasion phenotype and differential treatment responses associated with BRAF mutations in mCRC.

Recent studies have shown that BRAF-mutated tumors tend to exhibit a more immunosuppressive tumor microenvironment, characterized by reduced infiltration of effector T cells and increased immune regulatory factors [144]. Additionally, oncogenic BRAF signaling has been implicated in promoting T cell dysfunction and immune evasion [143]. The lower frequency of senescent $CD8^+$ T cells in BRAF-mutant patients may reflect diminished immune activation or altered senescence dynamics in this molecular subtype. These findings support the hypothesis that BRAF mutations are associated with distinct immune profiles and may influence the prognostic and therapeutic landscape in mCRC.

Immune_population	mediana_W	sd_W	mediana_M	sd_M	W_statistic	P_value
CD4+CD28+ (on CD3+)	63.70	13.14	52.40	15.64	199.00	0.007
CD4+CD28+TIGIT+ (on CD3+)	3.46	2.67	1.75	0.95	194.00	0.011
CD3+CD28+ (on CD3+)	79.20	11.80	65.00	15.09	193.00	0.013
CD4+ cells (on CD3+)	67.80	9.42	59.70	11.19	190.00	0.018
CD3+CD28- (on CD3+)	20.80	11.79	24.80	18.52	68.00	0.024
diff_CD4CD28eCD3CD57	47.60	22.53	36.36	26.39	187.00	0.024
CD4+CD28+PD-1+TIGIT+ (on CD3+)	0.44	1.22	0.18	0.18	177.00	0.064

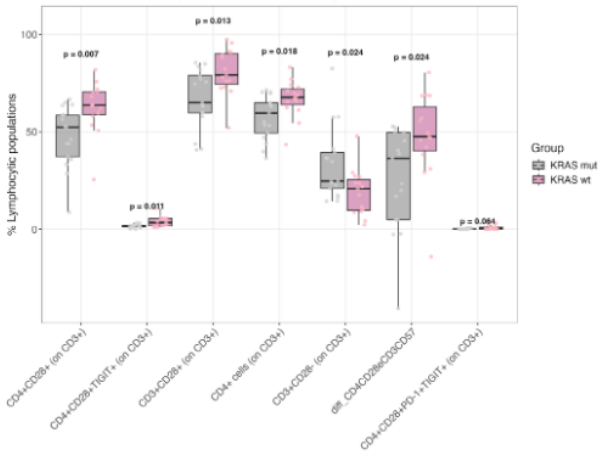

Figure 22 Mann-Withney test– Baseline T Cell subpopulation: KRAS wild type vs mutated

To further explore the immunological landscape associated with oncogenic drivers in mCRC, we performed a Mann–Whitney U test to compare baseline lymphocytic populations between KRAS-mutated and KRAS wild-type patients. As illustrated in Figure 22, several immune subpopulations demonstrated statistically significant differences between the two molecular groups. Specifically, KRAS wild-type patients showed significantly higher frequencies of $CD4^+CD28^+$ T cells (median: 63.70% vs. 52.40%, p = 0.007), $CD3^+CD28^+$ cells (79.20% vs. 65.00%, p = 0.007), and total $CD4^+$ T cells within the $CD3^+$ compartment (67.80% vs. 59.70%, p = 0.018), suggesting a more activated or functionally intact helper T cell profile in the KRAS wt cohort. Conversely, KRAS-mutated patients exhibited a higher proportion of $CD3^+CD28^-$ T cells (24.80% vs. 20.80%, p = 0.024), a phenotype commonly associated with T cell senescence or functional exhaustion. A trend toward reduced frequency of $CD4^+CD28^+PD\text{-}1^+TIGIT^+$ T cells was also observed in KRAS mut patients (0.18% vs. 0.44%, p = 0.064), suggesting subtle alterations in the composition of checkpoint-expressing subsets.

These findings align with emerging evidence that KRAS mutations can reshape the tumor immune microenvironment by modulating cytokine signaling, reducing antigen presentation, and impairing T cell recruitment or persistence. In particular, oncogenic KRAS signaling has been shown to suppress IFN-γ responses and enhance immunosuppressive networks, contributing to immune evasion and resistance to immune checkpoint inhibitors [151, 152]. The relative depletion of $CD28^+$ T cell subsets in KRAS-mutated tumors may reflect premature T cell aging or a chronically suppressed immune milieu, which may hold implications for therapeutic stratification.

Together, these data underscore distinct immunophenotypic profiles associated with KRAS mutational status, providing further evidence that oncogenic pathways can influence the functional composition of peripheral immune cells in mCRC.

Immune_population	mediana_S	sd_S	mediana_I	sd_I	W_statistic	P_value
CD4+CD28+PD-1+ (on CD3+)	1.97	3.75	0.20	0.65	86.00	0.094

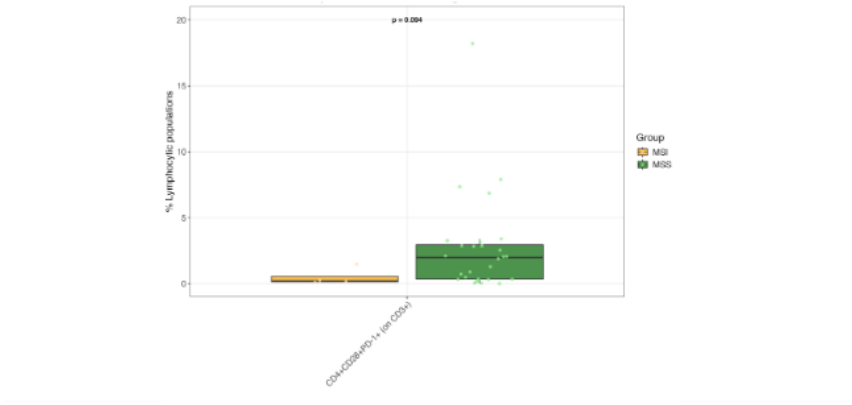

Figure 23 Mann-Withney test– Baseline T Cell subpopulation: MSS vs MSI

To investigate immunological differences associated with microsatellite status in mCRC, we evaluated the baseline frequency of $CD4^+CD28^+PD\text{-}1^+$ T cells (within $CD3^+$ lymphocytes) in patients with microsatellite instability (MSI) versus those with microsatellite stable (MSS) tumors. As depicted in Figure 23, MSI patients exhibited a higher median frequency of $CD4^+CD28^+PD\text{-}1^+$ T cells compared to MSS counterparts (1.97% vs. 0.20%), although the difference did not reach statistical significance ($p = 0.094$). Despite this borderline result, the observed trend is biologically relevant and aligns with established literature describing enhanced immune activation in MSI tumors. MSI is a well-recognized biomarker for favorable prognosis and heightened response to immune checkpoint inhibitors in colorectal cancer, attributed to the high mutational burden and resultant neoantigen load that enhances immunogenicity. The enrichment of $PD\text{-}1^+$ cells in the MSI cohort suggests a greater degree of T cell activation and checkpoint engagement, consistent with the immunologically "hot" tumor phenotype described in MSI-high CRC [153, 154]. Conversely, the markedly lower presence of $PD\text{-}1^+$ T cells in MSS patients may reflect a more immunologically inert or "cold" microenvironment, contributing to their known resistance to immunotherapy and reliance on chemotherapy.

Although statistical significance was not achieved in this comparison, the numerical trend supports the hypothesis that MSI status is associated with a distinct immunophenotype characterized by increased activation and checkpoint receptor expression. This reinforces the notion that microsatellite instability not only affects genomic integrity but also shapes systemic immune dynamics, with important implications for therapeutic stratification and response prediction in mCRC.

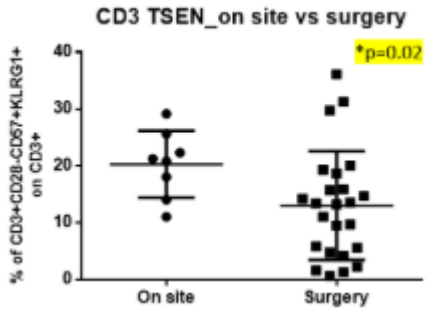

Figure 24 Dot Plot – Baseline T Senescent Cells: operated vs on site primary tumor

We analyzed the frequency of circulating senescent $CD3^{+}CD28^{-}CD57^{+}KLRG1^{+}$ T cells in the peripheral blood of patients with primary colorectal cancer, comparing individuals with a non-resected primary tumor ("On site") to those who had undergone surgical resection ("Surgery"). As illustrated in Figure 24, the percentage of senescent $CD3^{+}$ T cells was significantly lower in the surgery group compared to patients with an unresected primary tumor ($p = 0.02$). No significant differences were observed within the $CD4^{+}$ or $CD8^{+}$ senescent subsets (data not shown).

This reduction in circulating senescent T cells following tumor resection may reflect a state of diminished chronic immune stimulation. In patients with tumor on site, the persistent presence of the primary lesion may sustain peripheral immune activation, thereby delaying T cell senescence. In contrast, surgical removal of the tumor might interrupt this stimulatory loop, potentially resulting in a shift toward immune quiescence or remodeling of the systemic T cell pool.

These observations are in line with previous studies suggesting that tumor-associated antigenic exposure contributes to maintaining peripheral immune activation and may partially counteract immunosenescence [145, 146]. The decline in senescent T cells post-surgery might indicate a reconfiguration of immune homeostasis; however, whether this shift enhances or impairs immune competence remains to be elucidated. Importantly, these findings underscore the potential utility of circulating senescent T cells as dynamic biomarkers of immune status and disease trajectory in colorectal cancer patients.

Relationship with response

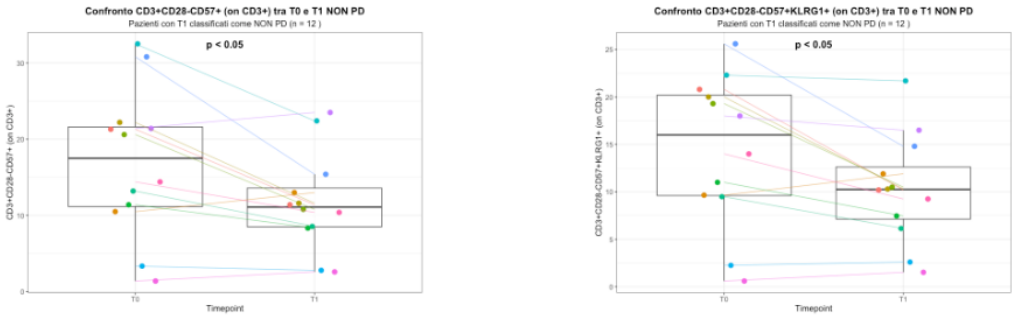

Variabile	n_campioni	T0_median	T1_median	p_value
CD3+CD28-CD57+ (on CD3+)	12	17.50	11.10	0.016
CD3+CD28-CD57+KLRG1+ (on CD3+)	12	16.00	10.25	0.016

Figure 25 Wilcoxon test: CD3+ Tsen T0 vs T1 in responsive group

We assessed the longitudinal changes in circulating senescent T cell subsets between baseline (T0) and the first radiological evaluation (T1) in 12 patients with mCRC who exhibited either disease stability or response at T1 (classified as NON PD). All patients received first-line systemic therapy between T0 and T1. As shown in Figure 25, using the Wilcoxon signed-rank test, a significant reduction was observed in the percentage of $CD3^{+}CD28^{-}CD57^{+}$ T cells ($p < 0.05$) and $CD3^{+}CD28^{-}CD57^{+}KLRG1^{+}$ T cells ($p < 0.05$) from T0 to T1. This decline in senescent T cell populations suggests a therapy-associated remodeling of the immune landscape, potentially reflecting reduced chronic antigenic stimulation and improved immunological fitness in patients achieving disease control. These findings support the relevance of senescent T cell dynamics as a peripheral biomarker of early treatment response in mCRC.

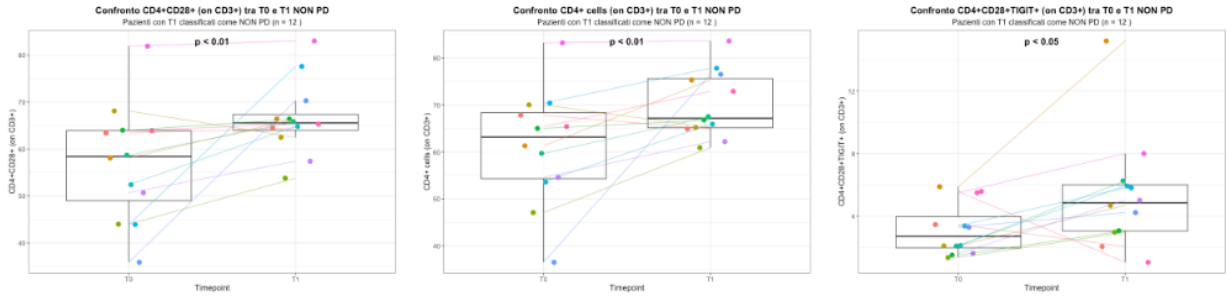

Variabile	n_campioni	T0_median	T1_median	p_value
CD4+CD28+ (on CD3+)	12	58.40	65.55	0.005
CD4+ cells (on CD3+)	12	63.15	67.15	0.009
CD4+CD28+TIGIT+ (on CD3+)	12	2.71	4.85	0.042

Figure 26 Wilcoxon test: CD4+ T cells T0 vs T1 in responsive group

In addition to the senescent T cell subsets previously described, we investigated further phenotypic alterations within the $CD4^{+}$ T cell compartment in the same cohort of 12 mCRC patients classified as

NON PD at T1, as illustrated in Figure 26. Paired analysis of peripheral blood samples collected at T0 and T1 revealed significant immunological shifts. Specifically, we observed a statistically significant increase in the percentage of $CD4^+CD28^+$ T cells (within $CD3^+$) from T0 to T1 ($p < 0.01$), suggesting a therapy-associated expansion of functionally competent $CD4^+$ T cells. This is paralleled by a concomitant rise in total $CD4^+$ T cells (within $CD3^+$; $p < 0.01$), which may reflect either a recovery from treatment-induced lymphopenia or a restoration of homeostatic T cell dynamics, in line with prior evidence linking $CD4^+$ T cell recovery to favorable immunological responses in cancer patients undergoing systemic therapies [147, 148].

Moreover, we detected a significant increase in the frequency of $CD4^+CD28^+TIGIT^+$ T cells (within $CD3^+$) at T1 compared to baseline ($p < 0.05$). The co-expression of TIGIT—a co-inhibitory receptor implicated in immune regulation—may denote a complex phenotype characterized by partial dysfunction but potentially retained suppressive or regulatory capacity. The expansion of this subset might reflect an adaptive response to therapy-induced immune activation, functioning to limit excessive inflammation or autoimmunity. These results underscore the heterogeneity of treatment-related T cell remodeling and highlight the importance of profiling discrete immune subpopulations to uncover immunological correlates of clinical benefit. Collectively, the observed shifts suggest not only a quantitative but also a qualitative remodeling of the $CD4^+$ T cell landscape, supporting the use of peripheral T cell dynamics as early biomarkers of therapeutic efficacy in mCRC.

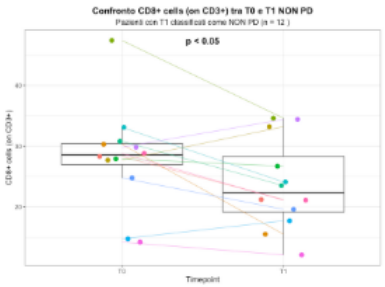

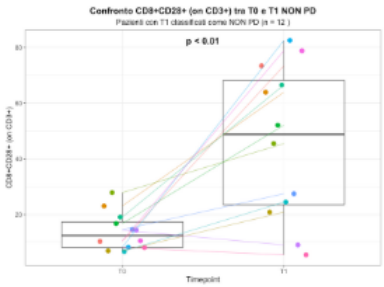

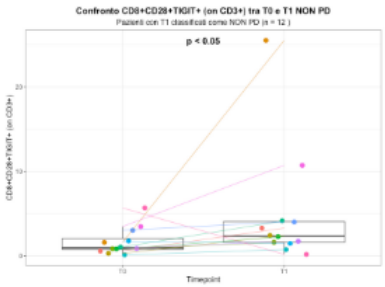

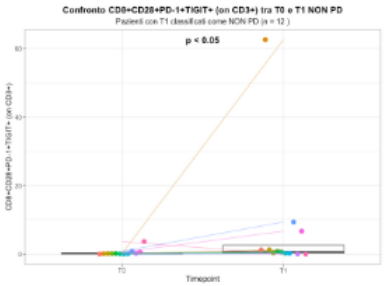

Variabile	n_campioni	T0_median	T1_median	p_value
CD8+CD28+ (on CD3+)	12	12.53	48.80	0.002
CD8+CD28+PD-1+TIGIT+ (on CD3+)	12	0.16	0.71	0.027
CD8+CD28+TIGIT+ (on CD3+)	12	0.94	2.34	0.027
CD8+ cells (on CD3+)	12	28.55	22.35	0.042

Figure 27 Wilcoxon test: CD8+ Tcell T0 vs T1 in responsive group

In parallel with the alterations observed in the $CD4^+$ T cell compartment, we analyzed the dynamics of circulating $CD8^+$ T cell subsets between T0 and T1 in the same cohort of 12 mCRC patients who achieved disease control (NON PD). The paired Wilcoxon signed-rank test revealed a statistically significant increase in the frequency of $CD8^+CD28^+$ T cells (within $CD3^+$) from a median of 12.53% at T0 to 48.80% at T1 ($p = 0.002$), indicating a robust expansion of functionally competent $CD8^+$ T cells following systemic therapy (Figure 27). CD28 expression on $CD8^+$ T cells is essential for

antigen-induced proliferation and survival; its upregulation post-treatment may reflect an immune reinvigoration consistent with reduced chronic stimulation and enhanced effector potential, in line with prior reports linking $CD28^+CD8^+$ T cell recovery to improved clinical outcomes in cancer patients undergoing immunotherapy or chemotherapy [148, 147].

In addition, a significant increase in $CD8^+CD28^+PD\text{-}1^+TIGIT^+$ T cells (median T0: 0.16%; T1: 0.71%; $p = 0.027$) and in $CD8^+CD28^+TIGIT^+$ T cells (median T0: 0.94%; T1: 2.34%; $p = 0.027$) was observed. These subsets, although expressing the co-inhibitory receptor TIGIT—and in one case, PD-1—may represent either a transiently exhausted phenotype amenable to functional rescue or a regulatory subset expanded in response to immune activation [149]. Their expansion, concurrent with the rise in $CD28^+CD8^+$ T cells, suggests the coexistence of effector and modulatory responses during early treatment phases. Interestingly, the total frequency of $CD8^+$ T cells (within $CD3^+$) decreased significantly from T0 to T1 (median T0: 28.55%; T1: 22.35%; $p = 0.042$). This reduction may represent a therapy-induced redistribution of cytotoxic lymphocytes to the tumor microenvironment or a selective contraction of senescent or bystander $CD8^+$ subsets, as previously reported in settings of effective anticancer immune responses [150]. Taken together, these results reveal a complex and coordinated remodeling of the $CD8^+$ T cell compartment, characterized by effector expansion, emergence of checkpoint-expressing subsets, and overall lymphocyte redistribution, supporting the potential of $CD8^+$ T cell dynamics as early immune correlates of clinical benefit in mCRC balance cytotoxicity and self-regulation.

Variabile	Coefficiente	OR	IC_2.5	IC_97.5	P_value
CD3+CD28-CD57+ (on CD3+)	**0.09**	**1.09**	**1.01**	**1.21**	**0.046**
CD3+CD28+LAG3+ (on CD3+)	4.37	78.72	0.96	23191.55	0.079

Figure 28 Logistic regression analysis (PD vs non PD)

As illustrated in Figure 28, logistic regression analysis was employed to further explore the association between specific peripheral T cell subpopulations and clinical response outcomes, providing an independent validation of the trends observed in our earlier analyses. Notably, a statistically significant association was identified between increased frequencies of peripheral $CD3^+CD28^-CD57^+$ T lymphocytes and a higher probability of experiencing PD ($p < 0.05$), thereby reinforcing the findings from our longitudinal and comparative analyses, which had previously highlighted the enrichment of this senescent subset in patients with poor clinical outcomes. Moreover, a trend toward increased likelihood of PD was also observed in patients with elevated levels of $CD3^+CD28^+LAG3^+$ cells, although this did not reach statistical significance. This further supports our earlier observations suggesting a possible role for checkpoint-expressing dysfunctional T cells in limiting effective antitumor responses. Overall, the logistic regression data corroborate the prognostic relevance of specific senescent and inhibitory T cell phenotypes, underscoring their potential utility as peripheral biomarkers of immune dysfunction and adverse clinical trajectories in mCRC.

Immune_population	ID_patinets	T0	T1	T2
CD3+CD28-CD57+ (on CD3+)	CRC03	22.20	11.60	35.10
	CRC11	32.50	22.40	61.20
	CRC15	30.80	15.40	9.24
CD3+CD28-CD57+KLRG1+ (on CD3+)	CRC03	20.00	10.30	31.40
	CRC11	22.30	21.70	16.90
	CRC15	25.60	14.80	8.00
CD4+ cells (on CD3+)	CRC03	70.00	65.20	57.10
	CRC11	53.60	65.90	18.90
	CRC15	36.52	76.50	76.70
CD4+CD28+ (on CD3+)	CRC03	68.10	62.50	52.70
	CRC11	52.40	64.80	18.10
	CRC15	35.89	70.30	76.20
CD4+CD28+TIGIT+ (on CD3+)	CRC03	2.10	4.68	5.13
	CRC11	2.12	5.93	1.25
	CRC15	3.29	4.23	3.08
CD8+ cells (on CD3+)	CRC03	27.70	33.20	41.10
	CRC11	33.10	24.10	57.40
	CRC15	24.76	19.60	14.10
CD8+CD28+ (on CD3+)	CRC03	7.02	20.90	17.20
	CRC11	6.74	24.50	15.10
	CRC15	14.62	27.50	8.78
CD8+CD28+PD-1+TIGIT+ (on CD3+)	CRC03	0.17	1.28	1.35
	CRC11	0.04	0.24	3.70
	CRC15	0.83	9.38	0.00
CD8+CD28+TIGIT+ (on CD3+)	CRC03	0.28	2.40	1.99
	CRC11	0.10	0.73	5.50
	CRC15	3.01	4.00	0.68

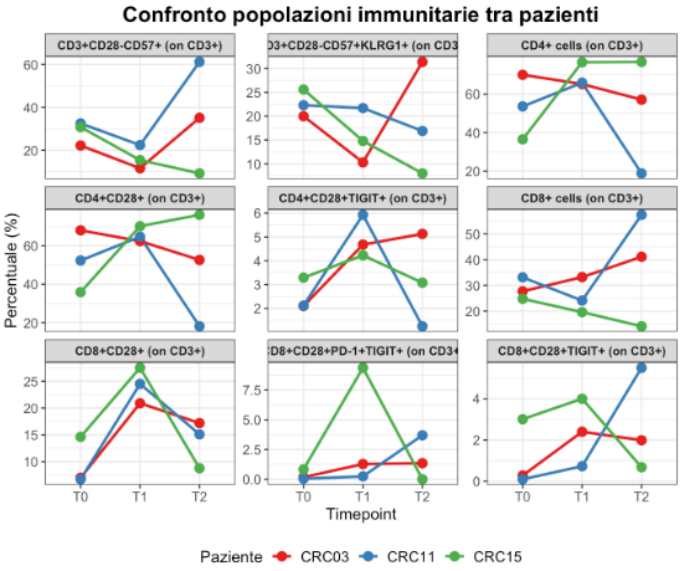

Figure 29 Evolution of Immune populations during treatment (T0vsT1vsT2)

To gain further insight into the temporal dynamics of T cell subpopulations in the context of therapeutic response and subsequent disease progression, we expanded our analysis to include a third timepoint (T2), corresponding to radiologically confirmed PD, in the three mCRC patients from the responder cohort who subsequently experienced PD. We assessed the longitudinal evolution of various T cell subsets at T0 (baseline), T1 (first evaluation with disease control), and T2 (progression). While most immune subsets displayed heterogeneous or patient-specific trajectories across timepoints, the frequency of $CD8^+CD28^+$ T cells (within $CD3^+$) demonstrated a remarkably consistent pattern across all three patients (Figure 29).

Specifically, a coordinated expansion of $CD8^+CD28^+$ T cells was observed from T0 to T1, consistent with the earlier findings at the cohort level, suggesting a treatment-induced reinvigoration of cytotoxic T cell functionality during the disease control phase. However, this expansion was followed by a marked contraction of the same subset at T2, coinciding with clinical progression. This temporal pattern was evident in all three patients, highlighting a possible link between the maintenance of CD28 expression on $CD8^+$ T cells and sustained antitumor immune surveillance. Given the central role of CD28 in promoting T cell activation, proliferation, and survival, the decline in $CD8^+CD28^+$ cells at progression may reflect a collapse in effector functionality, immune exhaustion, or tumor-mediated immunosuppression. These findings align with prior studies suggesting that loss of CD28 expression on $CD8^+$ T cells is associated with impaired immune competence and unfavorable clinical outcomes in cancer patients[147, 148]. In contrast, other $CD8^+$ T cell subsets—such as $CD8^+CD28^-TIGIT^+$ and $CD8^+CD28^+PD\text{-}1^+TIGIT^+$ cells—exhibited divergent trajectories among patients, precluding the identification of a common progression-associated pattern. Similarly, no consistent trends were observed in the $CD4^+$ T cell compartment across timepoints. These observations emphasize the potential of $CD8^+CD28^+$ T cell dynamics as a sensitive and reliable immunological correlate of treatment efficacy and emerging resistance in mCRC, warranting further investigation as a peripheral biomarker for longitudinal monitoring in clinical settings.

III.4 Metabolomic panel data

III.4.1 Stool metabolic panel data

Stool samples were analyzed at baseline, with data available for 22 patients. Results were compared between the cohort of 7 patients who subsequently experienced PD and the cohort of 15 patients who achieved disease control SD or PR.

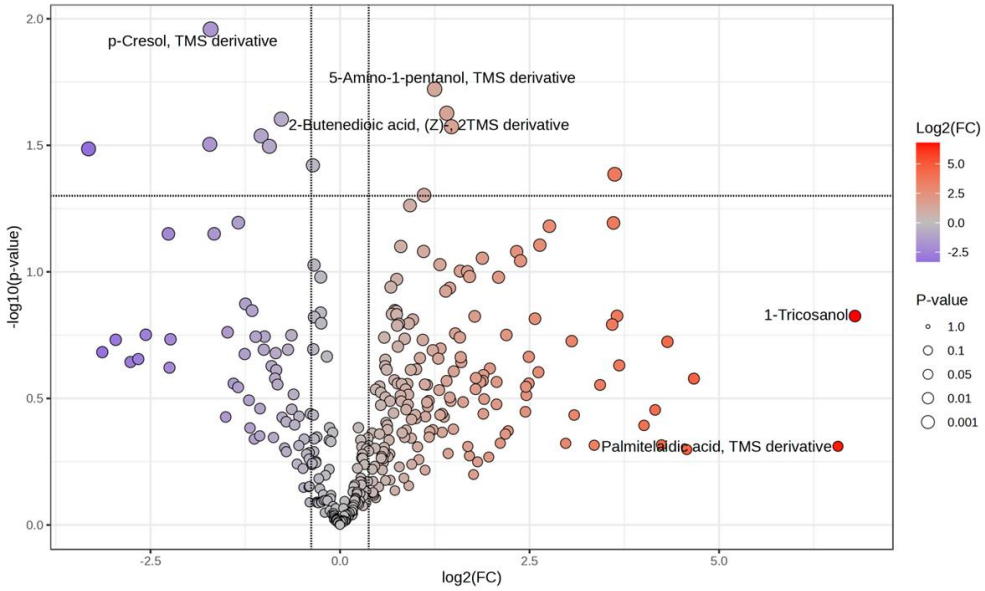

Figure 30 volcano plot stool metabolic analysis

This volcano plot reported in Figure 30 highlights metabolites that are differentially expressed between the two comparison groups. Several metabolites are labeled as they meet both the fold change and significance thresholds, indicating their potential biological and clinical relevance:

- 1-Tricosanol and Palmitelaidic acid, TMS derivative are among the most significantly upregulated metabolites.
- p-Cresol, TMS derivative, 2-Butenedioic acid, (Z)-2TMS derivative, and 5-Amino-1-pentanol, TMS derivative are significantly downregulated.

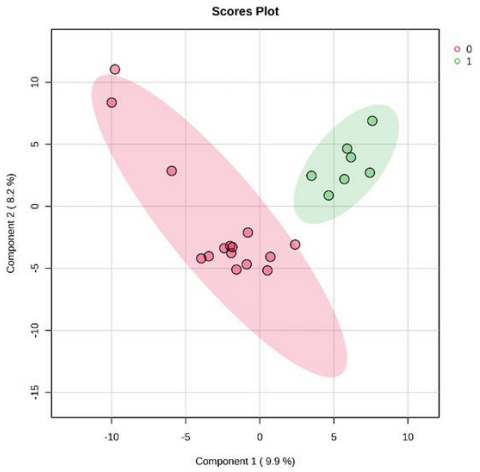

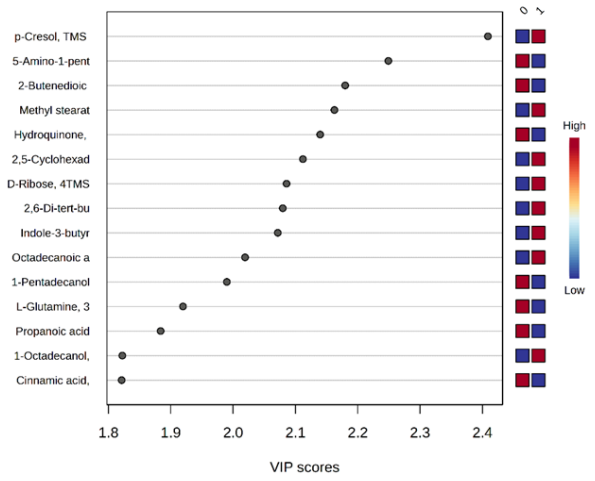

Figure 31 Score plot

Figure 32 VIP scores

Scores plot (Figure 31) indicates that there is a clear distinction between the two groups based on the metabolic assessment (PD group 1 vs response group 0). VIP (Variable Importance in Projection, Figure 32) score plot identifies the key metabolites that are most influential in separating the two subgroups.

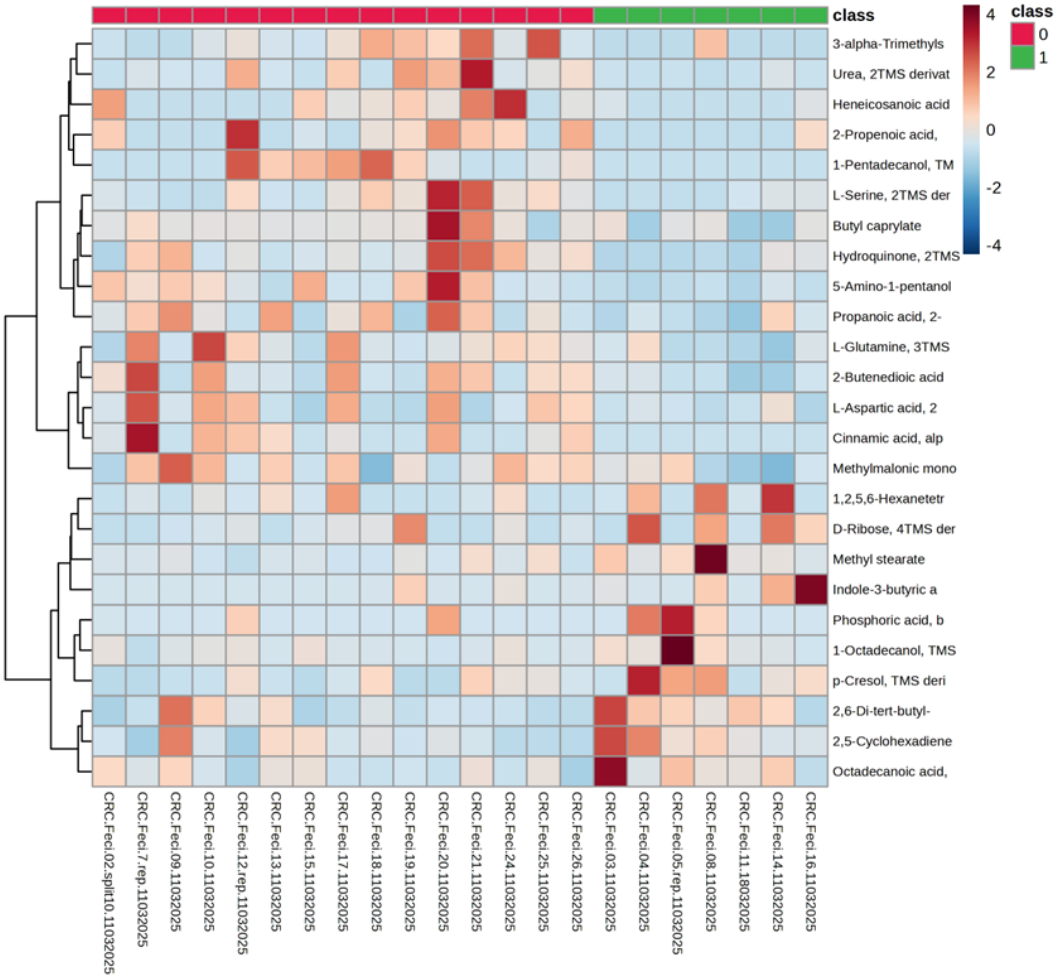

Figure 33 Heatmap metabolic analysis of fecal samples

A heatmap (Figure 33) was generated to visualize the relative abundance of the most discriminant metabolites, selected based on their VIP scores derived from multivariate analysis. The heatmap includes 22 patient samples, classified into two clinical outcome groups: progressive disease (PD, *n* = 7) and disease control (SD or PR, *n* = 15). Each row represents an individual metabolite, while columns correspond to patient samples. The color gradient reflects normalized metabolite intensity, with red indicating higher relative abundance and blue indicating lower levels.

Notably, several metabolites—including p-Cresol, 5-Amino-1-pentanol, and Fumaric acid—were found to be more abundant in the PD group, suggesting a possible association with unfavorable disease evolution. In contrast, other metabolites were enriched in patients who achieved disease control, potentially reflecting underlying metabolic pathways involved in therapeutic responsiveness.

L- Glutamine

Glutamine is a key metabolite that supports tumor viability and proliferation by meeting the metabolic and biosynthetic demands of rapidly dividing cells. In addition, it plays a crucial role in maintaining redox homeostasis by counteracting the accumulation of reactive oxygen species during enhanced proliferative activity. An in vitro study demonstrated that glutamine is essential for cell growth, and its deprivation leads to a significant reduction in the proliferation of CRC cells, accompanied by increased rates of apoptosis and necrosis [110]. In our cohort, we observed low levels of this metabolite in the fecal samples of patients who experienced PD, suggesting a potential association between glutamine availability and disease progression. Supporting this observation, a study by Su et al. (2022) identified serum glutamine as an independent prognostic biomarker for CRC progression. The authors also reported that glutamine deprivation may enhance the migratory and invasive capacities of CRC cells by promoting epithelial-to-mesenchymal transition (EMT) [109].

P-Cresol

p-Cresol is a microbial metabolite produced in the colon through bacterial fermentation of tyrosine, primarily by proteolytic bacteria associated with high-protein diets. It is rapidly absorbed and converted in the liver to *p*-cresol sulphate, a urinary metabolite proposed as a marker of protein intake and microbial activity. Unlike saccharolytic metabolites, *p*-cresol exhibits genotoxic properties. In vitro studies using colorectal cell lines (e.g., HT29, Caco-2) and colonic fermentation models have demonstrated that *p*-cresol induces DNA damage and disrupts cell cycle regulation at physiologically relevant concentrations, suggesting a role in colorectal carcinogenesis. Due to its efficient intestinal absorption, faecal levels may not accurately reflect mucosal exposure, making urinary *p*-cresol sulphate a potentially more reliable biomarker in diet–microbiota–host interaction studies in CRC. [111]. In our study, higher baseline levels of faecal *p*-cresol were observed in patients who experienced progressive disease, suggesting that a disbiotic environment characterized by elevated *p*-cresol may be associated with increased risk of progression.

2,6-di-tert-butylphenol

2,6-Di-tert-butylphenol (2,6-DTBP) is a synthetic phenolic compound commonly used as an antioxidant in industrial materials such as plastics, rubber, and fuels. In biological systems, it is

detected as an environmental xenobiotic, with both antioxidant properties and reported cytotoxic and endocrine-disrupting effects. Its presence in biological samples, including feces and plasma, may indicate exposure to environmental pollutants and reflect an altered xenobiotic metabolism. In our study, this metabolite was more abundant at baseline in patients who later experienced PD. Mechanistic studies have shown that 2,6-DTBP and its quinone derivative, 2,6-DTBQ, can promote carcinogenesis by disrupting the retinoic acid receptor beta (RARβ) pathway, leading to increased expression of p-Erk1/2 and COX-2, and thereby enhancing cancer cell proliferation and metastasis [112].

D-ribose

D-ribose is a naturally occurring pentose sugar derived both from nucleotide catabolism and bacterial fermentation, particularly by species such as *Clostridium* and *Bacteroides*, often enriched in dysbiotic microbiota. Elevated fecal levels of D-ribose have been associated with increased cellular turnover and microbial activity. Its phosphorylated derivative, D-ribose-5-phosphate (D5P), is a key intermediate of the pentose phosphate pathway (PPP) and functions as a metabolic checkpoint under glucose-limiting conditions. Recent evidence shows that D5P activates the YAP signaling pathway by facilitating MYH9-mediated LATS1 degradation, promoting cancer cell survival and proliferation. In our cohort, higher baseline levels of fecal D-ribose were observed in patients who progressed, suggesting its potential role as a marker of unfavorable prognosis. This may reflect both enhanced tissue turnover and the activation of oncogenic metabolic pathways, highlighting the relevance of D-ribose and D5P in tumor progression and their potential utility as biomarkers or therapeutic targets in colorectal cancer [113].

Octadecanol

Octadecanol (stearyl alcohol), a long-chain saturated fatty alcohol, has emerged as a potential fecal biomarker in CRC due to its involvement in lipid metabolism and its altered levels in disease states. Although its specific role in CRC remains underexplored, shifts in fecal lipid profiles, including long-chain fatty compounds, have been reported in CRC patients [114]. These metabolic changes may reflect tumor-associated dysregulation or microbiota-mediated lipid transformations [115]. While octadecanol itself is not consistently highlighted in existing panels, its structural similarity to other dysregulated lipids suggests potential relevance. Further targeted metabolomic studies are warranted to clarify its diagnostic and prognostic value in CRC.

Heneicosanoic acid and 1-Pentadecanol

These two very long-chain fatty acids (VLCFAs), primarily of dietary or plant origin, are also detectable in low concentrations in human cells. Currently, no direct evidence links them to alterations in cancer cell metabolism. However, elevated VLCFA levels may indicate a more intact intestinal barrier, potentially limiting endotoxin translocation and thereby reducing systemic and local inflammation. A less inflamed tumor microenvironment could contribute to improved treatment response and clinical outcomes. This hypothesis warrants further investigation in future studies [116].

2-butenedioic acid

In our cohort, patients with a positive response to treatment exhibited increased expression of 2-butenedioic acid (fumaric acid), a key intermediate of the TCA cycle. While fumarate's role in CRC is not well-established in fecal samples, its accumulation in tumors has been linked to metabolic reprogramming, including promotion of EMT and tumor aggressiveness. Dimethyl fumarate (DMF) has been shown to induce necroptosis in colon cancer cells via GSH depletion, ROS accumulation, and MAPK activation, though this effect is not observed with its metabolite monomethyl fumarate (MMF). The elevated fumarate levels in responders in our study suggest a potential link to better treatment outcomes, warranting further investigation into its role in CRC [117, 118].

Others

Several metabolites in our cohort showed unexpected trends or remain poorly characterized in CRC. *2,5-Cyclohexadiene*, an exogenous compound, has no known role in cancer but may relate to dysbiosis. *Indole-3-butyric acid*, which induces apoptosis in mCRC cells in vitro, was elevated in progressing patients, contradicting its reported antitumoral effect. Similarly, *octadecanoic acid*, known for its synergy with 5-FU, was higher in non-responders, opposing literature data. *1,2,5,6-Hexanetetrol* has not been studied in CRC but is linked to dysbiosis. *Phosphoric acid*, though not directly associated with CRC, was increased in progressing patients, possibly reflecting dysbiosis, dietary factors, or cell turnover. These findings highlight the complexity of metabolite dynamics and the need for further in vivo investigation.

III.4.2 Plasma metabolic panel data - responders vs non responders analysis

Plasma samples were analyzed at baseline, with data available for 23 patients. Results were compared between the cohort of 8 patients who subsequently experienced PD and the cohort of 15 patients who achieved disease control SD or PR.

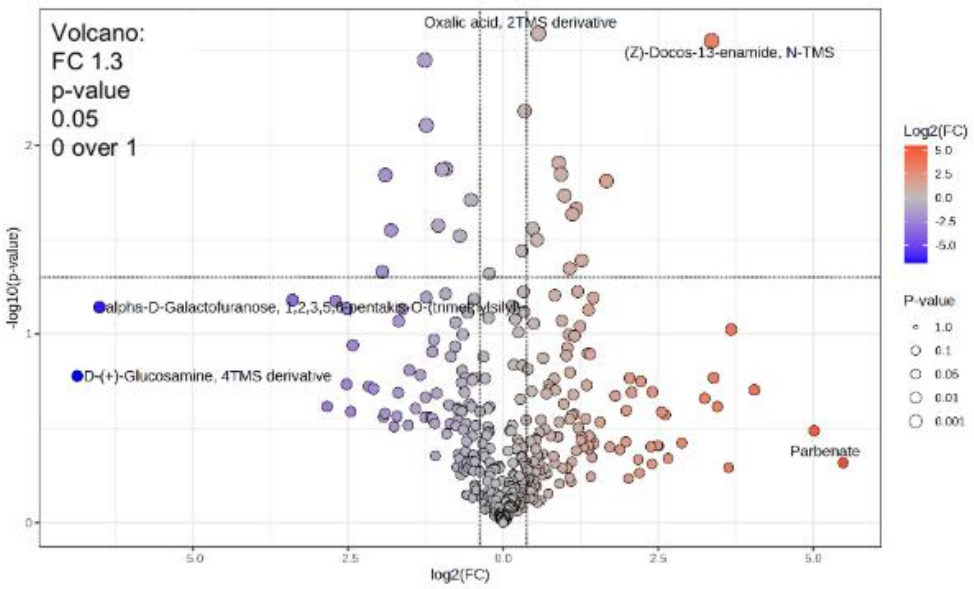

Figure 34 volcano plot plasma metabolic responders vs non responders analysis

The volcano plot in Figure 34 highlights metabolites that are differentially abundant between the two comparison groups. Notably increased were oxalic acid and (Z)-docos-13-enamide, while D-(+)-glucosamine was among the metabolites decreased. These findings suggest candidate metabolic biomarkers that may be predictive of treatment outcome.

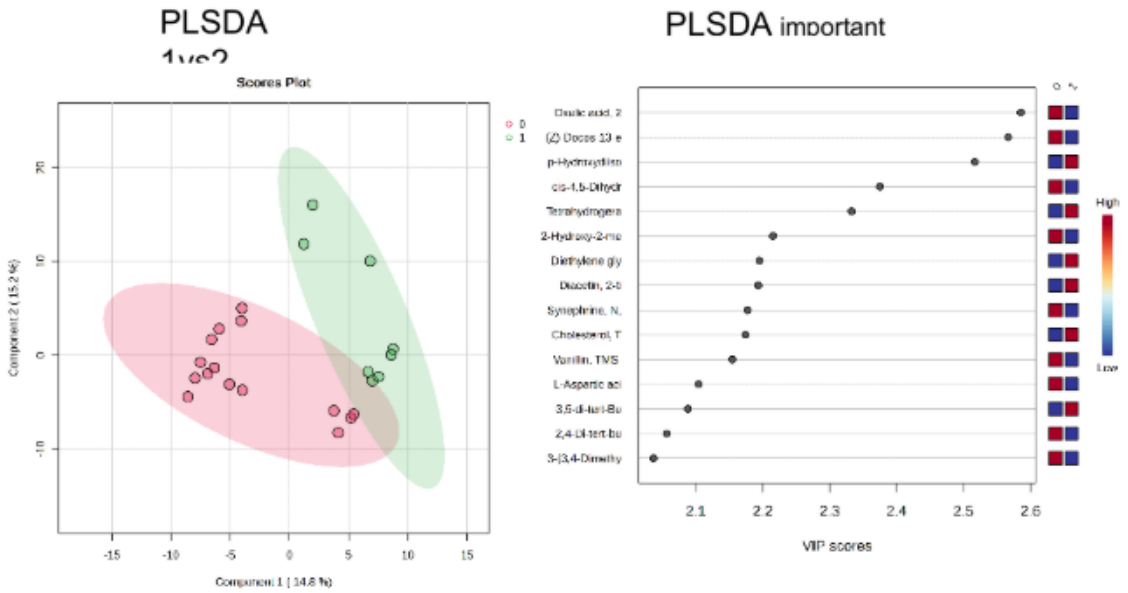

Figure 35 Score plot and VIP scores

In the Figure 35 the left panel shows the PLS-DA score plot comparing plasma metabolomic profiles at baseline between non-progressors (group 0, red) and progressors (group 1, green). A clear separation between the two groups is observed suggesting distinct metabolic signatures. Ellipses represent 95% confidence intervals. The right panel displays the VIP scores of the top discriminant metabolites (VIP > 2), indicating those contributing most to the group separation.

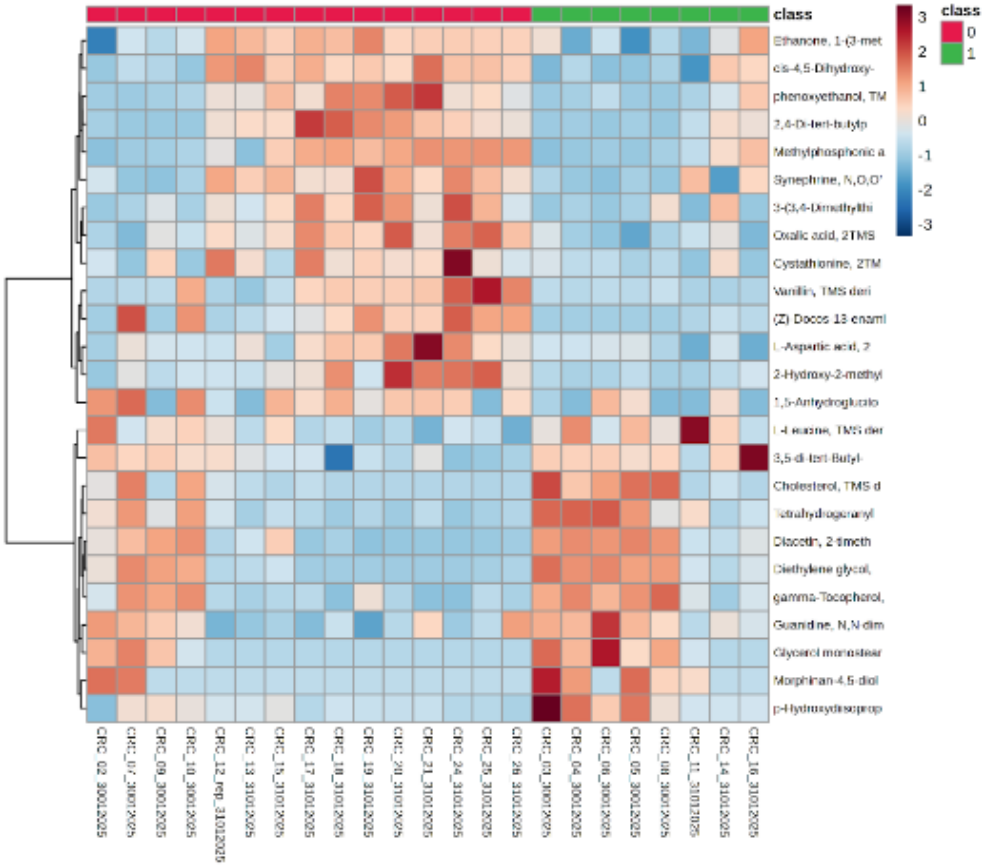

Figure 36 Heatmap of baseline plasma metabolites (0 progressors vs 1 non-progressors)

The heatmap in Figure 36 shows the relative abundance of key discriminant metabolites in baseline plasma samples. Samples are hierarchically clustered and annotated by clinical outcome: non-progressors (class 0, red) and progressors (class 1, green). Metabolites are organized by expression similarity. Distinct clustering patterns highlight metabolic differences between the two groups. For example, metabolites such as vanillin, (Z)-docos-13-enamide, and L-aspartic acid exhibited higher relative abundance in non-progressors, whereas cis-4,5-dihydroxy-2-cyclopenten-1-one, oxalic acid, and 2-hydroxy-2-methylbutyric acid were elevated in progressors. These alterations suggest distinct metabolic adaptations potentially associated with treatment response and disease progression.

III.4.3 Plasma metabolic panel data - pre vs post analysis

Baseline plasma samples were analyzed from a cohort of 26 patients with colorectal cancer, with follow-up data available for 13 patients (4 PD and 9 SD/PR). Comparative analyses were performed between the two evaluation time points (pre and post), regardless of the specific treatment response achieved.

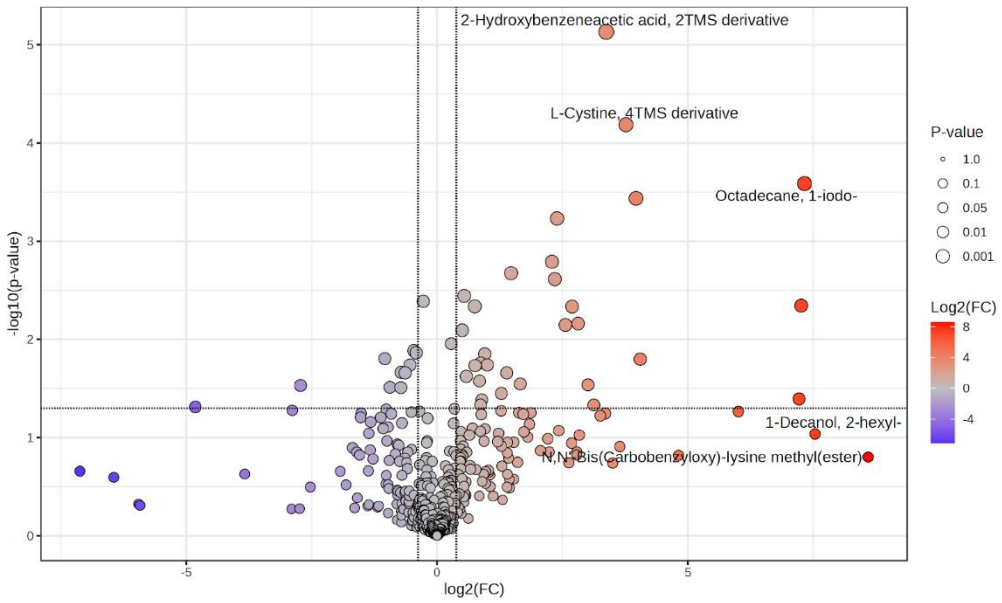

Figure 37 volcano plot plasma metabolic pre vs post analysis

The volcano plot illustrated in Figure 37 highlights metabolites that are differentially expressed between the two comparison groups. Several metabolites are labeled as they meet both the fold change and significance thresholds, indicating their potential biological and clinical relevance. Among the most prominently increased compounds were 2-Hydroxybenzeneacetic acid (2TMS derivative), L-Cystine (4TMS derivative), and Octadecane, 1-iodo-, 1-Decanol, 2-hexyl- and N,N-Bis(carboxymethyl)-lysine methyl(ester).

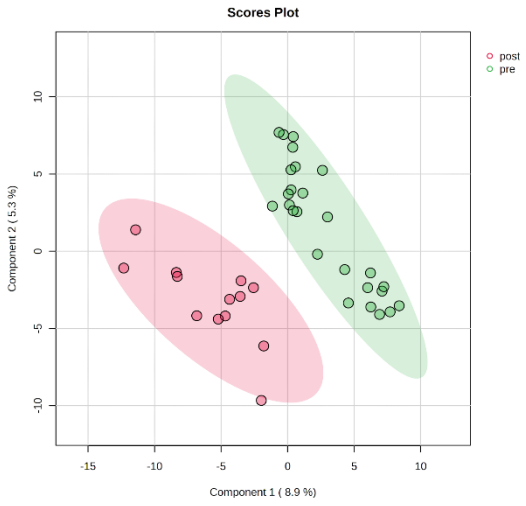

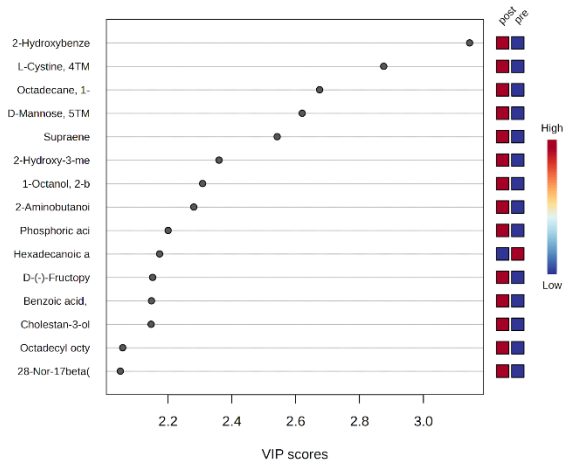

Figure 38 Score plot

Figure 39 VIP scores

Scores plot (Figure 38) indicates that there is a clear distinction between the two groups based on the metabolic assessment (post group vs pre-group). VIP score plot (Figure 39) identifies the key metabolites that are most influential in separating the two subgroups.

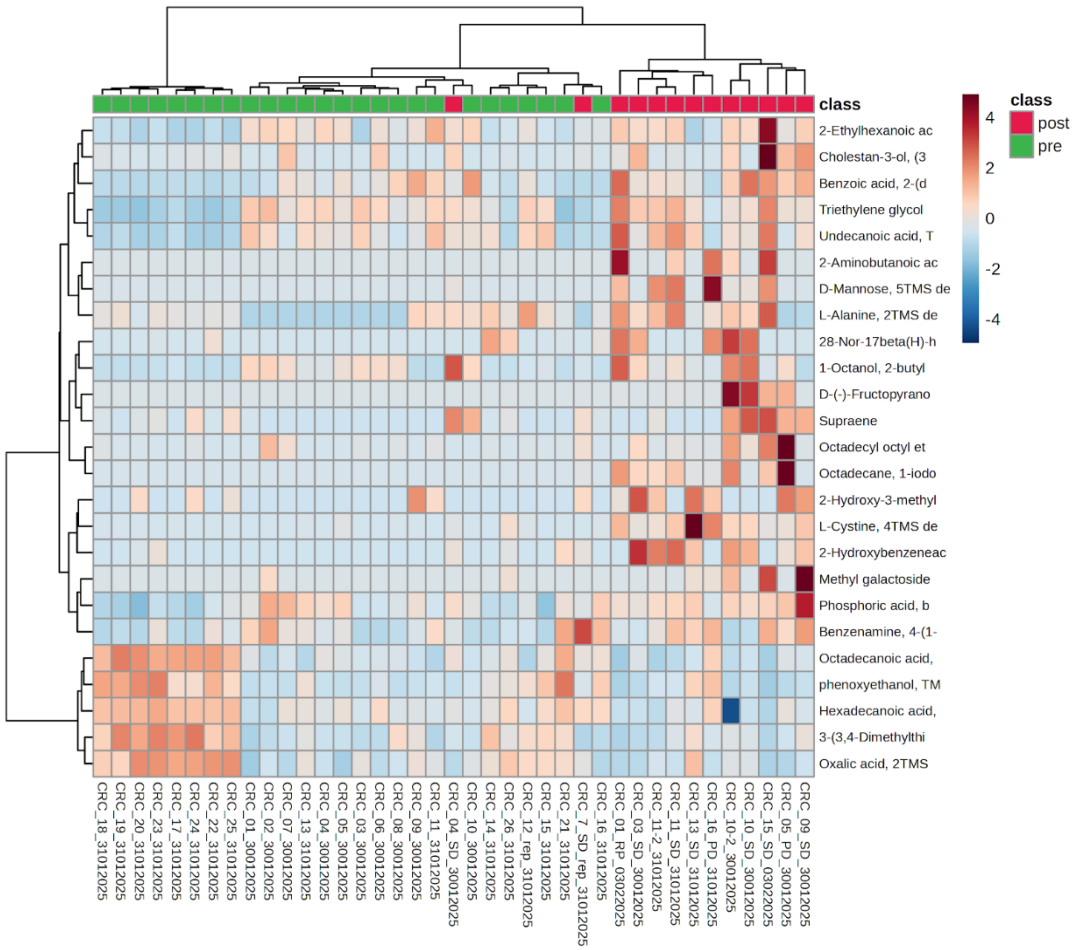

Figure 40 Heatmap metabolic analysis of plasma samples

Unsupervised hierarchical clustering of metabolomic data revealed distinct patterns differentiating pre- and post-treatment plasma samples (Figure 40). Several metabolites, including L-cystine, D-mannose, 2-hydroxybenzenacetic acid, and phosphoric acid, showed increased abundance in post-treatment samples, indicating metabolic adaptation or therapy-induced shifts. Conversely, compounds such as octadecanoic acid and triethylene glycol appeared more represented in pre-treatment samples or in patients not re-evaluated post-therapy. Notably, certain metabolites (e.g., methyl galactoside) displayed elevated levels only in specific post-treatment patients with stable disease, suggesting individualized metabolic responses. These findings highlight both group-level and patient-specific alterations in plasma metabolite profiles associated with treatment in metastatic colorectal cancer.

D-mannose

D-Mannose plays a central role in glycosylation processes, but emerging evidence suggests it also has direct implications in tumor immunity and cancer progression. Recent findings have shown that D-mannose can promote lysosomal degradation of PD-1, thereby enhancing T cell-mediated anti-tumor immunity [120]. This positions D-mannose not only as a metabolic substrate but also as an active modulator of immune checkpoint pathways. Additionally, elevated mannose levels have been associated with altered humoral immunity in cancer patients. Specifically, a recent study reported

decreased levels of natural IgM antibodies against mannose epitopes in gastric cancer, suggesting that mannose-related antigens may contribute to immune evasion mechanisms [119].

In this context, the observed enrichment of D-mannose in post-treatment plasma—particularly in patients with or eventually developing PD—may reflect both metabolic reprogramming and immunological dysregulation, supporting its relevance as a potential biomarker and therapeutic target in colorectal cancer.

L-alanine

D-Alanine, a microbiota-derived D-amino acid, was found to be more abundant in post-treatment plasma samples. This increased representation may reflect therapy-induced shifts in gut microbial composition or enhanced microbial-host metabolic exchange. Previous studies have associated alterations in circulating amino acid profiles with colorectal cancer progression and systemic inflammation [122,123]. In particular, alanine has been suggested to possess protective properties against the development of colon adenocarcinoma and may contribute to a more favorable disease prognosis. The consistent elevation of D-alanine following treatment supports its potential role as a marker of microbiome-associated metabolic remodeling in colorectal cancer. Furthermore, these findings raise the possibility that dietary modulation of alanine levels could represent a supportive strategy in the prevention or management of colorectal cancer.

Phosphoric acid

Phosphoric acid, an inorganic form of phosphate, was found to be more abundant in post-treatment plasma samples, independently of clinical response. This elevation may reflect altered phosphate homeostasis resulting from systemic metabolic changes, tumor burden, or treatment-related effects. Emerging evidence has highlighted the role of phosphate in cancer biology, suggesting that excessive phosphate availability can promote tumorigenesis and cancer cell proliferation by activating mitogenic signaling pathways and fostering a pro-tumoral microenvironment [123, 124].

The observed increase in circulating phosphoric acid post-treatment may therefore indicate a systemic shift toward phosphate dysregulation, potentially contributing to metabolic remodeling and disease progression. These findings support the notion that phosphate metabolism is a relevant, yet underexplored, target in the management of colorectal cancer.

L-cystine

L-Cystine, the oxidized dimeric form of cysteine, plays a crucial role in maintaining redox homeostasis and supporting glutathione biosynthesis, a key antioxidant defense mechanism in cancer cells. In our cohort, L-cystine levels were found to be elevated in post-treatment plasma samples, potentially reflecting increased metabolic demand for redox control following therapeutic stress. As highlighted by Bonifácio et al. [125], cystine uptake and its conversion to cysteine are essential for tumor cell survival, particularly under oxidative and metabolic stress. The observed post-treatment increase may therefore represent a systemic signature of tumor adaptation or host response to treatment-induced oxidative pressure.

2-Butyl-1-Octanol

2-Butyl-1-octanol, a branched-chain fatty alcohol, was found to be increased in post-treatment plasma samples. Although its role in cancer is not fully understood, such compounds are associated with lipid metabolism and membrane dynamics. The observed elevation may reflect therapy-induced metabolic adaptation or lipid remodeling, supporting its potential relevance as a marker of systemic metabolic response in colorectal cancer.

Methyl Galactoside

Methyl galactoside, a methylated sugar derivative, was generally detected at low levels across all samples. However, a relative increase was observed in post-treatment plasma, particularly in two patients with SD, where it appeared markedly elevated. Although its biological significance in colorectal cancer remains unclear, its selective enrichment may reflect patient-specific metabolic adaptations or alterations in glycosylation-related pathways following therapy.

Undecanoic Acid

Undecanoic acid, an odd-chain fatty acid, was slightly elevated in both pre- and post-treatment plasma samples, with higher levels observed post-therapy, particularly among responders. Recent studies suggest that odd-chain fatty acids, including undecanoic acid, may act as histone deacetylase 6 (HDAC6) inhibitors, modulating epigenetic regulation and tumor cell behavior [126]. Moreover, lipid metabolites such as these are increasingly recognized as active players in cancer-related signaling and metabolic adaptation [127]. The higher expression in responders may indicate a role in favorable metabolic reprogramming or epigenetic response to therapy in colorectal cancer.

Octadecanoic acid (stearic acid)

Octadecanoic acid was more abundant in pre-treatment plasma samples, particularly in a subgroup of patients who were not re-sampled post-therapy. Historically, stearic acid has been suggested to exert anti-carcinogenic effects [128], though its role remains context-dependent. Its early enrichment may reflect baseline lipid metabolic status or tumor-associated metabolic patterns prior to treatment initiation.

Phenoxyethanol

Phenoxyethanol, an aromatic alcohol with antimicrobial and solvent properties, was predominantly detected in pre-treatment plasma samples, particularly among patients who were not re-evaluated post-therapy. While its role in cancer biology remains poorly characterized, recent metabolomic studies suggest that baseline metabolic profiles, including exogenous compounds like phenoxyethanol, may influence treatment response and toxicity [129]. The observed enrichment may

reflect pre-treatment exposure, metabolic status, or individual pharmacokinetics, warranting further investigation into its potential relevance as a predictive or confounding factor in plasma metabolomics.

Hexadecanoic acid (Palmitic acid)

Hexadecanoic acid (palmitic acid), a key product of de novo lipogenesis, was more abundant in pre-treatment plasma samples and markedly reduced in one patient at the time of progressive disease (PD). Palmitic acid has been linked to colorectal cancer progression through multiple mechanisms, including β2-adrenergic receptor–dependent tumor growth [130], enhanced β-catenin palmitoylation via ACOX1 dephosphorylation [131], and CD36-mediated ferroptosis and ER stress signaling [132]. Its depletion at progression may reflect shifts in lipid metabolism or tumor cell adaptation. Notably, fatty acid synthase (FASN), the enzyme responsible for palmitate synthesis, is a therapeutic target currently under investigation. Oral FASN inhibitors such as TVB-2640 (Denifanstat) have shown promise in reducing palmitate levels and impairing cancer cell proliferation, highlighting the clinical relevance of palmitic acid in tumor metabolism and potential treatment strategies.

Oxalic Acid (ethanedioic acid)

Oxalic acid, a small dicarboxylic acid involved in various metabolic processes, was found to be more abundant in pretreatment plasma samples. Although its role in colorectal cancer remains unclear, elevated levels may reflect altered cellular metabolism or oxidative stress prior to therapy. This observation suggests a possible link between oxalate metabolism and the baseline metabolic state in colorectal cancer patients, warranting further investigation.

3-(3,4-Dimethylthieno[2,3-b]thiophen-2-yl)-1-methyl-5-methylsulfanyl-1H-pyrazole

The compound 3-(3,4-Dimethylthieno[2,3-b]thiophen-2-yl)-1-methyl-5-methylsulfanyl-1H-pyrazole was more highly expressed in pre-treatment plasma samples. While its biological function remains undefined, its structure—characterized by sulfur-containing heterocycles—suggests potential involvement in redox regulation or xenobiotic metabolism. The pre-treatment enrichment may reflect baseline metabolic conditions or exposure to exogenous compounds, and warrants further investigation for its potential as a marker of pre-therapeutic metabolic status.

III.4.4 Relationship between T Cells and baseline plasma metabolites

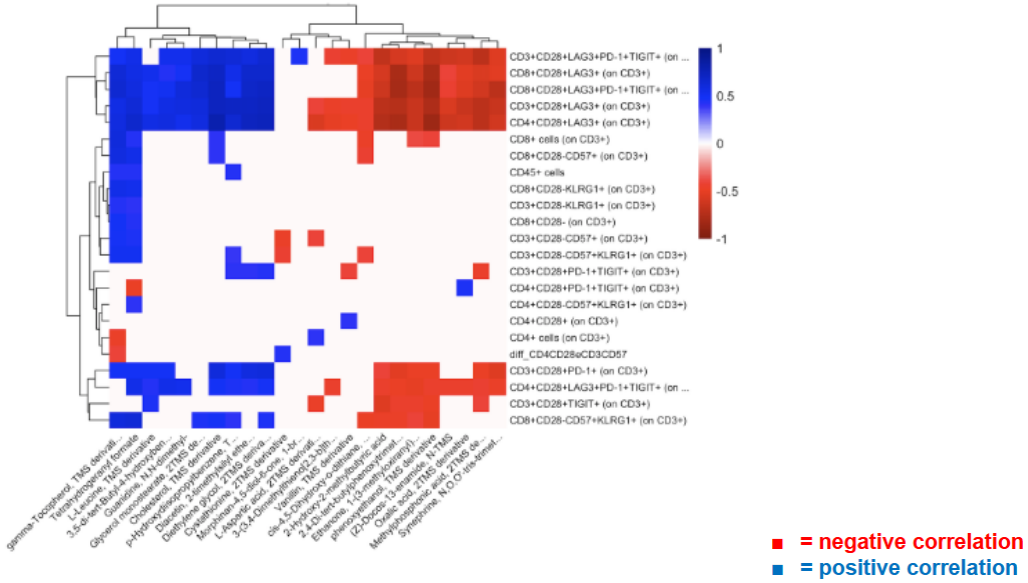

Figure 41 Spearman test: correlation between plasma metabolites and peripheral T-lymphocytes at baseline

To investigate the potential immunometabolic interactions in mCRC, we conducted a Spearman correlation analysis between baseline plasma metabolites (in responders and non responders populations) and peripheral T lymphocyte subpopulations. The heatmap in Figure 41 displays all statistically significant correlations ($p < 0.05$), with blue indicating positive correlations and red indicating negative correlations. The clustering of variables along both axes further reveals patterns of coordinated variation. Two major metabolic signatures emerged:

- Lipid-Enriched Metabolic Signature Associated with T Cell Exhaustion. Lipophilic metabolites, including gamma-Tocopherol, glycerophospholipids, and diacylglycerols, show strong positive correlations with dysfunctional and exhausted T cell phenotypes such as CD8+CD28+LAG3+PD-1+TIGIT+ and CD3+CD28+LAG3+ subsets. This profile suggests a pro-tumoral immunometabolic axis marked by T cell exhaustion and systemic lipid dysregulation.
- Mitochondrial-Linked Metabolic Profile Associated with Preserved T Cell Function. Short-chain acylcarnitines, bile acids, and intermediates of mitochondrial metabolism (e.g., methyl succinate), correlate with less differentiated or more functionally competent T cell subsets, including CD3+CD28+ and CD4+CD28+ populations. This points to a potentially protective or immunoresponsive metabolic milieu.

Together, these data reveal a tight coupling between systemic metabolism and T cell functional states in mCRC, suggesting that distinct metabolic environments may either fuel immune evasion or support

anti-tumor immunity. Prospective validation in a larger cohort will be crucial to determine causality and exploit these pathways therapeutically. Should these associations be confirmed, combined metabolic-immune biomarkers could refine risk stratification and identify patients who might benefit from metabolism-targeted adjuvant strategies in conjunction with standard chemotherapy.

III.4.5 Metabolomic Signatures Associated with T-cell Subsets Linked to Progression-Free Survival

To explore the functional relevance of immunometabolic crosstalk, we analyzed correlations between plasma metabolites and T-cell subpopulations previously associated with PFS. A distinct pattern emerged whereby T-cell subsets linked to a higher risk of progression (e.g., $CD3^+CD28^+LAG3^+$, $CD3^+CD28^+LAG3^+PD\text{-}1^+TIGIT^+$, and $CD8^+CD28^-CD57^+KLRG1^+$) showed positive correlations with metabolites reduced in patients with disease control (SD/PR), such as vanillin, phenoxyethanol, and oxalic acid, and negative correlations with protective metabolites, including γ-tocopherol, cystathionine, and L-leucine. These findings suggest that a lipid–phenolic metabolomic profile, enriched in patients with early progression, may foster or reflect T-cell exhaustion and senescence.

Conversely, T-cell subsets associated with favorable outcomes—including $CD4^+CD28^+$ and $CD4^+CD28^+PD\text{-}1^+TIGIT^+$—correlated positively with protective metabolites (e.g., γ-tocopherol and cystathionine) and negatively with immunosuppressive or dysregulated metabolic species such as vanillin or methylsuccinic acid. This is consistent with the hypothesis that a redox-competent, amino acid–rich metabolic environment supports immune functionality and treatment responsiveness.

Overall, these results reinforce the presence of a coordinated immunometabolic signature at baseline, in which plasma metabolites mirror and potentially modulate the functional status of peripheral T cells, aligning with clinical trajectories. These data support future development of circulating immuno-metabolomic biomarkers to stratify patients and tailor therapeutic approaches.

III.4.6 Relationship between T Cells and baseline faecal metabolites

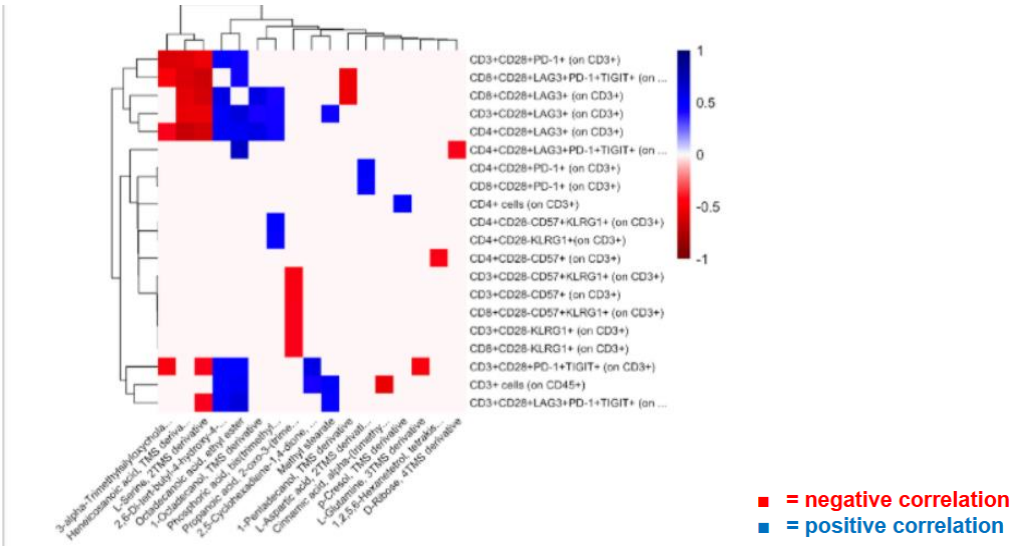

Figure 42 Spearman test: correlation between faecal metabolites and peripheral T-lymphocytes at baseline

To further explore the relationship between host immune status and metabolome, we performed a Spearman correlation analysis between baseline fecal metabolites and circulating T cell subsets in enrolled patients at baseline. As illustrated in Figure 42, the heatmap reveals distinct correlation patterns, with statistically significant associations highlighted in red (negative) and blue (positive). Notably, T cell subsets linked to an increased risk of disease progression—including $CD3^+CD28^+PD\text{-}1^+$, $CD3^+CD28^+LAG3^+$, and $CD3^+CD28^+PD\text{-}1^+TIGIT^+$ populations—displayed strong positive correlations with fecal metabolites found to be depleted in SD/RP patients. Conversely, these same T cell populations exhibited negative correlations with metabolites that were elevated in the SD/RP group. This opposing pattern suggests that the immunological milieu associated with poor clinical outcomes may be supported or shaped by a metabolomic environment less favorable to effective immune surveillance or anti-tumor activity. On the other hand, T cell subsets associated with more favorable prognostic profiles—including less exhausted or senescent phenotypes—tended to correlate positively with metabolites enriched in patients with disease stability or response, and negatively with those reduced in such individuals. These data collectively support the existence of a functional interplay between metabolome and systemic immune phenotypes, highlighting specific metabolites as potential modulators—or biomarkers—of T cell functionality in the tumor–host ecosystem. Altogether, these results provide novel evidence that fecal metabolites at baseline are not merely reflective of microbial composition, but are intimately connected to the systemic immune landscape. This immunometabolic crosstalk may hold mechanistic relevance in colorectal cancer progression and response to therapy, and merits further investigation to unravel causative pathways and therapeutic opportunities.

IV Discussion and conclusions

Therapeutic decision-making in mCRC is guided by the molecular profiling of the disease. It is essential to determine the microsatellite status and the mutational status of allRAS (KRAS, NRAS) and BRAF genes. RAS and BRAF wild-type tumors account for approximately 35–40% of cases. First-line treatments include combinations of fluoropyrimidine, irinotecan, and oxaliplatin, administered alongside a biological agent such as an anti-EGFR monoclonal antibody (cetuximab or panitumumab) in patients with all-RAS wild-type tumors, or an anti-angiogenic agent such as bevacizumab. In frail patients, monochemotherapy with fluoropyrimidine, with or without a monoclonal antibody, may be considered.

More recently, immunotherapy—such as pembrolizumab or the combination of nivolumab and ipilimumab—has been introduced into the treatment landscape for mCRC patients with high microsatellite instability (MSI-H) or mismatch repair deficiency (dMMR), who constitute approximately 4% of all mCRC cases.

The use of immunotherapy in cancers including mCRC enhances the immune system's ability to recognize tumor cells, strengthens immune responses, and eliminates mechanisms of immune evasion employed by tumor cells. One of the principal immune escape mechanisms exploited by neoplastic cells is immunosuppression mediated by regulatory T cells through pathways of exhaustion, anergy, and senescence. The process of immunosenescence is intrinsically linked to alterations in the cell cycle and immune cell function, including reduced proliferative capacity, delayed cell cycle progression, accumulation of senescent cells, impaired responses to proliferative and apoptotic stimuli, and decreased receptor diversity. Senescent cells are marked by increased expression of cell cycle inhibitors (e.g., p16 and p21), a characteristic surface phenotype ($CD28^-$ $CD27^+$ $CD57^+$ $KLRG1^+$), and a specific secretory profile known as the senescence-associated secretory phenotype (SASP).

The study and characterization of circulating T cells are increasingly recognized as valuable tools in evaluating their potential role as predictive and prognostic biomarkers. In oncology, elevated levels of circulating senescent T cells have been associated with significantly shorter overall survival in patients [85, 86]. Conversely, other studies have shown that baseline levels of senescent circulating T cells correlate with treatment response. Furthermore, post-chemotherapy changes in senescent T cell levels can serve as prognostic indicators for disease recurrence or treatment resistance [87, 88].

Another key consideration is the influence of the tumor microenvironment (TME) and numerous factors—such as cytokines, transcription factors, and cell-cell interactions—on immune cells, particularly in driving T cell exhaustion. Exhausted $CD3^+$ T lymphocytes express various inhibitory receptors including PD-1, LAG-3, CTLA-4, and TIM-3. These cells progressively lose their effector functions, becoming incapable of proliferation and cytokine production. Recent studies have demonstrated that elevated levels of circulating senescent cells are associated with reduced responsiveness to PD-1 inhibitors. Only exhausted $CD8^+$ $CD28^+$ $PD\text{-}1^+$ T cells can be reactivated via engagement of the PD-L1/PD-1 axis, whereas senescent T cells ($CD8^+$ $CD28^-$ $PD\text{-}1^-$) naturally remain in a non-functional, senescent state. Consequently, the prevalence of senescent T cells may serve as a potential predictive marker of response to immunotherapy [93, 95].

Currently, the number of clinically validated CRC-related biomarkers remains limited. Therefore, the identification of molecules detectable through non-invasive approaches represents a promising strategy for the dynamic monitoring of disease progression [96, 97].

Multiple studies have reported variations in the levels of different metabolites—including amino acids, fatty acids, and lysophosphatidylcholine—in CRC patients at different stages of disease when compared to healthy controls or individuals with adenomatous polyps. It is important to note that some of these metabolic differences may be influenced by variations in the composition of the gut microbiota [104].

The study "*CRC–Tsen: Assessment of the Predictive and Prognostic Role of Circulating T Cells in Patients with Colorectal Cancer Undergoing First-Line Treatment"* is a single-center, observational trial with a prospective and translational design. Its aim is to identify novel predictive and prognostic biomarkers of treatment response in patients with mCRC who are eligible for first-line therapy, consistent with current clinical standards.

The primary endpoint of this study is the evaluation of the predictive and/or prognostic role of senescent and exhausted $CD3^+$ T cell levels. Specifically, the study seeks to determine whether changes in these immune subpopulations are associated with treatment outcomes in mCRC patients. Additionally, the identification of a metabolomic signature with potential predictive or prognostic value is a key secondary objective of the investigation.

Between March 2024 and May 2025, 33 patients with mCRC were enrolled. The cohort had a median age of 69 years and was predominantly male (64%), with most patients being overweight or obese. Baseline plasma and fecal samples were collected from all participants, with follow-up plasma samples obtained in 14 cases based on clinical progression (2 patients) or response (12 patients). An additional follow-up plasma sample was collected at a third timepoint, corresponding to radiologically confirmed PD, in the three mCRC patients from the responder cohort who subsequently developed PD.

Primary tumors were mostly right-sided (45%), and one-third of patients had stage IV A disease. First-line treatments included anti-VEGF agents (45%), anti-EGFR therapy (33%), immunotherapy (12%), and chemotherapy alone (9%).

Molecular profiling revealed KRAS mutations in 52% of patients, with G12D as the most frequent variant. Additional alterations included BRAF V600E (12%), PIK3CA (21%), and TP53 (15%), with some patients showing co-occurring mutations. These findings underscore the molecular heterogeneity of mCRC and support the use of genomic profiling to inform targeted therapeutic strategies. As part of standard clinical practice, microsatellite status was assessed in all patients, revealing MSI-H in 4 cases (12%), all of whom received immunotherapy. Notably, the prevalence of MSI-H in our cohort is higher than typically reported in the literature (~4%), suggesting a potential selection bias or cohort-specific characteristics. Among the MSI-H patients, two also harbored concomitant BRAF mutations. None of the MSI-H cases were associated with a diagnosis of Lynch syndrome.

Our study provides novel evidence supporting the prognostic significance of senescent T cell subpopulations in patients with CRC. In particular, we observed a complex and dynamic immunophenotypic landscape in mCRC patients, with distinct patterns of T cell dysfunction and senescence emerging in association with disease progression, metastatic burden, and oncogenic drivers. Notably, the accumulation of $CD3^+CD28^-$ and $CD3^+CD28^-CD57^+$ T cells—phenotypes indicative of functional impairment and advanced immunosenescence—was significantly associated with shorter PFS, reinforcing their potential as prognostic biomarkers. The concurrent enrichment of $CD8^+CD28^+$LAG-3^+ transitional-exhausted T cells further underscores the detrimental impact of progressive T cell dysfunction on clinical outcomes, consistent with prior evidence linking co-inhibitory receptor expression to immune exhaustion and poor prognosis in malignancies [133, 134]. Importantly, these associations retained statistical significance in multivariate analysis, suggesting that immune parameters may independently inform prognosis beyond traditional clinicopathologic factors. Moreover, the potential protective role of statin use—implicated in immune modulation and tumor suppression through pleiotropic mechanisms [135]—further emphasizes the interplay between systemic immune status and therapeutic modifiers, advocating for their prospective evaluation in defined CRC immunophenotypes [136]. The observation that patients with limited metastatic spread (stage IVa) exhibited higher frequencies of $CD4^+$ senescent T cells, whereas those with extensive disease were enriched in globally exhausted phenotypes, points to a stage-dependent divergence in immune regulation, potentially reflecting differential histories of antigenic exposure and immune surveillance efficacy [137–140]. These findings suggest that senescence and exhaustion may not represent merely convergent dysfunctional states but may instead constitute context-dependent immune adaptations with variable clinical implications. Additionally, the divergent immunophenotypic profiles observed in relation to BRAF and KRAS mutational status reveal that oncogenic pathways may actively sculpt systemic T cell composition, favoring immune evasion through reduced $CD28^+$ subsets and enhanced dysfunctionality [143, 144, 151, 152]. The trend toward increased checkpoint-expressing $CD4^+CD28^+$PD-1^+ T cells in MSI patients, although not statistically significant, aligns with the recognized immunogenicity of MSI tumors and reinforces their known responsiveness to immunotherapy [153, 154]. Finally, the reduction in circulating senescent T cells following surgical removal of the primary tumor supports the hypothesis that persistent antigenic stimulation contributes to peripheral immune aging, and that its interruption may remodel immune dynamics toward a less senescent profile [145, 146].

The present study provides compelling evidence that dynamic changes in specific circulating T cell subsets may serve as early immunological correlates of clinical response in patients with mCRC undergoing first-line systemic therapy. In particular, we observed a significant decline in peripheral senescent T cells—characterized by $CD3^+CD28^-CD57^+$ and $CD3^+CD28^-CD57^+$KLRG1^+ phenotypes—in patients achieving disease control at first evaluation (NON PD), supporting the notion that therapeutic response is associated with a reduction in chronic antigenic stimulation and immune senescence. These results extend previous findings by demonstrating the reversibility of T cell senescence in a clinically meaningful context, and by reinforcing the prognostic relevance of these phenotypes in mCRC.

In parallel, functionally competent T cell subsets displayed a therapy-associated expansion, particularly $CD28^+$-expressing $CD4^+$ and $CD8^+$ T cells. The increase in $CD4^+CD28^+$ and $CD8^+CD28^+$

T cells from baseline to first radiological assessment suggests an immunological reinvigoration characterized by enhanced costimulatory signaling capacity. Notably, $CD8^+CD28^+$ T cells, essential for robust cytotoxic activity and long-term memory formation, increased substantially during disease control and subsequently declined upon progression in longitudinally followed patients, thus delineating a dynamic signature of immune surveillance failure. These findings align with prior evidence indicating that sustained CD28 expression on $CD8^+$ T cells is critical for maintaining antitumor immunity [147, 148].

The expansion of checkpoint-expressing subsets, such as $CD4^+CD28^+TIGIT^+$ and $CD8^+CD28^+PD\text{-}1^+TIGIT^+$ T cells, further highlights the complexity of the immune response during therapy. While TIGIT and PD-1 expression are typically associated with T cell dysfunction, their presence within the $CD28^+$ compartment suggests the coexistence of adaptive regulatory mechanisms alongside effector responses. This duality may reflect a transiently activated or partially exhausted state, potentially amenable to immune checkpoint blockade, and warrants further functional characterization [149].

Of particular note, logistic regression analysis confirmed that elevated baseline levels of $CD3^+CD28^-CD57^+$ T cells are significantly associated with progressive disease, corroborating the hypothesis that senescent T cell accumulation impairs therapeutic responsiveness. Although increased frequencies of $CD3^+CD28^+LAG3^+$ T cells also trended toward association with poor outcomes, the lack of statistical significance may reflect limited sample size or functional heterogeneity within this subset.

Finally, the three-patient longitudinal case analysis highlighted a reproducible pattern of $CD8^+CD28^+$ T cell contraction coinciding with disease progression, underscoring their potential as a robust and sensitive biomarker for real-time monitoring of immune competence during therapy. In contrast, other subsets, including $TIGIT^+$ or $PD\text{-}1^+$-expressing $CD8^+$ populations, demonstrated divergent trajectories, suggesting that $CD28^+CD8^+$ dynamics may represent a more consistent and clinically relevant indicator of therapeutic efficacy.

Collectively, these data suggest that effective treatment in mCRC is associated with a reduction in peripheral immune senescence, an expansion of costimulatory-competent T cells, and the emergence of regulatory or partially exhausted phenotypes that may either facilitate or constrain antitumor immunity. The longitudinal assessment of peripheral T cell phenotypes—particularly the CD28 axis—emerges as a promising strategy for identifying early responders, monitoring immune competence, and anticipating therapeutic resistance.

Our analysis of stool samples from 22 CRC patients revealed distinct metabolic profiles associated with PD and response to treatment (SD/PR). Key metabolites such as p-cresol, 5-amino-1-pentanol, and fumaric acid were significantly elevated in the PD group, suggesting a dysbiotic environment linked to unfavorable disease progression. p-Cresol, produced by microbial fermentation of tyrosine, is known for its genotoxic properties, which may contribute to carcinogenesis. Similarly, fumaric acid, a TCA cycle intermediate, is involved in epithelial-to-mesenchymal transition (EMT) and may reflect metabolic reprogramming in CRC. Surprisingly, elevated fumarate levels were also found in responders, suggesting potential therapeutic implications.

In contrast, metabolites like 1-tricosanol and palmitelaidic acid were enriched in the disease control group, potentially reflecting altered lipid metabolism supportive of treatment response. Additionally, L-glutamine levels were lower in PD patients, aligning with its role in tumor proliferation and survival.

Unexpectedly, indole-3-butyric acid and octadecanoic acid, compounds previously associated with antitumoral effects, were elevated in non-responders, contradicting existing literature. Other metabolites like 2,5-cyclohexadiene and phosphoric acid remain poorly characterized in CRC but may indicate microbial dysbiosis and metabolic alterations, warranting further investigation.

The differential metabolomic profiles observed at baseline between patients who achieved disease control (SD or PR) and those who progressed (PD) provide compelling evidence of the prognostic value of systemic metabolic states. The identification of metabolites such as oxalic acid and (Z)-docos-13-enamide, which were elevated in non-progressors, suggests the presence of metabolic pathways potentially involved in enhanced immune surveillance or tumor suppression. In contrast, the reduction of D-(+)-glucosamine in the same group may reflect decreased activity in glycosylation pathways linked to tumor proliferation or immune evasion.

The clear separation in PLS-DA analysis and distinct clustering observed in the heatmap further support the existence of structured metabolic differences with clinical relevance. Elevated levels of vanillin, L-aspartic acid, and (Z)-docos-13-enamide in non-progressors may reflect a more immunologically favorable or metabolically restrained tumor microenvironment. Conversely, the increase in oxalic acid, cis-4,5-dihydroxy-2-cyclopenten-1-one, and 2-hydroxy-2-methylbutyric acid among progressors points to metabolic reprogramming events that may underlie immune escape, tumor aggressiveness, or treatment resistance.

These results are consistent with the broader paradigm that metabolic alterations can shape both tumor behavior and immune response, reinforcing the importance of integrating metabolomic profiling into predictive models. Overall, the baseline plasma metabolome emerges as a promising non-invasive source of biomarkers to stratify patients by risk of progression and to tailor therapeutic strategies accordingly.

Longitudinal plasma metabolomic profiling revealed substantial biochemical remodeling following treatment in patients with mCRC, irrespective of clinical response. Several metabolites showed consistent post-treatment increases, including L-cystine, 2-hydroxybenzeneacetic acid, and D-mannose, indicating systemic metabolic adaptations. The rise in L-cystine suggests enhanced glutathione biosynthesis, reflecting a compensatory response to therapy-induced oxidative stress. The increase in D-mannose, recently implicated in immunomodulation via PD-1 degradation and altered humoral immunity [153], further supports a role for treatment-driven immune-metabolic reprogramming. Phosphoric acid, also elevated post-treatment, may reflect increased activity in phosphate-dependent signaling pathways involved in tumor proliferation and survival [152]. Similarly, 2-butyl-1-octanol enrichment may reflect shifts in lipid remodeling or detoxification pathways. Metabolites such as methyl galactoside and undecanoic acid were selectively elevated in patients with stable disease, suggesting their potential association with favorable therapeutic outcomes. Notably,

undecanoic acid has been identified as a selective HDAC6 inhibitor [151], pointing to a possible epigenetic mechanism underlying clinical benefit.

Conversely, metabolites enriched at baseline in progressors—such as octadecanoic acid, hexadecanoic acid, and phenoxyethanol—may represent a pro-tumoral metabolic signature. Of particular interest, palmitic acid (hexadecanoic acid) was decreased post-treatment, aligning with previous evidence of its involvement in colorectal carcinogenesis and resistance via fatty acid synthase (FASN) activity [149]. This supports the hypothesis that FASN-related lipogenic pathways are dynamically regulated during treatment and may represent actionable metabolic vulnerabilities.

Finally, elevated pre-treatment levels of oxalic acid and 3-(3,4-dimethylthieno[2,3-b]thiophen-2-yl)-1-methyl-5-methylsulfanyl-1H-pyrazole may reflect systemic oxidative stress or environmental exposures, reinforcing the complexity of host–tumor metabolic interactions in mCRC.

Collectively, these findings highlight a dynamic and patient-specific modulation of the circulating metabolome in response to therapy. This evolving metabolic landscape may influence immune function, treatment efficacy, and resistance mechanisms, underscoring the potential of plasma metabolomics as a powerful tool for biomarker discovery and patient stratification.

Building upon the identified associations between T cell subsets and baseline plasma and fecal metabolites, these findings collectively underscore the critical role of systemic immunometabolic crosstalk in shaping tumor-immune dynamics in mCRC. The dichotomous metabolic signatures—lipid-enriched profiles linked to exhausted T cell phenotypes versus mitochondrial and amino acid–associated profiles correlated with preserved T cell function—highlight the metabolic plasticity that may underlie immune evasion or effective antitumor immunity. Importantly, the parallel patterns observed in fecal metabolomics reinforce the concept that the gut microenvironment exerts a profound influence on peripheral immune competence, likely via modulating metabolite availability and systemic immune tone. These integrative data suggest a bidirectional interaction where altered systemic metabolism not only reflects but potentially drives the phenotypic and functional remodeling of T cell compartments critical for clinical outcomes. Such insights pave the way for innovative biomarker development that combines circulating metabolite profiles with immune phenotyping to enhance risk stratification and predict therapeutic response. Moreover, these findings invite exploration of therapeutic strategies targeting metabolic pathways—either to reverse T cell exhaustion or to potentiate mitochondrial and redox-dependent T cell fitness—thereby complementing existing immuno-oncologic treatments. Future longitudinal and mechanistic studies are essential to validate causality and to translate these metabolically informed immunomodulatory approaches into clinical practice, ultimately aiming to improve prognosis and personalize treatment in mCRC.

Taken together, this work advances the understanding of mCRC biology by highlighting the prognostic relevance of circulating immune dysfunction and by establishing metabolomic signatures as complementary, non-invasive biomarkers of treatment response and disease progression. These findings support the development of integrated immunometabolic classifiers to inform early stratification, monitor immune fitness, and anticipate resistance to systemic therapies. Future studies should aim to validate these results in larger, independent cohorts and elucidate the mechanistic basis

of immunometabolic interactions. Moreover, therapeutic strategies targeting metabolic pathways—such as fatty acid synthesis inhibition or redox modulation—may represent promising avenues to restore immune competence and enhance treatment efficacy in mCRC.

In conclusion, this study identifies circulating T cell phenotypes and plasma/fecal metabolites as interrelated and clinically informative parameters in mCRC. Their combined analysis holds substantial potential for improving prognostic accuracy, guiding treatment decisions, and ultimately, personalizing care for patients with advanced colorectal cancer.

V Future perspectives

The results of this study open several promising avenues for future research. First, validating these findings in larger and more diverse patient cohorts will be crucial to strengthen their clinical relevance and statistical significance. Increasing the sample size will allow for a more accurate stratification of patients and better capture the biological heterogeneity of mCRC. Expanding the analytical scope to include lipidomics and microvesicle profiling could provide deeper insights into the metabolic and intercellular communication networks that shape the immune response and tumor behavior. In parallel, studying the gut microbiota—a powerful modulator of both immunity and metabolism—may uncover additional layers of regulation that influence treatment response and resistance. A key objective will be to integrate these biological dimensions and correlate them with tumor sidedness (right- vs. left-sided) and with molecular features such as RAS/BRAF mutations and microsatellite instability (MSI) status. These correlations may help explain inter-patient variability and support the development of more refined prognostic and predictive models. Ultimately, combining immune profiling, metabolic signatures, extracellular vesicle content, and microbiome composition into a multidimensional framework—possibly supported by artificial intelligence and machine learning—may pave the way for a new generation of non-invasive biomarkers. These tools could guide personalized therapeutic strategies, identify patients at risk of resistance earlier, and enhance clinical outcomes in mCRC. Such a systems-level approach holds the potential to move precision oncology from theory to practice.

VI Bibliography

1. GLOBOCAN Project 2022. http://globocan.iarc.fr

2. Bonadonna G., Robustelli Della Cuna G., Valgussa P. Elsevier Masson, Medicina oncologica Ottava Edizione. Capitolo 43. 1078-1079

3. Center MM, Jemal A, Smith RA, Ward E. Worldwide variations in colorectal cancer. CA Cancer J Clin 2009; 59: 366–78.

4. G. Argilés, J. Tabernero, R. Labianca, D. Hochhauser R. Salazar, T. Iveson, P. Laurent-Puig, P. Quirke, T. Yoshino,J. Taieb, E. Martinelli & D. Arnold on behalf of the ESMO Guidelines Committee Localised colon cancer: ESMO Clinical Practice Guidelines for diagnosis, treatment and follow-up 2020

5. Bonadonna G., Robustelli Della Cuna G., Valgussa P. Elsevier Masson, Medicina oncologica Ottava Edizione. Capitolo 43. 1078-1079

6. AIOM, AIRTUM e CCM. I numeri del cancro in Italia 2024

7. Surveillance Epidemiology and End Results (SEER), U.S National Instituites of Health. Stage distribution by Age at Diagnosi/Death, Colon and Rectum, All Races, Both Sexes 2000-2010 2003-2010

8. Siegel RL, Miller KD, Goding Sauer A, et al. Colorectal cancer statistics, 2020. CA Cancer J Clin 2020.

9. Bailey CE, Hu CY, You YN, et al. Increasing disparities in the age- related incidences of colon and rectal cancers in the United States, 1975- 2010. JAMA Surg 2014:1-6.

10. Doll R, Peto R. The causes of cancer: quantitative estimates of avoidable risks of cancer in the United States today. J Natl Cancer Inst. 1981;66:1191–308.

11. Chen J, Giovannucci EL, Hunter DJ. MTHFR polymorphism, methyl-replete diets and the risk of colorectal carcinoma and adenoma among U.S. men and women: an example of gene-environment interactions in colorectal tumori-genesis. J Nutr. 1999;129(2 Suppl):560S–4S.

12. Cuzick J, Otto F, Baron JA, Brown PH, Burn J, Greenwald P, Jankowski J, La Vecchia C, Meyskens F, Senn HJ, Thun M, Aspirin and non-steroidal anti-inflammatory drugs for cancer prevention: an international consensus statement. Lancet Oncol. 2009 May;10(5):501-7. doi: 10.1016/S1470-2045(09)70035-X.

13. Cao Y, Nishihara R, Wu K, et al. Population-wide impact of long-term use of aspirin and the risk for cancer. JAMA Oncol 2016;2:762-769

14. Chung M, Lee J, Terasawa T, Lau J, Trikalinos TA. Vitamin D with or without calcium supplementation for prevention of cancer and fractures: an updated meta-analysis for the U.S. Preventive Services Task Force. Ann Intern Med. 2011 Dec 20;155(12):827-38. doi: 10.7326/0003-4819-155-12-201112200-00005.

15. Gorham ED1, Garland CF, Garland FC, Grant WB, Mohr SB, Lipkin M, Newmark HL, Giovannucci E, Wei M, Holick MF. Optimal vitamin D status for colorectal cancer prevention: a quantitative meta analysis. Am J Prev Med. 2007 Mar;32(3):210-6.

16. Lappe JM1, Travers-Gustafson D, Davies KM, Recker RR, Heaney RP.Vitamin D and calcium supplementation reduces cancer risk: results of a randomized trial. Am J Clin Nutr. 2007 Jun;85(6):1586-91.

17. Ma Y1, Zhang P, Wang F, Yang J, Liu Z, Qin H Association between vitamin D and risk of colorectal cancer: a systematic review of prospective studies. J Clin Oncol. 2011 Oct 1;29(28):3775-82. doi: 10.1200/JCO.2011.35.7566. Epub 2011 Aug 29.

18. Fedirko V, Riboli E, Tjønneland A, Ferrari P, Olsen A, Bueno-de-Mesquita HB, van Duijnhoven FJ, Norat T, Jansen EH, Dahm CC, Overvad K, Boutron-Ruault MC, Clavel-Chapelon F, Racine A, Lukanova A, Teucher B, Boeing H, Aleksandrova K, Trichopoulou A, Benetou V, Trichopoulos D, Grioni S, Vineis P, Panico S, Palli D, Tumino R, Siersema PD, Peeters PH, Skeie G, Brustad M, Chirlaque MD, Barricarte A, Ramón Quirós J, Sánchez MJ, Dorronsoro M, Bonet C,Palmqvist R, Hallmans G, Key TJ, Crowe F, Khaw KT, Wareham N, Romieu I, McKay J, Wark PA, Romaguera D, Jenab M. Prediagnostic 25-hydroxyvitamin D, VDR and CASR polymorphisms, and survival in patients with colorectal cancer in western European ppulations. Cancer Epidemiol Biomarkers Prev. 2012 Apr;21(4):582-93. doi: 10.1158/1055-9965.EPI-11-1065. Epub 2012 Jan 25.

19. Ng K1, Meyerhardt JA, Wu K, Feskanich D, Hollis BW, Giovannucci EL, Fuchs CS Circulating 25-hydroxyvitamin d levels and survival in patients with colorectal cancer. J Clin Oncol. 2008 Jun 20;26(18):2984-91. doi: 10.1200/JCO.2007.15.1027.

20. Zgaga L, Theodoratou E, Farrington SM, Din FV, Ooi LY, Glodzik D, Johnston S, Tenesa A, Campbell H, Dunlop MG. Plasma vitamin D concentration influences survival outcome after a diagnosis of colorectal cancer. J Clin Oncol. 2014 Aug 10;32(23):2430-9. doi: 10.1200/JCO.2013.54.5947. Epub 2014 Jul 7.

21. Ng K, Sargent DJ, Goldberg RM, Meyerhardt JA, Green EM, Pitot HC, Hollis BW, Pollak MN, Fuchs CS.Vitamin D status in patients with stage IV colorectal cancer: findings from Intergroup trial N9741. J Clin Oncol. 2011 Apr 20;29(12):1599-606. doi: 10.1200/JCO.2010.31.7255. Epub 2011 Mar 21.

22. Ströhle A et al. Nutrition and colorectal cancer. Med Monatsschr Pharm. 2007 Yan; 30(1): 25-32.

23. Correa Lima et al. Colorectal cancer: lifestyle and dietary factors. Nutr Hosp. 2005 Yul-Aug; 20 (4): 235-41.

24. AIOM Linee guida – Tumori del colon, edizione 2024

25. Stoffel EM, Mangu PB, Gruber SB, et al. Hereditary colorectal cancer syndromes: American Society of Clinical Oncology Clinical Practice Guideline endorsement of the

familial risk-colorectal cancer: European Society for Medical Oncology Clinical Practice Guidelines. J Clin Oncol. 2015;33(2):209-17

26. Biller LH, Syngal S, Yurgelun MB. Recent advances in Lynch syndrome. Fam Cancer. 2019;18(2):211-9.

27. Sepulveda AR, Hamilton SR, Allegra CJ, et al. Molecular Biomarkers for the evaluation of Colorectal Cancer: guideline from the American Society for Clinical Pathology, College of American Pathologists, Association for Molecular Pathology, and the American Society of Clinical Oncology. J Clin Oncol. 2017;35(13):1453-86.

28. National Institute for Health and Care Excellence NICE. Molecular testing strategies for Lynch syndrome in people with colorectal cancer; 2017

29. Zhang R et al. A meta-analysis of the prevalence of somatic mutations in the hMLH1 and hMSH2 genes in colorectal cancer. Colorectal Dis 2012; 14(3): e80-9

30. Warusavitarne J et al. The role of chemotherapy in microsatellite unstable (MSI-H) colorectal cancer. Int J Colorectal Dis 2007; 22 (7):739-48.

31. Barry Iacopetta et al. Microsatellite instability in colorectal cancer. Asia Pacific Journal of Clinical Oncology 2010 Dec; (4):260-9.

32. Wimmer K et al. Constitutional mismatch repair-deficiency syndrome: have we so far seen only the tip of an iceberg? Hum Genet 2008 Sp, 124(2): 105-22

33. Wang H et al. Signaling from DNA mismatch repair excision site despite interventing blockades. The EMBO journal. 2004 May 19;23(10):2126-33.

34. Halling KC et al. Nicrosatellite instability and 8p allelic imbalance in stage B2 and C colorectal cancers. J natl Cancer Inst. 1999 Aug 4;91(15):1295-303

35. Gryfe R et al. Tumor microsatellite instabily and clinical outcome in young patients with colorectal cancer. N Engl J Med 2000 Jan 13;42(2):69-77.

36. Kochhar R et al. Allelic imbalance and microsatellite instability in resected Duke's D colorectal cancer. Diagn Mol Pathol 1997 Apr;6(2):78-84.

37. Kuebler JP et al. Oxaliplatin combined with weekly bolus fluorouracil and leucovorin as surgical adjuvant chemotherapy for stage II and III colon cancer: results from NSABP. J Clin Oncol. Jun 2007 Jun 1; 25(16): 2198-204

38. Robbins C. Elsevier Masson. Le basi patologiche delle malattie Ottava Edizione. Capitolo 17. 809-810

39. Roth A. et al. Stage-specific prognostic value of molecular markers in colon cancer: Results of the translational study on the PETACC 3-EORTC 40993-SAKK 60-00 trial. J Clin Oncol 2009

40. Bianco AR. McGraw-Hill editor, 2007. Manuale di oncologia clinica IV edizione, capitolo 11. 177-190

41. Yarden Y. The EGFR family and its ligands in human cancer signaling mechanism and therapeutic opportunities. Eur J Cancer 2001; 37 (Suppl): S3-S8

42. Mayer A, Takimoto M, Fritz E et al. The prognostic significance of proliferating cell nuclear antigen, epidermal growth factor receptor and mdr gene expression in colorectal. Cancer 1993; 71:2454-2460

43. Sartore-Bianchi A, Di Nicolantonio F, Nichelatti M et al. Multi-determinants Analysis of molecular Alterations for Predicting Clinical Benefits to EGFR- Targeted Monoclonal Antibodies in Colorectal Cancer. PloS ONE 2009; 4(10): e7287

44. Lievre A, Bachet JB, Boige V et al. KRAS mutations as an independent prognostic factor in patients with advanced colorectal cancer treated with Cetuximab. J Clin Oncol 2008; 26: 374-379.

45. Bokemeyer C, Van Cutsem E, Rougier P et al. Addition of Cetuximab to chemotherapy as first-line treatment for KRAS wild-type metastatic colorectal cancer: pooled analysis of the CRYSTAL and OPUS randomised clinical trials. Eur J Cancer 48: 1466-1475.

46. Douillard JY, K O, Siena S et al. Panitumumab–FOLFOX4 Treatment and RAS Mutations in Colorectal Cancer N Engl J Med 2013; 369:1023-1034.

47. Schwartzberg LS, Rivera F, Karthaus M et al. PEAK: A Randomized, Multicenter Phase II Study of Panitumumab Plus Modified Fluorouracil, Leucovorin, and Oxaliplatin (mFOLFOX6) or Bevacizumab Plus mFOLFOX6 in Patients With Previously Untreated, Unresectable, Wild-Type KRAS Exon 2 Metastatic Colorectal Cancer. J Clin Oncol.

48. Heinemann V, von Weikersthal LF, Decker T et al. FOLFIRI plus Cetuximab versus FOLFIRI plus Bevacizumab as first-line treatment for patients with metastatic colorectal cancer (FIRE-3): a randomised, open-label, phase 3 trial. Lancet Oncol 15: 1065-1075.

49. De Roock W1, Jonker DJ, Di Nicolantonio F, Sartore-Bianchi A, Tu D, Siena S, Lamba S, Arena S, Frattini M, Piessevaux H, Van Cutsem E, O'Callaghan CJ, Khambata-Ford S, Zalcberg JR, Simes J, Karapetis CS, Bardelli A, Tejpar S. Association of KRAS p.G13D mutation with outcome in patients with chemotherapy-refractory metastatic colorectal cancer treated with Cetuximab. JAMA. 2010 Oct 27;304(16):1812-20. doi: 10.1001/jama.2010.1535.

50. Tejpar S, Celik I, Schlichting M, Sartorius U, Bokemeyer C, Van Cutsem E. Association of KRAS G13D tumor mutations with outcome in patients with metastatic colorectal cancer treated with first-line chemotherapy with or without Cetuximab. J Clin Oncol. 2012 Oct 10;30(29):3570-7. doi: 10.1200/JCO.2012.42.2592. Epub 2012 Jun 25.

51. Artale S, Sartore-Bianchi A, Veronese SM et al. Mutations of KRAS and BRAF in primary and matched metastatic sites of colorectal cancer. J Clin Oncol 2008; 26: 4217-4219

52. Michela Pucci, Mattia Lauriola, Resistance to EGFR Targeting Treatments in Colorectal Cancer, Oncogenomics 2019

53. Loupakis F et al. KRAS codon 61, 146 and BRAF mutations predict resistance to Cetuximab plus Irinotecan in KRAS codon 12 and 13 wild-type metastatic colorectal cancer. Br J cancer 2009 Aug 18; 101(4): 715-21.

54. Di Nicolantonio F et al. Wild-type BRAF is required for response to Panitumumab or Cetuximab in metastatic colorectal cancer. JCO 2008 Dec 10; 26 (35):5705-12

55. Van Cutsem E LI, Folprecht G et al. Cetuximab plus FOLFIRI in the treatment of metastatic colorectal cancer (mCRC): The influence of KRAS and BRAF biomarkers on outcome: Update data from CRYSTAL trial. ASCO Gastrointestinal Cancer Symposium 2010 28(May 20 suppl): 3570.

56. Davies H1, Bignell GR, Cox C, Stephens P, Edkins S, Clegg S, Teague J, Woffendin H, Garnett MJ, Bottomley W, Davis N, Dicks E, Ewing R, Floyd Y, Gray K, Hall S, Hawes R, Hughes J, Kosmidou V, Menzies A, Mould C, Parker A, Stevens C, Watt S, Hooper S, Wilson R, Jayatilake H, Gusterson BA, Cooper C, Shipley J, Hargrave D, Pritchard-Jones K, Maitland N, Chenevix-Trench G, Riggins GJ, Bigner DD, Palmieri G, Cossu A, Flanagan A, Nicholson A, Ho JW, Leung SY, Yuen ST, Weber BL, Seigler HF, Darrow TL, Paterson H, Marais R, Marshall CJ, Wooster R, Stratton MR, Futreal PA. Mutations of the BRAF gene in human cancer. Nature. 2002 Jun 27;417(6892):949-54. Epub 2002 Jun 9.

57. Ikenoue T, Hikiba Y, Kanai F, Tanaka Y, Imamura J, Imamura T, Ohta M, Ijichi H, Tateishi K, Kawakami T, Aragaki J, Matsumura M, Kawabe T, Omata M.Functional analysis of mutations within the kinase activation segment of B-Raf in human colorectal tumors. Cancer Res. 2003 Dec 1;63(23):8132-7.

58. Wan PT, Garnett MJ, Roe SM, Lee S, Niculescu-Duvaz D, Good VM, Jones CM, Marshall CJ, Springer CJ, Barford D, Marais R; Cancer Genome Project. Mechanism of activation of the RAF-ERK signaling pathway by oncogenic mutations of B-RAF. Cell. 2004 Mar 19;116(6):855-67.

59. Bokemeyer C, Van Cutsem E, Rougier P, Ciardiello F, Heeger S, Schlichting M, Celik I, Köhne CH. Addition of Cetuximab to chemotherapy as first-line treatment for KRAS wild-type metastatic colorectal cancer: pooled analysis of the CRYSTAL and OPUS randomised clinical trials. Eur J Cancer. 2012 Jul;48(10):1466-75. doi: 10.1016/j.ejca.2012.02.057. Epub 2012 Mar 23.

60. Van Cutsem E, Köhne CH, Láng I, Folprecht G, Nowacki MP, Cascinu S, Shchepotin I, Maurel J, Cunningham D, Tejpar S, Schlichting M, Zubel A, Celik I,Rougier P, Ciardiello F. Cetuximab plus Irinotecan, fluorouracil, and leucovorin as first-line treatment for metastatic colorectal cancer: updated analysis of overall survival according to tumor KRAS and BRAF mutation status. J Clin Oncol. 2011 May 20;29(15):2011-9. doi: 10.1200/JCO.2010.33.5091. Epub 2011 Apr 18.

61. Maughan TS, Adams RA, Smith CG, Meade AM, Seymour MT, Wilson RH, Idziaszczyk S, Harris R, Fisher D, Kenny SL, Kay E, Mitchell JK, Madi A, Jasani B,James MD, Bridgewater J, Kennedy MJ, Claes B, Lambrechts D, Kaplan R, Cheadle JP; MRC COIN Trial Investigators. Addition of Cetuximab to oxaliplatin-based first-line combination chemotherapy for treatment of advanced colorectal cancer: results of the randomised phase 3 MRC COIN trial. Lancet. 2011 Jun 18;377(9783):2103-14. doi: 10.1016/S0140-6736(11)60613-2. Epub 2011 Jun 5.

62. Roth AD, Tejpar S, Delorenzi M, Yan P, Fiocca R, Klingbiel D, Dietrich D, Biesmans B, Bodoky G, Barone C, Aranda E, Nordlinger B, Cisar L, Labianca R,Cunningham D, Van Cutsem E, Bosman F. Prognostic role of KRAS and BRAF in stage II and III resected colon cancer: results of the translational study on the PETACC-3, EORTC 40993, SAKK 60-00 trial. J Clin Oncol. 2010 Jan 20;28(3):466-74. doi: 10.1200/JCO.2009.23.3452. Epub 2009 Dec 14.

63. Van Cutsem E, Köhne CH, Láng I, Folprecht G, Nowacki MP, Cascinu S, Shchepotin I, Maurel J, Cunningham D, Tejpar S, Schlichting M, Zubel A, Celik I,Rougier P, Ciardiello F Cetuximab plus Irinotecan, fluorouracil, and leucovorin as first-line treatment for metastatic colorectal cancer: updated analysis of overall survival according to tumor KRAS and BRAF mutation status. J Clin Oncol. 2011 May 20;29(15):2011-9. doi: 10.1200/JCO.2010.33.5091. Epub 2011 Apr 18.

64. Price TJ, Hardingham JE, Lee CK, Weickhardt A, Townsend AR, Wrin JW, Chua A, Shivasami A, Cummins MM, Murone C, Tebbutt NC Impact of KRAS and BRAF Gene Mutation Status on Outcomes From the Phase III AGITG MAX Trial of Capecitabine Alone or in Combination With Bevacizumab and Mitomycin in Advanced Colorectal Cancer. J Clin Oncol. 2011 Jul 1;29(19):2675-82. doi: 10.1200/JCO.2010.34.5520. Epub 2011 Jun 6.

65. Safaee Ardekani G, Jafarnejad SM, Tan L, Saeedi A, Li G. The prognostic value of BRAF mutation in colorectal cancer and melanoma: a systematic review and meta-analysis. PLoS One. 2012;7(10):e47054. doi: 10.1371/journal.pone.0047054. Epub 2012 Oct 9.

66. Samowitz WS, Sweeney C, Herrick J, Albertsen H, Levin TR, Murtaugh MA, Wolff RK, Slattery ML. Poor survival associated with the BRAF V600E mutation in microsatellite-stable colon cancers. Cancer Res. 2005 Jul 15;65(14):6063-9.

67. Saridaki Z, Papadatos-Pastos D, Tzardi M, Mavroudis D, Bairaktari E, Arvanity H, Stathopoulos E, Georgoulias V, Souglakos J. BRAF mutations, microsatellite instability status and cyclin D1 expression predict metastatic colorectal patients' outcome. Br J Cancer. 2010 Jun 8;102(12):1762-8. doi: 10.1038/sj.bjc.6605694. Epub 2010 May 18.

68. Xu Q, Xu AT, Zhu MM, Tong JL, Xu XT, Ran ZH. Predictive and prognostic roles of BRAF mutation in patients with metastatic colorectal cancer treated with anti-epidermal growth factor receptor monoclonal antibodies: a meta-analysis. J Dig Dis. 2013 Aug;14(8):409-16. doi: 10.1111/1751-2980.12063.

69. Topalian SL, Hodi FS, Brahmer JR, et al. Safety, activity, and immune correlates of anti-PD-1 antibody in cancer. N Engl J Med 2012;366:2443-2454.

70. Drilon A, Laetsch TW, Kummar S, et al. Efficacy of Larotrectinib in TRK Fusion-Positive Cancers in Adults and Children. N Engl J Med 2018;378:731-739.

71. De Roock W, Claes B, Bernasconi D et al. Effects of KRAS, BRAF, NRAS, and PIK3CA mutations on the efficacy of Cetuximab plus chemotherapy in chemotherapy-refractory metastatic colorectal cancer: a retrospective consortium analysis. Lancet Oncol 11: 753-762.

72. Yarden Y, Pines G. The ERBB network: at last, cancer therapy meets systems biology. Nat Rev Cancer. 2012 Jul 12;12(8):553-63

73. Arteaga CL, Engelman JA. ERBB receptors: From oncogene discovery to basic science to mechanism-based cancer therapeutics. Cancer Cell 2014 Mar 17;25(3):282-303.

74. Gelfo V, Rodia MT, Pucci M, Dall'Ora M, Santi S, Solmi R, et al. A module of inflammatory cytokines defines resistance of colorectal cancer to EGFR inhibitors. Oncotarget. 2016. Nov 1;7(44):72167-72183

75. Gelfo V, Mazzeschi M, Grilli G, Lindzen M, Santi S, D'Uva G, Győrffy B, Ardizzoni A, Yarden Y and Lauriola M. A novel role for the interleukin-1 receptor axis in resistance to anti-EGFR therapy. Cancers (Basel). 2018 Sep 26;10(10):355.

76. Chen et al Efficacy of Adding Bevacizumab in the First-Line Chemotherapy of Metastatic Colorectal Cancer: Evidence from Seven Randomized Clinical Trials Gastroenterol Res Pract. 2014;2014:594930. doi: 10.1155/2014/594930. Epub 2014 May 25

77. Heinemann v et al.FOLFIRI plus cetuximab versus FOLFIRI plus bevacizumab as first-line treatment for patients with metastatic colorectal cancer (FIRE-3): a randomised, open-label, phase 3 trial. Lancet Oncol 2014 Sep

78. Venook AND, Lenz HJ, et al. CALGB/SWOG 80405: phase III trial of irinotecan/5-FU/leucovorin (FOLFIRI) or oxaliplatin/5-FU/leucovorin (mFOLFOX6) with bevacizumab (BV) or cetuximab (CET) for patients (pts) with KRAS wild-type (wt) untreated metastatic adenocarcinoma of the colon or rectum (MCRC). J Clin Oncol. 2015;32:5s. 2014 (suppl; abstr LBA3).

79. Revised RECIST Guideline Version 1.1

80. Cervantes, A., Adam, R., Roselló, S., Arnold, D., Normanno, N., Taïeb, J., Seligmann, J., De Baere, T., Osterlund, P., Yoshino, T., et al. (2023). Metastatic colorectal cancer: ESMO Clinical Practice Guideline for diagnosis, treatment and follow-up. Ann Oncol 34, 10–32. 10.1016/j.annonc.2022.10.003.

81. Sung, H., Ferlay, J., Siegel, R.L., Laversanne, M., Soerjomataram, I., Jemal, A., and Bray, F. (2021). Global Cancer Statistics 2020: GLOBOCAN Estimates of Incidence and Mortality Worldwide for 36 Cancers in 185 Countries. CA: A Cancer Journal for Clinicians 71, 209–249. 10.3322/caac.21660.

82. LINEE GUIDA TUMORI DEL COLON (2024) - AIOM.

83. Reynolds, L.E., Maallin, S., Haston, S., Martinez-Barbera, J.P., Hodivala-Dilke, K.M., and Pedrosa, A.-R. (2023). Effects of senescence on the tumour microenvironment and response to therapy. FEBS J. 10.1111/febs.16984.

84. Niklander, S.E., Lambert, D.W., and Hunter, K.D. (2021). Senescent Cells in Cancer: Wanted or Unwanted Citizens. Cells 10, 3315. 10.3390/cells10123315.

85. Giunco, S., Petrara, M.R., Bergamo, F., Del Bianco, P., Zanchetta, M., Carmona, F., Zagonel, V., De Rossi, A., and Lonardi, S. (2019). Immune senescence and immune activation in elderly colorectal cancer patients. Aging (Albany NY) 11, 3864–3875. 10.18632/aging.102022.

86. Falci, C., Gianesin, K., Sergi, G., Giunco, S., De Ronch, I., Valpione, S., Soldà, C., Fiduccia, P., Lonardi, S., Zanchetta, M., et al. (2013). Immune senescence and cancer in elderly patients: results from an exploratory study. Exp Gerontol 48, 1436–1442. 10.1016/j.exger.2013.09.011.

87. Zhang, J., He, T., Xue, L., and Guo, H. (2021). Senescent T cells: a potential biomarker and target for cancer therapy. EBioMedicine 68, 103409. 10.1016/j.ebiom.2021.103409.

88. Xu, X., Wei, F., Xiao, L., Wu, R., Wei, B., Huang, S., Yi, J., and Cui, W. (2023). High proportion of circulating CD8 + CD28- senescent T cells is an independent predictor of distant metastasis in nasopharyngeal carcinoma after radiotherapy. Journal of Translational Medicine 21, 64. 10.1186/s12967-023-03912-2.

89. Hu, J., Han, C., Zhong, J., Liu, H., Liu, R., Luo, W., Chen, P., and Ling, F. (2021). Dynamic Network Biomarker of Pre-Exhausted CD8+ T Cells Contributed to T Cell Exhaustion in Colorectal Cancer. Front Immunol 12, 691142. 10.3389/fimmu.2021.691142.

90. Jiang, Y., Li, Y., and Zhu, B. (2015). T-cell exhaustion in the tumor microenvironment. Cell Death Dis 6, e1792–e1792. 10.1038/cddis.2015.162.

91. Blank, C.U., Haining, W.N., Held, W., Hogan, P.G., Kallies, A., Lugli, E., Lynn, R.C., Philip, M., Rao, A., Restifo, N.P., et al. (2019). Defining “T cell exhaustion.” Nat Rev Immunol 19, 665–674. 10.1038/s41577-019-0221-9.

92. Akce, M., Farran, B., Switchenko, J.M., Rupji, M., Kang, S., Khalil, L., Ruggieri-Joyce, A., Olson, B., Shaib, W.L., Wu, C., et al. (2023). Phase II trial of nivolumab and metformin in patients with treatment-refractory microsatellite stable metastatic colorectal cancer. J Immunother Cancer 11, e007235. 10.1136/jitc-2023-007235.

93. Ye, J., and Peng, G. (2015). Controlling T cell senescence in the tumor microenvironment for tumor immunotherapy. Oncoimmunology 4, e994398. 10.4161/2162402X.2014.994398.

94. Liu, X., Si, F., Bagley, D., Ma, F., Zhang, Y., Tao, Y., Shaw, E., and Peng, G. (2022). Blockades of effector T cell senescence and exhaustion synergistically enhance antitumor immunity and immunotherapy. J Immunother Cancer 10, e005020. 10.1136/jitc-2022-005020.

95. Huff, W.X., Kwon, J.H., Henriquez, M., Fetcko, K., and Dey, M. (2019). The Evolving Role of CD8+CD28- Immunosenescent T Cells in Cancer Immunology. Int J Mol Sci 20, 2810. 10.3390/ijms20112810.

96. Prakash, A., Gates, T., Zhao, X., Wangmo, D., and Subramanian, S. (2023). Tumor-derived extracellular vesicles in the colorectal cancer immune environment and immunotherapy. Pharmacol Ther 241, 108332. 10.1016/j.pharmthera.2022.108332.

97. Xiong, L., Wei, Y., Jia, Q., Chen, J., Chen, T., Yuan, J., Pi, C., Liu, H., Tang, J., Yin, S., et al. (2023). The application of extracellular vesicles in colorectal cancer metastasis and drug resistance: recent advances and trends. Journal of Nanobiotechnology 21, 143. 10.1186/s12951-023-01888-1.

98. Glass, S.E., and Coffey, R.J. (2022). Recent Advances in the Study of Extracellular Vesicles in Colorectal Cancer. Gastroenterology 163, 1188–1197. 10.1053/j.gastro.2022.06.039.

99. Brocco, D., Simeone, P., Buca, D., Marino, P.D., De Tursi, M., Grassadonia, A., De Lellis, L., Martino, M.T., Veschi, S., Iezzi, M., et al. (2022). Blood Circulating CD133+ Extracellular Vesicles Predict Clinical Outcomes in Patients with Metastatic Colorectal Cancer. Cancers (Basel) 14, 1357. 10.3390/cancers14051357.

100. Kaushik, A.K., and DeBerardinis, R.J. (2018). Applications of Metabolomics to Study Cancer Metabolism. Biochim Biophys Acta Rev Cancer 1870, 2–14. 10.1016/j.bbcan.2018.04.009.

101. Definition of cellular metabolism - NCI Dictionary of Cancer Terms - NCI (2011). https://www.cancer.gov/publications/dictionaries/cancer-terms/def/cellular-metabolism.

102. Claudino, W.M., Goncalves, P.H., di Leo, A., Philip, P.A., and Sarkar, F.H. (2012). Metabolomics in cancer: a bench-to-bedside intersection. Crit Rev Oncol Hematol 84, 1–7. 10.1016/j.critrevonc.2012.02.009.

103. Schmidt, D.R., Patel, R., Kirsch, D.G., Lewis, C.A., Vander Heiden, M.G., and Locasale, J.W. (2021). Metabolomics in cancer research and emerging applications in clinical oncology. CA Cancer J Clin 71, 333–358. 10.3322/caac.21670.

104. Gold, A., Choueiry, F., Jin, N., Mo, X., and Zhu, J. (2022). The Application of Metabolomics in Recent Colorectal Cancer Studies: A State-of-the-Art Review. Cancers (Basel) 14, 725. 10.3390/cancers14030725.

105. Krauß, D., Fari, O., and Sibilia, M. (2022). Lipid Metabolism Interplay in CRC—An Update. Metabolites 12, 213. 10.3390/metabo12030213.

106. Scott Kopetz et al. BREAKWATER: Analysis of first-line encorafenib + cetuximab + chemotherapy in BRAF V600E-mutant metastatic colorectal cancer.. JCO 43, 16-16(2025).

107. Kopetz S, Grothey A et al. Encorafenib, Binimetinib, and Cetuximab in BRAF V600E-Mutated Colorectal Cancer.N Engl J Med. 2019 Oct 24;381(17):1632-1643. doi: 10.1056/NEJMoa1908075. Epub 2019 Sep 30.

108. Bhatt, K.; Orlando, T.; Meuwis, M.-A.; Louis, E.; Stefanuto, P.-H.; Focant, J.-F. Comprehensive Insight into Colorectal Cancer Metabolites and Lipids for Human Serum: A Proof-of-Concept Study. Int. J. Mol. Sci. 2023, 24, 9614. https://doi.org/10.3390/ijms24119614

109. Sun H, Zhang C, Zheng Y, Liu C, Wang X, Cong X. Glutamine deficiency promotes recurrence and metastasis in colorectal cancer through enhancing epithelial-mesenchymal transition. J Transl Med. 2022 Jul 22;20(1):330. doi: 10.1186/s12967-022-03523-3. PMID: 35869517; PMCID: PMC9308325.

110. Spada M, Piras C, Diana G, Leoni VP, Frau DV, Serreli G, Simbula G, Loi R, Noto A, Murgia F, Caria P, Atzori L. Glutamine Starvation Affects Cell Cycle, Oxidative Homeostasis and Metabolism in Colorectal Cancer Cells. Antioxidants (Basel). 2023 Mar 10;12(3):683. doi: 10.3390/antiox12030683. PMID: 36978930; PMCID: PMC10045305.

111. Al Hinai EA, Kullamethee P, Rowland IR, Swann J, Walton GE, Commane DM. Modelling the role of microbial p-cresol in colorectal genotoxicity. Gut Microbes. 2019;10(3):398-411. doi: 10.1080/19490976.2018.1534514. Epub 2018 Oct 25. PMID: 30359553; PMCID: PMC6546321

112. Cui S, Yu Y, Zhan T, Gao Y, Zhang J, Zhang L, Ge Z, Liu W, Zhang C, Zhuang S. Carcinogenic Risk of 2,6-Di-tert-Butylphenol and Its Quinone Metabolite 2,6-DTBQ Through Their Interruption of RARβ: In Vivo, In Vitro, and In Silico Investigations. Environ Sci Technol.

113. Tu CE, Liu YF, Liu HW, Jiao CM, Liu Q, Hung MC, Li P, Wan XB, Fan XJ, Wang YL. D-ribose-5-phosphate inactivates YAP and functions as a metabolic checkpoint. J Hematol Oncol. 2025 Jan 4;18(1):2. doi: 10.1186/s13045-024-01655-1. PMID: 39755622; PMCID: PMC117004462022 Jan 4;56(1):480-490. doi: 10.1021/acs.est.1c06866. Epub 2021 Dec 19. PMID: 34927421.

114. Kim, E. R., et al. (2018). Fecal Fatty Acid Profiling as a Potential New Screening Biomarker in Patients with Colorectal Cancer. Annals of Coloproctology, 34(4), 206–211.

115. Xie, Y., et al. (2023). Metabolomic analysis of gut metabolites in patients with colorectal cancer: Association with disease development and outcome. Oncology Letters, 26(1), 1–12.

116. The intestinal barrier: a pivotal role in health, inflammation, and cancer Neurath, Markus F et al.The Lancet Gastroenterology & Hepatology, Volume 10, Issue 6, 573 - 592

117. Gwenny M. Fuhler, Hester Eppinga, Maikel P. Peppelenbosch, Fumarates and Cancer, Trends in Molecular Medicine, Volume 23, Issue 1, 2017, pages 3-5, ISSN 1471-4914, https://doi.org/10.1016/j.molmed.2016.12.001.

118. Xie X, Zhao Y, Ma CY, Xu XM, Zhang YQ, Wang CG, Jin J, Shen X, Gao JL, Li N, Sun ZJ, Dong DL. Dimethyl fumarate induces necroptosis in colon cancer cells through GSH

depletion/ROS increase/MAPKs activation pathway. Br J Pharmacol. 2015 Aug;172(15):3929-43. doi: 10.1111/bph.13184. Epub 2015 Jun 12. PMID: 25953698; PMCID: PMC4523346.

119. Nikulin MP, Shilova NV, Lipatnikov AD, Stilidi IS, Semyanikhina AV, Bovin NV, Tupitsyn NN. Innate IgM antibodies to mannose in patients with gastric cancer. Cancer Biol Med. 2023 Nov 17;21(3):193–7. doi: 10.20892/j.issn.2095-3941.2023.0156. PMID: 37975248; PMCID: PMC10976321

120. Dong W, Lin M, Zhang R, Sun X, Li H, Liu T, Xu Y, Lv L. d-mannose targets PD-1 to lysosomal degradation and enhances T cell-mediated anti-tumor immunity. Cancer Lett. 2024 Jun 1;591:216883. doi: 10.1016/j.canlet.2024.216883. Epub 2024 Apr 12. PMID: 38615929.

121. Wang Y, Jia Z, Wang Q, Zhu Z. Amino acids and risk of colon adenocarcinoma: a Mendelian randomization study. BMC Cancer. 2023 Oct 28;23(1):1041. doi: 10.1186/s12885-023-11514-w. PMID: 37898769; PMCID: PMC10612249

122. Sirniö, P., Väyrynen, J.P., Klintrup, K. et al. Alterations in serum amino-acid profile in the progression of colorectal cancer: associations with systemic inflammation, tumour stage and patient survival. Br J Cancer 120, 238–246 (2019). https://doi.org/10.1038/s41416-018-0357-6

123. Brown RB, Razzaque MS. Phosphate toxicity and tumorigenesis. Biochim Biophys Acta Rev Cancer. 2018 Apr;1869(2):303-309. doi: 10.1016/j.bbcan.2018.04.007. Epub 2018 Apr 21. PMID: 29684520.

124. Arnst JL, Beck GR Jr. Modulating phosphate consumption, a novel therapeutic approach for the control of cancer cell proliferation and tumorigenesis. Biochem Pharmacol. 2021 Jan;183:114305. doi: 10.1016/j.bcp.2020.114305. Epub 2020 Oct 28. PMID: 33129806; PMCID: PMC9667393.

125. Bonifácio, V.D.B., Pereira, S.A., Serpa, J. et al. Cysteine metabolic circuitries: druggable targets in cancer. Br J Cancer 124, 862–879 (2021). https://doi.org/10.1038/s41416-020-01156-1

126. Meran Keshawa Ediriweera, Ngoc Bao To, Yoongho Lim, Somi Kim Cho,»Odd-chain fatty acids as novel histone deacetylase 6 (HDAC6) inhibitors»

127. You, M., Xie, Z., Zhang, N. et al. Signaling pathways in cancer metabolism: mechanisms and therapeutic targets. Sig Transduct Target Ther 8, 196 (2023). https://doi.org/10.1038/s41392-023-01442-3

128. Habib NA, Wood CB, Apostolov K, Barker W, Hershman MJ, Aslam M, Heinemann D, Fermor B, Williamson RC, Jenkins WE, et al. Stearic acid and carcinogenesis. Br J Cancer. 1987 Oct;56(4):455-8. doi: 10.1038/bjc.1987.223. PMID: 3689663; PMCID: PMC2001814

129. Fang Z, Ren G, Ke S, Xu Q, Chen Y, Shi X, Guo C, Huang J. Serum metabolomic profiling for predicting therapeutic response and toxicity in breast cancer neoadjuvant

chemotherapy: a retrospective longitudinal study. Breast Cancer Res. 2025 Jan 6;27(1):2. doi: 10.1186/s13058-024-01956-w. PMID: 39762945; PMCID: PMC11706045

130. Fatima, S., Hu, X., Huang, C. et al. High-fat diet feeding and palmitic acid increase CRC growth in β2AR-dependent manner. Cell Death Dis 10, 711 (2019). https://doi.org/10.1038/s41419-019-1958-6

131. Zhang, Q., Yang, X., Wu, J. et al. Reprogramming of palmitic acid induced by dephosphorylation of ACOX1 promotes β-catenin palmitoylation to drive colorectal cancer progression. Cell Discov 9, 26 (2023). https://doi.org/10.1038/s41421-022-00515-x

132. Palmitic acid-induced ferroptosis via CD36 activates ER stress to break calcium-iron balance in colon cancer cells, Hao Kuang, Xuehua Sun, Ying Liu, Meng Tang, Yan Wei, Yingying Shi, Ruibin Li, Guohui Xiao, Jinlin Kang, Fen Wang, Jin Peng, Hui Xu, Fuxiang Zhou

133. Anderson AC, Joller N, Kuchroo VK. Lag-3, Tim-3, and TIGIT: Co-inhibitory Receptors with Specialized Functions in Immune Regulation. Immunity. 2016 May 17;44(5):989-1004. doi: 10.1016/j.immuni.2016.05.001. PMID: 27192565; PMCID: PMC4942846.

134. Thommen DS, Schumacher TN. T Cell Dysfunction in Cancer. Cancer Cell. 2018 Apr 9;33(4):547-562. doi: 10.1016/j.ccell.2018.03.012. PMID: 29634943; PMCID: PMC7116508.

135. Mei Z, Liang M, Li L, Zhang Y, Wang Q, Yang W. Effects of statins on cancer mortality and progression: A systematic review and meta-analysis of 95 cohorts including 1,111,407 individuals. Int J Cancer. 2017 Mar 1;140(5):1068-1081. doi: 10.1002/ijc.30526. PMID: 27859151.

136. Liusheng Li, Ning Cui, Tengteng Hao, Jianhua Zou, Wu Jiao, Kangjun Yi, Wu Yu, Statins use and the prognosis of colorectal cancer: a meta-analysis, Clinics and Research in Hepatology and Gastroenterology, Volume 45, Issue 5, 2021, 101588, ISSN 2210-7401, https://doi.org/10.1016/j.clinre.2020.101588.

137. Kroemer M, Turco C, Spehner L, Viot J, Idirène I, Bouard A, Renaude E, Deschamps M, Godet Y, Adotévi O, Limat S, Heyd B, Jary M, Loyon R, Borg C. Investigation of the prognostic value of CD4 T cell subsets expanded from tumor-infiltrating lymphocytes of colorectal cancer liver metastases. J Immunother Cancer. 2020 Nov;8(2):e001478. doi: 10.1136/jitc-2020-001478. PMID: 33229508; PMCID: PMC7684804.

138. Li, M., Zhu, W., Lu, Y. et al. Identification and validation of a CD4+ T cell-related prognostic model to predict immune responses in stage III-IV colorectal cancer. BMC Gastroenterol 25, 153 (2025). https://doi.org/10.1186/s12876-025-03716-2

139. Zhang J, He T, Yin Z, Shang C, Xue L, Guo H. Ascitic Senescent T Cells Are Linked to Chemoresistance in Patients With Advanced High-Grade Serous Ovarian Cancer. Front

Oncol. 2022 Jul 7;12:864021. doi: 10.3389/fonc.2022.864021. PMID: 35875098; PMCID: PMC9301961.

140. Thoma, O.-M.; Neurath, M.F.; Waldner, M.J. T Cell Aging in Patients with Colorectal Cancer—What Do We Know So Far? Cancers 2021, 13, 6227. https://doi.org/10.3390/cancers13246227

141. Wherry, E., Kurachi, M. Molecular and cellular insights into T cell exhaustion. Nat Rev Immunol 15, 486–499 (2015). https://doi.org/10.1038/nri3862. https://doi.org/10.1038/nri3862

142. Yaeger R, Cercek A. Colorectal cancer genetics: What's new and how it impacts therapy. Curr Oncol Rep. 2015;17(2):17.

143. Liu D, Schilling B, Liu D, et al. Integrative molecular and clinical modeling of clinical outcomes to PD1 blockade in patients with metastatic melanoma. Nat Med. 2020;26(9):1401–1412

144. Cen, Y., Liu, Y., Zheng, Y., Shan, L., Jing, Y., Gao, Y., Pan, Y., Bai, Y., & Liu, Y. (2021). BRAF Mutation as a Potential Therapeutic Target for Checkpoint Inhibitors: A Comprehensive Analysis. Frontiers in Immunology, 12, 727. https://doi.org/10.3389/fimmu.2021.727

145. Galon J, Costes A, Sanchez-Cabo F, et al. Type, density, and location of immune cells within human colorectal tumors predict clinical outcome. Science. 2006;313(5795):1960–1964.

146. Fridman WH, Pagès F, Sautès-Fridman C, Galon J. The immune contexture in human tumours: impact on clinical outcome. Nat Rev Cancer. 2012;12(4):298–306.

147. Akbar, A. N., & Henson, S. M. (2011). Are senescence and exhaustion intertwined or unrelated processes that compromise immunity? Nature Reviews Immunology, 11(4), 289–295. https://doi.org/10.1038/nri2959

148. Larbi, A., & Fulop, T. (2014). From "truly naïve" to "exhausted senescent" T cells: When markers predict functionality. Cytometry Part A, 85(1), 25–35. https://doi.org/10.1002/cyto.a.22351

149. Wherry, E. J. (2011). T cell exhaustion. *Nature Immunology*, 12(6), 492–499. https://doi.org/10.1038/ni.2035

150. Im, S. J., et al. (2016). Defining $CD8^+$ T cells that provide the proliferative burst after PD-1 therapy. *Nature*, 537(7620), 417–421. https://doi.org/10.1038/nature19330

151. Liao W, Overman MJ, Boutin AT, Shang X, Zhao D, Dey P, Li J, Wang G, Lan Z, Li J, Tang M, Jiang S, Ma X, Chen P, Katkhuda R, Korphaisarn K, Chakravarti D, Chang A, Spring DJ, Chang Q, Zhang J, Maru DM, Maeda DY, Zebala JA, Kopetz S, Wang YA, DePinho RA. KRAS-IRF2 Axis Drives Immune Suppression and Immune Therapy

Resistance in Colorectal Cancer. Cancer Cell. 2019 Apr 15;35(4):559-572.e7. doi: 10.1016/j.ccell.2019.02.008. Epub 2019 Mar 21. PMID: 30905761; PMCID: PMC6467776.

152. Liu J, Huang X, Liu H, Wei C, Ru H, Qin H, Lai H, Meng Y, Wu G, Xie W, Mo X, Johnson CH, Zhang Y, Tang W. Immune landscape and prognostic immune-related genes in KRAS-mutant colorectal cancer patients. J Transl Med. 2021 Jan 7;19(1):27. doi: 10.1186/s12967-020-02638-9. PMID: 33413474; PMCID: PMC7789428.

153. Le, D. T., et al. (2015). *PD-1 Blockade in Tumors with Mismatch-Repair Deficiency*. New England Journal of Medicine, 372(26), 2509–2520. https://doi.org/10.1056/NEJMoa1500596

154. Llosa, N. J., et al. (2015). The vigorous immune microenvironment of microsatellite instable colon cancer is balanced by multiple counter-inhibitory checkpoints. Cancer Discovery, 5(1), 43–51. https://doi.org/10.1158/2159-8290.CD-14-0863

VII List of publications of the candidate

- Colangelo M, Di Martino M, Polidoro MA, Forti L, **Tober N,** Gennari A, Pagano N, Donadon M. Management of intrahepatic cholangiocarcinoma: a review for clinicians. Gastroenterol Rep (Oxf). 2025 Jan 26;13:goaf005. doi: 10.1093/gastro/goaf005. PMID: 39867595; PMCID: PMC11769681.
- Filippini DM, Carosi F, Panepinto O, Neri G, Nobili E, **Tober N**, Giusti R, Di Maio M. Health-related quality of life assessment in head and neck cancer: A systematic review of phase II and III clinical trials. Heliyon. 2024 Nov 24;10(23):e40671. doi: 10.1016/j.heliyon.2024.e40671. PMID: 39687101; PMCID: PMC11647859.

- Calcitonin-secreting neuroendocrine tumor of the larynx, a diagnostic challenge of a rare neoplasm: a case report and literature review. Daria Maria Filippini, Andi Abeshi, **Nastassja Tober**, Paola Valeria Marchese, Elisa Andrini, Giuseppe Lamberti, Roberto Agosti, Giulia Molinari, Matteo Fermi, Livio Presutti. *AME Case Rep* 2024;8:21

- HER2-targeted therapies for salivary gland cancers. Filippini DM, Pagani R, **Tober N**, Lorini L, Riefolo M, Molinari G, Burato A, Alfieri S, Bossi P, Presutti L.Oral Oncol. 2024 Jan;148:106612

- G07 Health-related Quality of Life assessment in Head and Neck cancer: a Systematic Review of phase 2 and 3 clinical trials published in the last 15 years. Carosi F., Neri G., **Tober N.**, Panepinto O., Nobili E., Di Maio M., Filippini DM Tumori Journal abstract book, vol. 109 n 25 Oct 2023 [Abstract XXV Congresso Nazionale AIOM 2023]

- C69 CARTOON: a study of cardiovascular toxicity of Lonsurf ™. Leone F, Fiamma *V.*, Crivelli F., Paris M.K., Forti L.G., Brizzi M.P., Sperti E., Laface R., **Tober N.**, Salerno F., Traverso E.S., Parlagreco E. Nepote A., Giuli A, Bonessio E., Nicolì E., Bertola B.,

Montagnani F. Tumori Journal abstract book, vol. 109 n 25 Oct 2023 [Abstract XXV Congresso Nazionale AIOM 2023]

- Mosca M, Filippini DM, **Tober N**, Rojas FL, Rihawi K, Di Fabio F. Unexpected response to fourth-line paclitaxel in a patient with metastatic oropharyngeal squamous cell carcinoma, immunotherapy-refractory: a case report. Anticancer Drugs. 2022 Aug 1;33(7):691-695. doi: 10.1097/CAD.0000000000001302. Epub 2022 Mar 23.PMID: 35324531

- **N. Tober** and others. P-144 Quality of life assessment in biliary tract cancer: A systematic review of phase 2 and 3 clinical trials published between 2010 and 2021. Annals of Oncology 33:S301 June 2022 [abstract ESMO World Congress on Gastrointestinal Cancer 2022]

- Andi Abeshi, Daria Maria Filippini, **Nastassja Tober**, Paola Valeria Marchese, Giuseppe Lamberti, Roberto Agosti, Livio Presutti, Giulia Molinari, Matteo Fermi. A rare case of serum calcitonin-secreting neuroendocrine tumor of the larynx [abstract 8° congresso nazionale AIOCC, 2022]